FAKULTÄT FÜR MEDIZIN

Influence of mitochondrial thioredoxin reductase on KrasG12D-mediated pancreatic carcinogenesis

KERSTIN NADINE PFISTER

Vollständiger Abdruck der von der Fakultät für Medizin der Technischen Universität München zur Erlangung des akademischen Grades **einer Doktorin der Medizin** genehmigten Dissertation.

Vorsitzende: Prof. Dr. Gabriele Multhoff

Prüfende /-r der Dissertation:

1. Prof. Dr. Roland M. Schmid

2. apl. Prof. Dr. Katharina S. Götze

Die Dissertation wurde am 20.04.2021 bei der Technischen Universität München eingereicht und durch die Fakultät für Medizin am 12.10.2021 angenommen.

TABLE OF CONTENTS

I. Abstract

Reactive oxygen species and antioxidant enzymes are believed to play a pivotal role in pancreatic cancer development. One under investigated antioxidant enzyme is mitochondrial thioredoxin reductase (Txnrd2). We deleted Txnrd2 in a *Kras*^{G12D}-driven mouse pancreatic tumor model.

Despite an initial increase in precursor lesions, tumor incidence was significantly decreased. We isolated cancer cell lines from these genetically engineered mice and observed impaired proliferation and colony formation, with fewer cells in S phase. Reactive oxygen species and some antioxidant enzymes were increased, whereas H_2O_2 resistance was not diminished. Measurement of mitochondrial bioenergetics showed no impairment of oxidative phosphorylation.

We found significant changes in RAS abundance and RAS activity in Txnrd2-deficient cell lines. The mRNA levels of RAS isoforms were slightly decreased. We could show that eNOS phosphorylation and NO signaling is altered, providing evidence for a model for the low tumor incidence observed: Via enhanced NO signaling, protein nitrosylation is altered such that the activity of mutated Kras is reduced. This might help understand pancreatic carcinogenesis and enable new therapeutic approaches.

II. List of Abbreviations

5-FU	5- Fluoruracil
BrdU	Bromodeoxyuridine
BSC	Best supportive care
CAT	Catalase
cre	Cyclic recombinase
DMEM	Dulbecco's modified Eagle Medium
EDTA	Ethylenediaminetetraacetic
FBS	Fetal Bovine Serum
FPKM	Fragments per kilobase per million mapped reads
FU	Fluoruracil
GEF	Guanine nucleotide exchange factor
GEMM	Genetically engineered mouse models
GPX	Glutathione peroxidase
GR	Glutathione reductase
GRX	Glutaredoxin
GSH	Reduced, monomeric glutathione
GSSG	Oxidized, dimeric glutathione
GTP	Guanosine-5'-triphosphate
IL	Interleukine
IPMN	Intraductal papillary mucinous neoplasm
KRAS	Kirsten Rat Sarcoma viral oncogene
MAPK	Mitogen-associated protein kinase
MCN	Mucinous cystic neoplasm
NAC	N-Acetylcystein
Nor-3	(±)-(E)-4-Ethyl-2-[(E)-hydroxyimino]-5-nitro-3-hexeneamide
OXPHOS	Oxidative phosphorylation
PanIN	Pancreatic intraepithelial neoplasia
PBS	Phosphate buffered saline
PDAC	Pancreatic ductal adenocarcinoma
PRDX	Peroxiredoxin
PTIO	2-Phenyl-4,4,5,5-tetramethylimidazoline-1-oxyl 3-oxide
Rcf	Relative centrifugal force
ROS	Reactive oxygen species

SOD	Superoxide dismutase
TXN	Thioredoxin
TXNIP	Thioredoxin interacting protein
Txnrd	Thioredoxin reductase
VDUP	Vitamin D3-upregualted protein

Table II-1 List of Abbreviations

III. Introduction

III.1 Pancreatic cancer

Pancreatic ductal adenocarcinoma (PDAC), commonly referred to as pancreatic cancer, is one of the deadliest cancers. While survival of cancers of other entities, like breast, colon, or cervix, could have been improved over the last decades, the prognosis of pancreatic cancer is still poor with a 5-year survival rate of 3-9% (Hidalgo, 2010; Jemal et al., 2011; R. Siegel, Ma, Zou, & Jemal, 2014; R. L. Siegel, Miller, & Jemal, 2019). As of now, it is the fourth leading cause of cancer-related deaths in the United States of America (R. L. Siegel, Miller, & Jemal, 2018). However, in 2030, it will become the second leading cause of cancer-related deaths in the USA and Germany, following lung cancer (Quante et al., 2016; Rahib et al., 2014) (see Fig. II-1 A).

Whereas incidents of other cancers show an upwards trend, new cases of PDAC have been constantly rising and will continue to do so in the future (Quante et al., 2016).

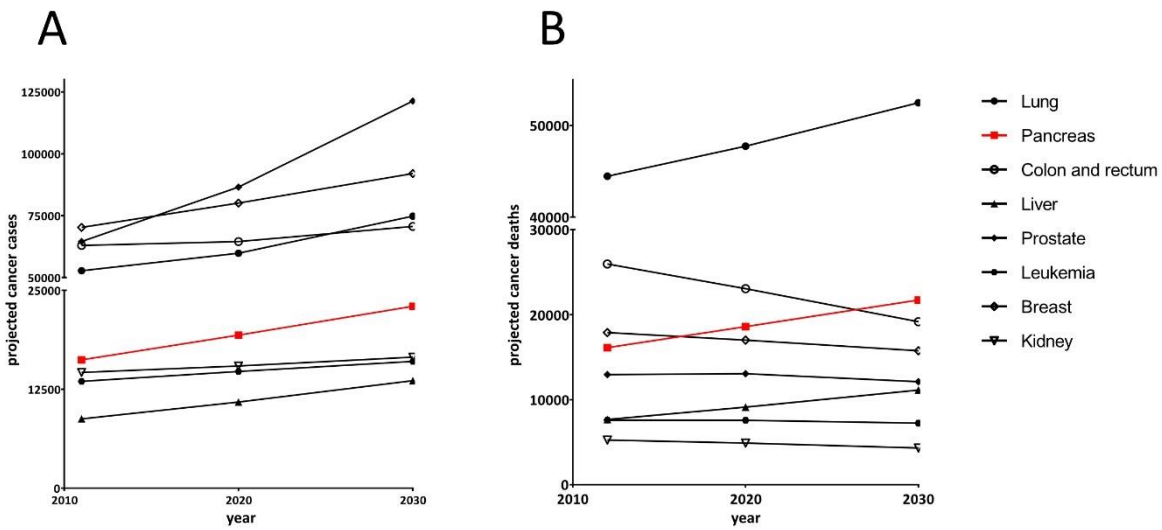

Figure III-1 Projected incident cancer cases (A) and cancer deaths (B) in the years 2020 and 2030.
The 8 most common cancer entities in Germany are shown. The absolute number of cancer cases / deaths is depicted. Data taken from (Quante et al., 2016). For statistical analysis, see the original publication.

Pancreatic ductal adenocarcinoma originates from the exocrine tissue of the pancreas and is classified according to the predominantly existing histological patterns. As for PDAC, these are duct-like structures. It is the most prevalent pancreatic tumor, accounting for about 85% of all cases (Hezel, Kimmelman, Stanger, Bardeesy, & Depinho, 2006). However, tumors can also develop from endocrine tissue, i.e. the islet cells of the pancreas. These pancreatic endocrine tumors account for

1-2% of all cases (Mulkeen, Yoo, & Cha, 2006) and are named after the predominantly produced hormone, i.e. Insulinoma, Gastrinoma, Glucagonoma, and others. Other, rare pancreatic tumors include pancreatic acinar cell carcinoma, pancreatoblastoma, and mixed acinar-endocrine carcinoma (Holen et al., 2002). Also, lymphatic tumors can localize in the pancreas and often mimic primary pancreatic cancer (Volmar, Routbort, Jones, & Xie, 2004). Lastly, in 2-5% of all pancreatic tumors, the pancreas is the site of metastases of primary tumors of different origin, mainly the kidney, skin, lung colon, and breast cancer (Pan, Lee, Rodriguez, Lee, & Saif, 2012).

Due to the absence of early and specific symptoms, pancreatic cancer is usually diagnosed in advanced stages. Several factors contribute to this delay, including the retroperitoneal location of the pancreas without surrounding fibrous capsula (i.e. expansion is not hindered by fibrous tissue) and the small circumferences of preneoplastic lesions (i.e. hard to detect by commonly used radiologic techniques) (Hingorani, Petricoin, et al., 2003). Symptoms of PDAC are mostly general like weight loss, abdominal pain, jaundice, night sweat, etc., and thus challenging to diagnose (DiMagno, Reber, & Tempero, 1999; Huggett & Pereira, 2011). Diagnosis is made by a combination of endoscopic procedures like ERCP and fine-needle aspiration, computer tomography / magnetic resonance imaging, and combined techniques as MR-cholangio-pancreatography or endoscopic ultrasound (Miura et al., 2006).

Commonly used screening methods (like the colonoscopy for early detection of colon cancer) are, as of now, not available for PDAC. The only tumor marker that is commonly used in clinics is CA 19-9 (Swords, Firpo, Scaife, & Mulvihill, 2016). It has been shown to have a very low positive predictive value of 0.4% (Homma & Tsuchiya, 1991), making it not applicable in the screening of unimpaired patients. A better screening parameter is thus urgently needed.

When detected, therapeutic options are limited as most patients already have advanced cancer stages or metastases and only 14% present themselves as candidates for primarily curative resection, i.e. surgical therapy (DiMagno et al., 1999). Even with those cancers, adjuvant chemotherapy consisting of either i. Gemcitabine or ii. Fluorouracil (5-FU) improves survival (Neoptolemos et al., 2004; Oettle et al., 2007; Ueno et al., 2009). The choice of the therapeutic regimen depends on pre-existing conditions and tolerance of the drug, and new therapeutic regimens are developed, tested, and administered every year. Median disease-free survival after adjuvant Gemcitabine was 11.4 months vs. 5.0 months (Ueno et al., 2009) and 5-year survival was 21 percent vs. 8 percent (Neoptolemos et al., 2004), thus showing the benefit of adjuvant chemotherapy, but also the very limited survival altogether.

The better part of patients presenting with PDAC relies on conventional therapeutic strategies in a palliative setting. As first-line therapy, there are 3 regimens commonly used in Germany (Leitlinienprogramm Onkologie der AWMF; Deutschen Krebsgesellschaft e.V. und Deutschen Krebshilfe e.V., 2013):

i.) Gemcitabine as a mono-therapeutic

ii.) Gemcitabine with the addition of the targeted therapeutic Erlotinib (Leitlinienprogramm Onkologie der AWMF; Deutschen Krebsgesellschaft e.V. und Deutschen Krebshilfe e.V., 2013)

iii.) FOLFIRINOX, a regime consisting of 5-FU, Irinotecan, and Oxaliplatin, in cases of good general condition, as is ECOG 0-1 (a score assessing the patient's abilities to perform

in every-day life, see (Oken et al., 1982), a bilirubin value under 1.5 fold of the upper limit and patients under the age of 75)

If the patient suffers progression of the tumor under the above listed first-line therapy, a regimen of 5- FU plus Oxaliplatin can be administered (Leitlinienprogramm Onkologie der AWMF; Deutschen Krebsgesellschaft e.V. und Deutschen Krebshilfe e.V., 2013), leading to a survival benefit of 4.82 vs. 2.30 months with best supportive care (BSC) (Pelzer et al., 2011).

Taken together, it is the shared expert's opinion that detection and treatment of PDAC are extremely challenging, thus resulting in very poor prognoses for the patients. New diagnostic and therapeutic strategies are therefore urgently needed.

III.1.2 Development of pancreatic ductal adenocarcinoma

It is believed that PDAC develops in most cases from preneoplastic lesions, analogous to the adenoma-carcinoma theory of Vogelstein (Fearon & Vogelstein, 1990). Whereas intraductal papillary mucinous neoplasm (IPMN) and mucinous cystic neoplasm (MCN) can also be the origin of pancreatic ductal adenocarcinoma, mostly it originates from pancreatic intraepithelial neoplasia (PanIN) or cystic lesions (Reichert, Blume, Kleger, Hartmann, & von Figura, 2016). These PanIN develop due to accumulations of mutations that benefit survival, metabolism, immunosuppression, suppression of apoptosis, and stromal accumulation (Hanahan & Weinberg, 2000, 2011; Makohon-Moore & Iacobuzio-Donahue, 2016). The theory is that, due to enabling mutations, normal pancreatic tissue develops into low-grade preneoplastic lesions, high-grade PanIN, and finally invasive cancer with metastases. In shared expert's opinion, these mutations are in most cases the following (Biankin et al., 2012; Hezel et al., 2006; Jones et al., 2008; Waddell et al., 2015) (see Fig. III-1):

i.) An enabling mutation in the small GTPase Kirsten Rat Sarcoma viral oncogene (KRAS) in virtually all cases of pancreatic cancer (Almoguera et al., 1988)
ii.) Telomere shortening to allow further mutations (short telomeres become “sticky ends” and lead to chromosomal breakage–fusion–bridge cycles in dividing cells and, thus, more genetic alterations) in virtually all cases of pancreatic cancer (Campbell et al., 2010; Iacobuzio-Donahue, 2012; van Heek et al., 2002)
iii.) A disabling mutation in the CDKN2A / p16 gene in about 90% of all cases of pancreatic cancer (Caldas et al., 1994)
iv.) A disabling mutation in the TP53 gene in 50-75% of all pancreatic cancer (Redston et al., 1994)
v.) A disabling mutation in the SMAD4 gene in about 55% of all pancreatic cancers (Xia et al., 2015)

Besides these major driver mutations, Jones et al. could show in their pioneering work the heterogeneity of mutations in PDAC with the detection of over 1000 somatic mutations, clustering into twelve core signaling pathways (Jones et al., 2008).

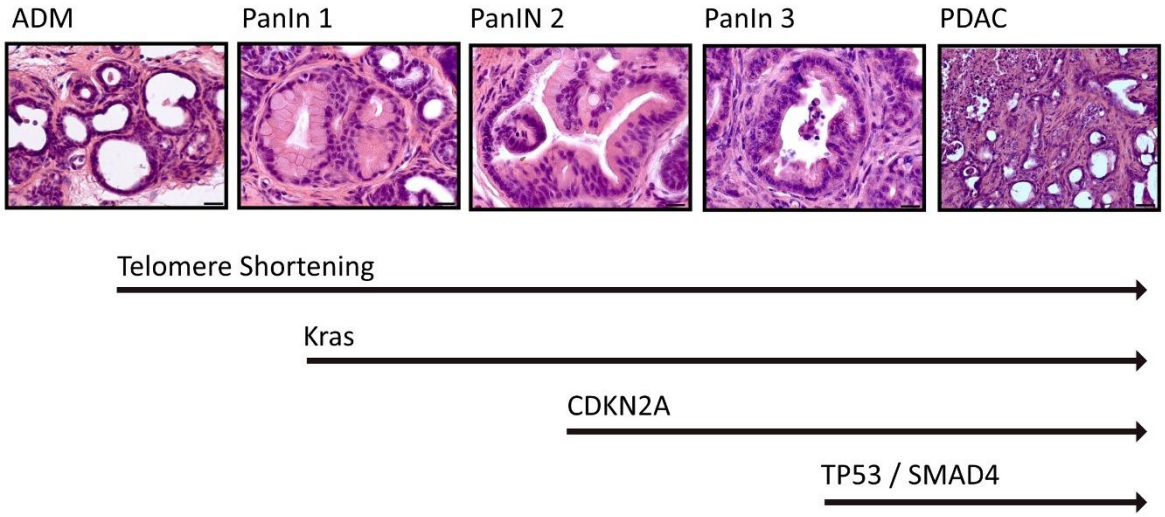

Figure III-2: Genetic mutations in PDAC development
The emergence of invasive PDAC, originating normal epithelium, over different-graded PanIN lesions relies on the sequential accumulation of mutations of the indicated, PDAC-driving genes. Histological images kindly provided by Dr. med. Einwächter, data taken from (Iacobuzio-Donahue, 2012).

There are still vivid discussions concerning the cells or origin for PanIN – and, following, PDAC – formation. Discoveries over the last decade have taken together, given conclusive reasons for acinar cells as the cells of origin, and a metaplastic event (acinar-to-ductal metaplasia) as the primary incident in PDAC development (De La et al., 2008; Kopp et al., 2012; Yamaguchi, Yokoyama, Kokuryo, Ebata, & Nagino, 2018).

Especially during the last years, focus in pancreatic cancer research has broadened, also considering e.g. epigenetic changes in tumor development (review (Paradise, Barham, & Fernandez-Zapico, 2018)) and inflammation (Guerra et al., 2007), thus providing a more detailed insight into this pathology and opening new therapeutic windows.

III.1.3 Mouse models for pancreatic cancer

With the knowledge of these driving genes of PDAC, genetically engineered mouse models (GEMM) were implemented over the last decade. These models underly the principle of the Cre / LoxP system consisting of the bacterial cyclic recombinase (cre), expressed under pancreas-specific promotors and Lox – cassettes flanking the locus of interest, as primarily described in lung cancer (Jackson et al., 2001; Johnson et al., 2001). In the case of KRAS, the most common mutation in pancreatic cancer, a heterozygous knock-in allele of a conditional mutated KRAS insert (*Kras*^{G12D}) is silenced by a transcriptional STOP cassette flanked by two Lox-cassettes at the endogenous locus, thus completing the LSL-Kras$^{+/G12D}$ model, in this study called Kras$^{+/G12D}$. By cross-breeding these

$Kras^{+/G12D}$ mice with $p48^{+/cre}$ mice, specific KRAS-mutational activation of pancreatic cells could be realized, as firstly done by David Tuveson and Ronald DePinho (Aguirre et al., 2003; Hingorani, Jacobetz, Robertson, Herlyn, & Tuveson, 2003).

Since then, a variety of other GEMMs have been developed and used for a better understanding of PDAC progression and formation. In this study, the focus lies on the deficiency of mitochondrial Thioredoxin Reductase, and the respective conditional knockout has previously been described in the vascular system and heart (Conrad et al., 2004; Hellfritsch et al., 2015; Kiermayer et al., 2015). For a detailed explanation of the construction of the knockout see the paper of Conrad et al. (Conrad et al., 2004).

III.2 Reactive Oxygen Species and defense systems

III.2.1 Reactive Oxygen Species

Reactive oxygen species, or ROS, is the elaborated term for radicals, ions, or molecules with an unpaired electron in their outermost shell of electrons. This makes them highly chemically reactive. ROS can be categorized into two categories (Liou & Storz, 2010):

1. Radicals, including superoxide (O_2•−), hydroxyl radical (•OH), nitric oxide (NO•), organic radicals (R•), peroxyl radicals (ROO•), alkoxyl radicals (RO•), thiyl radicals (RS•), sulfonyl radicals (ROS•), thiol peroxyl radicals (RSOO•), and disulfides (RSSR)

2. Non-Radicals, like hydrogen peroxide (H_2O_2), singlet oxygen ($^1O_2$), ozone/trioxygen (O_3), organic hydroperoxides (ROOH), hypochloride (HOCl), peroxynitrite (ONO−), nitrosoperoxycarbonate anion ($O=NOOCO_2-$), nitrocarbonate anion (O_2NOCO_2-), dinitrogen dioxide (N_2O_2), nitronium (NO_2+), as well as highly reactive lipid-or carbohydrate-derived carbonyl compounds

These molecules are generated endogenously for a great part as byproducts in oxidative phosphorylation (OXPHOS). During this process, electrons pass complexes via oxidation-reduction reactions, with each complex showing increasing redox potential. These complexes are, as it has long been known, the following: complex I (NADH dehydrogenase (ubiquinone)), complex II (succinate dehydrogenase), complex III (ubiquinol-cytochrome c reductase), and complex IV (cytochrome c oxidase), where, during the last RedOx reaction, O_2 is reduced to water. However, up to 2% of oxygen is not reduced but oxidized to form superoxide (O_2•−)(X. Li et al., 2013). This is then leaked towards the mitochondrial matrix (via complex I and III) and intermembrane space (via complex III) (Han, Canali, Rettori, & Kaplowitz, 2003; Madamanchi & Runge, 2007; Weinberg et al., 2010). Subsequently, superoxide is dismutated by superoxide dismutase 1 (SOD 1, cytosolic) and 2 (SOD 2, mitochondrial, see Equation 1). Hydrogen peroxide can thus overcome the compartmentalization e.g. with the aid of aquaporins, that are not only obtainable by water, as Bienert et al. could show (Bienert et al., 2007), and then form other ROS compounds or react with DNA / proteins / lipids, respectively (see III.2.2.1 and 0).

$$2\ O_2^{\cdot -} + 2H^+ \xrightarrow{SOD} H_2O_2 + O_2$$

Equation 1

Reactive Oxygen Species in the form of superoxide is also being generated by NADPH oxidase. This enzyme catalyzes the reduction of O_2, generating O_2•− with NADPH as an electron donor. NADPH oxidases were primarily found in cells of the innate immune system (responsible for the 'respiratory burst' (Quinn & Gauss, 2004)), but more recently have been found to be expressed in numerous other cell types including the vascular system, colon, and also pancreas (Cheng, Cao, Xu, van Meir, & Lambeth, 2001; Geiszt, 2006).

Another main site of ROS generation (but also scavenging) is peroxisomes. Hydrogen peroxide is produced by peroxisomal oxidases during e.g. fatty acid metabolism, by oxidases transferring hydrogen from metabolites to O_2 (Dansen & Wirtz, 2001), or by xanthine oxidases in purine metabolism (Bonekamp, Volkl, Fahimi, & Schrader, 2009). In the liver, it has been shown that about 20% of oxygen consumption accounts for peroxisomal oxidase activity (Reddy & Mannaerts, 1994), thus substantially contributing to cellular ROS-production.

There are numerous more sites of ROS generation in eukaryotic cells. Also, ROS can be produced exogenously by e.g. pollutants, tobacco, drugs, xenobiotics, heavy metal ions, or ionizing radiation.

III.2.2 Effect of ROS on eukaryotic cells

Reactive Oxygen species have diverse effects on eukaryotic cells. The effect and the resulting fate of the cell depend on the level of ROS – i.e. moderate levels of ROS are part of cellular signaling and high ROS-levels ('oxidative stress') will result in apoptosis (X. Li et al., 2013). Hereby the threshold of 'physiological' and 'pathological' is nowhere clear and depends on the cell cycle state, microenvironment, and cell type.

III.2.2.1 Effects of moderate levels of ROS

ROS in physiological concentrations is part of cellular signaling. Many pathways are influenced by ROS. The MEK / Erk pathway will be explained in more detail, as it is also part of this study (see below). Many other pathways, like the PI3K/Akt or IKK/NFκB pathway, have been shown to interact with ROS. Mostly, enhanced ROS levels lead to higher phosphorylation rates of respective signaling molecules, thus benefiting survival and growth (Burdick et al., 2003; Q. Li & Engelhardt, 2006; Manna, Zhang, Yan, Oberley, & Aggarwal, 1998; Mochizuki et al., 2006; S. A. Park, Na, Kim, Cha, & Surh, 2009; Y. Wang et al., 2007).

The MEK / Erk 1,2 pathway: As shown in III.1.2, KRAS is the gene most often found with mutations in pancreatic cancer, thus leading to upregulation of the MEK / Erk pathway. It consists of a small G-Protein (RAS) as a recipient of extracellular signaling (via GEFs – Guanine nucleotide exchange

factors), then forwarding the signal to Raf, then Mek and Erk 1,2. This then leads to increased cell growth, proliferation, and survival (McCain, 2013).
p21/RAS can be activated through oxidation at Cys-Residue 118, resulting in loss of GTPase activity and thus constant activation of RAS (Lander et al., 1997). Also, it could be shown that ROS inactivates $p90^{RSK}$, an inhibitor of Erk 1 and 2, thus resulting in higher activity of the MEK / Erk cascade in ovarian cancer (D. W. Chan et al., 2008).
Recently, studies have been done to limit RAS/Raf/MEK/Erk cascade activity by ROS-scavenging. In breast cancer cells, it could be shown that treatment with salvicine, a topoisomerase II inhibitor shown to increase levels of ROS, lead to higher activity of MEK / Erk pathways, whereas a ROS-scavenger (N-acetyl-l-cysteine) stalls it, thus promoting adhesion and apoptosis (Zhou, Chen, Lang, Lu, & Ding, 2008). The same effect could be observed in skin cancer: keratinocytes lacking Tiam1, an activator of Erk 1 and 2, show low levels of ROS and concomitant impaired Erk-phosphorylation and survival signaling (Rygiel, Mertens, Strumane, van der Kammen, & Collard, 2008).
In pancreatic cancer, vitamin E, that has been shown to act as antioxidant (Pathania, Syal, Pathak, & Khanduja, 1999), has proven to inhibit RAS / Mek / Erk signaling and thus cancer growth (Hodul et al., 2013), as Husain et al. could show, by inhibition of pancreatic cancer stem-like cells (Husain et al., 2017).

III.2.2.2 Effects of oxidative stress

High levels of ROS lead to changes in DNA, Proteins, and lipids, but can affect all molecules and organelles in the cell. The first reaction of an oxidant with a macromolecule alters this nucleotide, protein, or lipid and develops it into a second radical, thus a chain reaction arises (Kannan & Jain, 2000).

ROS modifications of DNA

DNA: ROS production and accumulation leads to alterations in the genome. It can affect all structures of deoxyribonucleic acid (DNA):

i.) **Single base lesions**. The mutations are mediated by hydroxyl radicals. The bases are modified as follows:
Thymine: The hydroxyl radical mediates two main reactions: addition across the 5,6-pyrimidine bond and H-atom abstraction from the methyl group. This leads, via different oxidation/reduction steps to the formation of the following molecules: thymine 5,6-glycols (Thy-Gly), 5-hydroxy-5-methylhydantoin (Hyd-Thy), 5-hydroxymethyluracil (5-HmUra), and 5-formyluracil (5-FoUra) (Cadet & Wagner, 2013).
These mutations have only a limited mutagenic potential, as they mainly pair with adenine, however, thymidine glycols are strong DNA polymerase inhibitors *in vitro (Evans et al., 1993)*.
Moreover, one intermediate molecule, 5-(uracilyl)-methyl radical, can also react with neighboring guanine or adenine to create intrastrand cross-links like G[8-5 m]T (Cadet & Wagner, 2013).

Guanine: There exist two main degradation products of guanine: 8-oxo-7,8-dihydroguanine (8-oxoGua) and 2,6-diamino-4-hydroxy-5-formamidopyrimidine (Fapy-Gua) (Cadet & Wagner, 2013). 8-oxoGua is one of the most mutagenic DNA lesions, as a mispairing with adenine instead of cysteine occurs. It thus leads to a guanine-to-thymine conversion with an efficiency of up to 5% per 8-oxoGua mutation (Fraga, Shigenaga, Park, Degan, & Ames, 1990; Moriya, 1993; Wood, Dizdaroglu, Gajewski, & Essigmann, 1990). The presence of 8-oxoGua in telomeric regions of the chromosome inhibits telomerase activity, leading to decreased telomere length, which can lead to chromosomal instability and thus apoptosis or carcinogenesis (Coluzzi et al., 2014; Opresko, Fan, Danzy, Wilson, & Bohr, 2005).

Adenine: The oxidative modification of adenine resembles the modification of guanine, resulting in 8-oxo-7,8-dihydroadenine (8-oxoAde) and 4,6-diamino-5-formamidopyrimidine (Fapy-Ade). 8-oxoAde mutation holds mutagenic potential as it can be replaced by guanine or cytosine, respectively (Kamiya et al., 1995).

Cytosine: Oxidation of cytosine leads to the following products: 5-hydroxycytosine (5-OHCyt), 5-hydroxyuracil (5-OHUra), 5,6-dihydroxy-5,6- dihydrouracil (Ura-Gly), 5-hydroxyhydantoin (Hyd-Ura), and 1-carbamoyl-4,5-dihydroxy-2-oxoimidazolidine (Imid-Cyt) (Cadet & Wagner, 2013). In 10-30% of cases, Cyt-Gly is demaninated to Ura-Gly (Tremblay & Wagner, 2008).
A very common mutation of cytosine is 5-methylcytosine, which is believed to play a pivotal role in evolution (C. A. Lewis, Jr., Crayle, Zhou, Swanstrom, & Wolfenden, 2016). Remarkably, upon oxidation, 5-methylcytosine evolves into thymidine glycol (Zuo, Boorstein, & Teebor, 1995).

ii.) **Tandem-base lesions**: These lesions are formed by either hydroxy radicals or one-electron oxidants, forming pyrimidine peroxyls, which are then able to efficiently add to adjacent purine (Cadet & Wagner, 2013). For example, thymine can be developed into a hydroxyperoxyl radical that subsequently can react with guanine, resulting in the formation of tandem formamide and 8-oxoGua lesions (Cadet & Wagner, 2013). It has been shown, that over 40% of 8-oxoGua lesions are refractory to repair by DNA glycosylases (Bergeron, Auvre, Radicella, & Ravanat, 2010).

iii.) **DNA-protein crosslinks**: Especially upon UV-radiation, but also by hydroxy radicals, DNA-protein crosslinks can develop via guanine radicals (see above) reacting with lysine, forming lysine-guanine cross-link between the ε-amino group and the C8 position of guanine (Cadet & Wagner, 2013; Perrier et al., 2006).

iv.) **Base-sugar crosslinks**: Purine 5',8-Cyclonucleosides, interstrand base-sugar connections, are being formed by oxidation of exocyclic 5'-hydroxymethyl group, followed by intramolecular cyclization (Cadet & Wagner, 2013). This cross-link mutation also leads to DNA-distortion, thus has to be repaired by nucleotide excision repair, hence imposing great difficulties in cells where this system is

damaged or lost (e.g. in Xeroderma pigmentosum, leading to a 1000-fold increase in skin-cancer prevalence (Torgovnick & Schumacher, 2015)).

v.) **DNA interstrand crosslinks:** There are two main oxidative pathways described, which result in interstrand cross-links by opposite DNA strands (Cadet & Wagner, 2013): a. Cross-links by C4' abasic sites, favored by adenine or cytosine opposite and b. cross-links involving nucleophilic addition to guanine radicals, as in iii.) described, can also take place in opposite DNA strands.

In non-cancerous cells, frequently arising mutations are checked and repaired by numerous DNA repair mechanisms (see relevant literature). However, in cancer cells, these mechanisms often are disabled, leading to a potentiated rate of carcinogenic mutations (see e.g. (Chae et al., 2019)).

ROS modification of proteins

Modifications of proteins include a transformation of methionine to sulfoxide and cysteine to sulfenic, sulfinic, and sulfonic acid (Grimsrud, Xie, Griffin, & Bernlohr, 2008). Modification of proteins leads to i.) alterations in intracellular signal (see above) and ii.) targeted degradation by ubiquitin-dependent proteasome. For this degradation, proteins are e.g. marked by carbonylation with 4-hydroxy-2-nonenal (4-HNE), a product of lipid peroxidation (see below). Remarkably, high levels of ROS can lead to 4-HNE modification and inhibition of the proteasome itself, thus benefiting ROS accumulation (Ferrington & Kapphahn, 2004).

ROS modifications of lipids

Polyunsaturated fatty acid side chains are the main parts of organelles' membranes by providing a pivotal role in the cell's integrity and structure; and are regularly affected by lipid peroxidation due to their reactive methylene bridges (Gaschler & Stockwell, 2017). The formation of lipid peroxides precedes the removal of a hydrogen atom from a methylene carbon, resulting in a radical, that then reacts with molecular oxygen to form lipid peroxide, the two most common being 4-HNE (see above) and malondialdehyde (Gaschler & Stockwell, 2017). The reaction is either enzymatical (via Lipoxygenases) or non-enzymatic (Gaschler & Stockwell, 2017). Lipid peroxidation leads to diverse effects on the cell's membrane: i.) the impairment of membrane fluidity by inhibition of lateral diffusion (Borst, Visser, Kouptsova, & Visser, 2000), ii.) reorientation of lipid peroxides in bilayer membranes, leading to a decrease in membrane thickness (Wong-Ekkabut et al., 2007), iii.) the generation of lysophospholipids, increasing membrane's permeability (Wong-Ekkabut et al., 2007), and iv.) the generation of new oxidational reactions, e.g. by reaction with ferrous iron, producing alkoxy radicals that can further oxidize macromolecules (Gaschler & Stockwell, 2017).

III.2.3 Cellular detoxification from ROS

As a perturbation of ROS homeostasis can lead to numerous disadvantages for the cell (see 0), it is compulsory to keep ROS-levels balanced. This is provided by the fine regulation of antioxidant enzymes and molecules. The big antioxidant systems (thioredoxin, glutathione, catalase, peroxiredoxin, and glutaredoxin), will be explained in more detail below and in Figure III-3. Additional antioxidants include dietary antioxidants like Vitamine A, C, and E, bilirubin, urate, and others, and detailed information can be obtained in various publications.

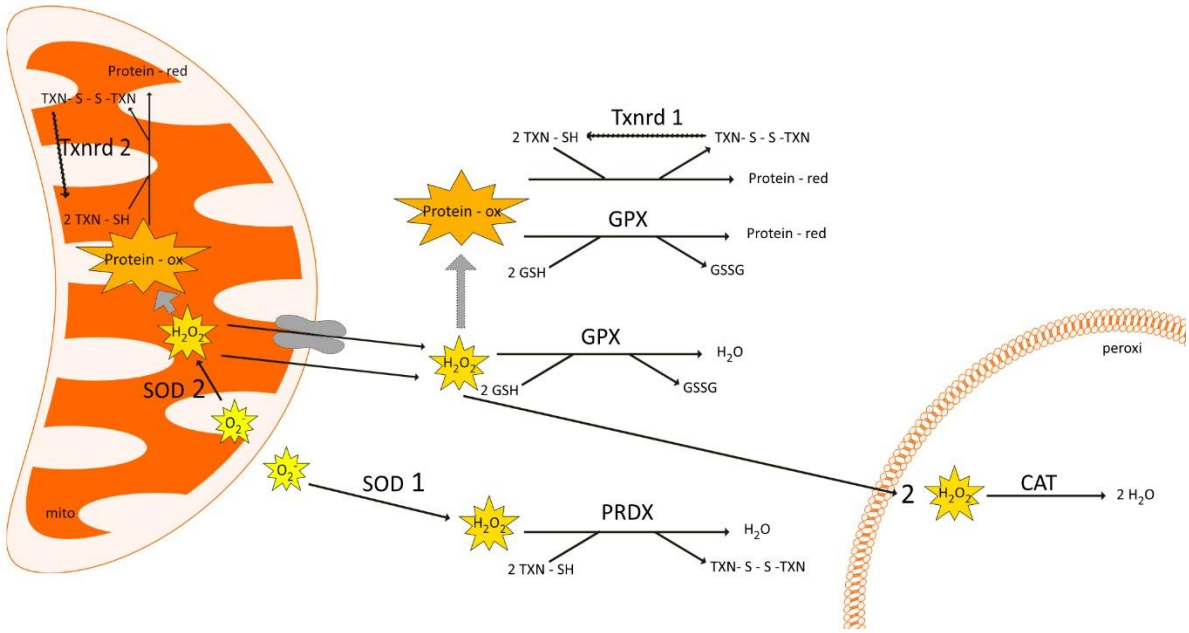

Figure III-3 Antioxidant defense systems in the cell
Defense of mitochondrial ROS (mtROS) in the cell. Superoxide formed during oxidative phosphorylation is being dismutated by SOD 1 (in the cytoplasm) and 2 (in the mitochondria), with the product being hydrogen peroxide. Superoxide can pass through membranes due to its neutral electric charge but can also cross barriers through aquaporins (Bienert et al., 2007). H_2O_2 is reduced by GPX or PRDX with the help of reduced glutathione or thioredoxin, respectively. H_2O_2 can also lead to modifications ("oxidations") of proteins, that can be reversed by GPX or Txnrd. Lastly, H_2O_2 can also diffuse into peroxisomes and is reduced there by catalase.
TXN = Thioredoxin, Txnrd = Thioredoxin Reductase, SOD = Superoxide dismutase, GPX = glutathione peroxidase, PRDX = peroxiredoxin, CAT = catalase, mito = mitochondrium, peroxi = peroxisome
Data taken from (Begas, Liedgens, Moseler, Meyer, & Deponte, 2017; Bhabak & Mugesh, 2010; Gong, Hou, Liu, & Zhang, 2015; Kirkman & Gaetani, 2007; Y. H. Park et al., 2016; Radi et al., 1991; Rhee, Chae, & Kim, 2005; Sabens & Mieyal, (2009)).

III.2.3.1 Thioredoxin Reductases (Txnrd)

The Thioredoxin system is a highly conserved system consisting of Thioredoxin (TXN), Thioredoxin Reductase (Txnrd), and NADPH and catalyzes the reduction of intra- and intermolecular disulfides and sulfenic acids to their respective sulfhydryl moieties.

Txnrds are, together with e.g. glutathione peroxidases and iodothyronine deiodases, some of the 50 identified enzymes containing selenocysteine, thus being selenoproteins (Labunskyy, Hatfield, & Gladyshev, 2014).

Thioredoxins have a dithiol/disulfide active site and act as electron donors for various proteins, to control intracellular redox state, signal transduction by thiols, defense of oxidative stress, and aiding miscellaneous enzymes, e.g. the ribonucleotide reductase, which produces deoxyribonucleotides, an essential step for DNA-synthesis. Thioredoxin reductases then reduce the formed disulfide bond with the help of NADPH (equation 3) (Arner & Holmgren, 2000).

$$2\ TXN - SH + R - S\text{-}S - R \rightarrow TXN - S\text{-}S - TXN + 2\ R - SH$$

Equation 2

$$TXN - S\text{-}S - TXN + NADPH + H^{+} \xrightarrow{Txnrd} TXN - SH + NADP^{+}$$

Equation 3

There are three distinct forms of thioredoxin and, therefore, thioredoxin reductases, known in human tissues. TXN1 and thus Txnrd1 is localized in the cytosol and extracellular, TXN2, and Txnrd2 in the mitochondria, and Txnrd3 has only been observed in testis (Arner, 2009).

III.2.3.2 Glutathione Peroxidase (GPX) and Glutaredoxin (GRX)

As previously described, superoxide is quickly dismutated into hydrogen peroxide (see equation 1), which is then reduced to water by e.g. glutathione. Glutathione peroxidase (GPX), a selenoenzyme, uses reduced, monomeric glutathione (GSH) to reduce H_2O_2, producing H_2O, O_2, and oxidized, dimeric glutathione (GSSG) (see equation 2).

$$2\ GSH + H_2O_2 \xrightarrow{GPX} GS{-}SG + 2\ H_2O$$

Equation 4

Glutaredoxin (GRX) possesses two distinct glutathione binding sites, one site interacting with the oxidized disulfide substrate and the other site activating GSH as the reducing agent (Begas et al., 2017).

$$GSH + GS\text{-}SR \xrightarrow{GRX} GS\text{-}SG + RSH$$

Equation 5

$$2\ GSH + RS - SR \xrightarrow{GRX} GS - SG + RSH + HSR$$

Equation 6

In both cases, GSSG is then reduced with the help of glutathione reductase (GR) and NADPH as co-enzyme, thus completing the circle (equation 3) (Bhabak & Mugesh, 2010).

$$GS - SG + NADPH + H^+ \xrightarrow{GR} 2\ GSH + NADP^+$$

Equation 7

III.2.3.3 Catalase (CAT)

This enzyme also catalyzes the inactivation of H_2O_2 (see equation 4), however, catalases are mainly located in the peroxisomes (exceptions could be observed in the rat heart mitochondria, see (Radi et al., 1991)). Mammalian Catalase contains four heme groups, thus requires iron as a cofactor (Kirkman & Gaetani, 2007).

$$2\ H_2O_2 \xrightarrow{CAT} 2\ H_2O + O_2$$

Equation 8

III.2.3.4 Peroxiredoxin (PRDX)

This enzyme reduces hydroperoxides (and peroxynitrites) with the use of electrons provided by thioredoxin or other thiols. Peroxiredoxins contain a central Cystein residue and use this to detoxify H_2O_2, then undergoing a cycle of peroxide-dependent oxidation and thiol-dependent reduction (Rhee et al., 2005).

$$H_2O_2 + PRDX - SH \rightarrow H_2O + PRDX - SOH$$

$$PRDX - SOH + PRDX - SH \rightarrow PRDX - S - S - PRDX + H_2O$$

$$2\ TXN - SH + PRDX - S - S - PRDX \rightarrow TXN - S - S - TXN + 2\ PRDX - SH$$

Equation 9

Interestingly, PRDXs have recently been found to be tumor-accelerating in hepatic cellular carcinoma (HCC), as homozygous depletion of PRDX II upregulates RAS expression and promotes RAS dependent tumor growth and proliferation (Y. H. Park et al., 2016). In esophageal squamous cell carcinoma, an interaction with the mTOR / p70S6K pathway and thus enhanced tumorigenesis was observed (Gong et al., 2015).

III.2.4 ROS and ROS-defense in cancer

The role of reactive oxygen species and antioxidants in oncogenesis, tumor growth, and metastasis are big topics of research as of the time being. It has been shown that ROS contributes pivotally to some of the hallmarks of cancer described by Hanahan and Weinberg, being cancer heterogeneity, sustained tumor proliferation, resisting cell death, deregulation of cellular energetics, tumor-promoting inflammation, inducing angiogenesis, evading growth suppressors, avoiding immune destruction, activating invasion and metastasis, and enabling replicative immortality (Hanahan & Weinberg, 2011). This is fulfilled by the activation of oncogenes and/or the inactivation of tumor suppressor-acting genes.

i.) Cancer heterogeneity
As shown in 0, ROS can lead to a variety of mutations in DNA, leading to genetic instability. These mutations can benefit the tumor by increasing its genetic instability, hence gaining “facilitating characteristics”, and by aiding cancer heterogeneity.

ii.) Sustained tumor proliferation
It has been shown that sustained proliferative signaling, one key characteristic of cancer cells, is influenced by ROS, one key regulator being SOD2. This antioxidant enzyme is regulated by levels of superoxide or hydrogen peroxide, and decreased SOD2 activity drives proliferation (Liou & Storz, 2010; M. Wang et al., 2005). Likewise, it could be shown that a stable ectopic expression of SOD2 leads to decreased growth rate in pancreatic cancer cells (Cullen et al., 2003). Contrarily, Estrogen-dependent ROS have been shown to upregulate mRNA levels of different cyclins, leading to sustained proliferative signaling in breast cancer, whereas antioxidants like NAC were able to stall these pathways (Felty, Singh, & Roy, 2005).

iii.) Resisting cell death
Whereas high levels of ROS in normal cells generally lead to apoptosis via mitochondrial / endoplasmic reticulum or death receptor pathway due to accumulating macromolecular damage and e.g. p53 - activation (Redza-Dutordoir & Averill-Bates, 2016), it has recently been shown that moderate levels of ROS can lead to pro-survival signaling. For example, the elevation of mitochondrial ROS (mtROS)-levels activates protein-kinase D1 and NFκB, subsequently leading to upregulation of antioxidant enzymes such as SOD2 and anti-apoptotic molecules like A20 and cIAPs (Liou & Storz,

2010; Mihailovic et al., 2004; Song et al., 2009; Storz, Doppler, Ferran, Grey, & Toker, 2005).

iv.) Deregulation of cellular energetics

The Warburg-effect, a switch from oxidative phosphorylation to glycolysis, is a phenomenon observable in various cancer types (Liberti & Locasale, 2016). During high ROS-levels, the cell experiences cumulative damages to membranes and proteins (see 0), i.e. also to the mitochondrial membrane, disrupting the complex-aggregation and efficiency of the electron transport chain, and to the complexes themselves, impairing their function (de Sa Junior et al., 2017; Ernster & Dallner, 1995; Paradies et al., 2004; Petrosillo, Ruggiero, Di Venosa, & Paradies, 2003). Through this metabolic switch, the cells do not rely as much on the function of the electron transport chain, ensuring adequate energy supply, and limit the production of more, damaging ROS (see III.2.1). Interestingly, complex I, responsible for much of the mtROS, presents a higher quantity of mutations than the others in various tumors, whilst mutations in complex I lead to increased ROS-production (Lu, Sharma, & Bai, 2009).

v.) Tumor-promoting inflammation

The first findings on the connection of inflammation ("irritation") and cancer had been described in Aryuvedic medicine about 5000 years ago (Garodia, Ichikawa, Malani, Sethi, & Aggarwal, 2007). Since then, the relationship of oxidative stress leading to chronic inflammation, due e.g. the oxidative burst as part of the innate immune response, and subsequently cancer, has been accepted (Weitzman & Gordon, 1990). This has been underlined by epidemiologic data of higher tumor incidences in patients with chronic inflammation, e.g. Crohn's disease and colon carcinoma or *Helicobacter pylori*-induced gastritis and gastric cancer (Balkwill & Mantovani, 2001; Mantovani, Allavena, Sica, & Balkwill, 2008). The common opinion is that up to 15% of all worldwide cases of cancer are attributed to infections and resulting in chronic inflammation (Kuper, Adami, & Trichopoulos, 2000).

It is believed, that higher ROS – production of immune cells leads to a higher mutation rate in the (pre)malignant cells, whereas mutations themselves contribute to enhanced inflammation e.g. by recruiting neutrophils to the locus of tumor promotion (Dibra, Mishra, & Li, 2014).

III.2.4.1 ROS in pancreatic cancer

It has been shown that levels of mtROS increase over the development from normal pancreatic tissue, to ADM, PanIN lesions, and finally, PDAC, in the context of mutant KRAS, which is the gene most commonly mutated in pancreatic cancer (see III.1.2) (Liou et al., 2016). Responsible for the big amounts of mtROS is i.) the inefficiency of the respiratory chain, leading to higher levels of ROS (Weinberg et al., 2010) and ii.) the high activity of NADPH oxidase, mainly acting in mitochondria (Vaquero, Edderkaoui, Pandol, Gukovsky, & Gukovskaya, 2004; Wu et al., 2011).

One main response of (pre)cancerous pancreatic cells to oxidative stress is the upregulation of NRF2 (K. Chan, Han, & Kan, 2001; Kovac et al., 2015; Nguyen, Nioi, & Pickett, 2009). Activation of NRF2 depends on several pathways, like the MAPK pathway (see above) and PI3K pathway (Martinez-

Useros, Li, Cabeza-Morales, & Garcia-Foncillas, 2017). NRF2 is the transcription factor for various genes also a variety of antioxidants, players of the immune response and inflammatory reaction, carcinogenesis, and fibrosis (Martinez-Useros et al., 2017). Also, it could be shown, that NRF2 regulates mtROS production through both respiratory chain and NADPH oxidases, mainly NOX4 (Kovac et al., 2015).

One main characteristic of PDAC is hypoxia, due to the massive accumulation of stroma surrounding the cancerous cells (Yuen & Diaz, 2014). Hypoxia induces Hif-1α, hypoxia-inducible factor 1α, which then acts as a transcription factor for various gene products benefiting metabolic adaption to hypoxic states and increase cellular oxidation (Movafagh, Crook, & Vo, 2015; Semenza, 2004). It is commonly accepted that ROS levels increase under hypoxic conditions (Clanton, 2007). The mediator of hypoxia to Hif-1α seems to be ROS, as ROS have been shown to regulate Hif-1α stabilization via MAPK and PI3K pathway, respectively (Movafagh et al., 2015).

Taken together, it seems like the role of ROS in PDAC, like in other cancers, depends on the homeostasis. Medium levels of ROS seem to promote tumor growth, enhancing the tumor's enabling characteristics (see III.2.4), whereas imbalance and oxidative stress hinders the cancerous cells from further expansion and lead to apoptosis (Martinez-Useros et al., 2017; Zhang, Cao, Toole, & Xu, 2015).

III.2.4.2 Txnrd2 in pancreatic cancer

This study focuses on the role of mitochondrial Thioredoxin reductase in PDAC. Until now, there has been no published research in this area. Txnrd2 has been intensively studied in the context of cardiovascular disease (Conrad et al., 2004; Hellfritsch et al., 2015; Horstkotte et al., 2011; Sibbing et al., 2011; Yoshioka, 2015), but the role in pancreatic cancer has yet remained elusive.

The human protein atlas is a brilliant tool for the screening of expression levels of various types of cancer (" Human Protein Atlas "; Ponten, Jirstrom, & Uhlen, 2008). The Kaplan-Meier-Curves of low and high expressed Txnrd2 gene in patients diagnosed with PDAC can be found in Figure III-4. Other analysis like the one of the GEPIA project shows similar results (Tang et al., 2017). Together it shows that indeed, different expression levels of Txnrd2 lead to significant differences in survival, indicating a promising and essential topic of current research.

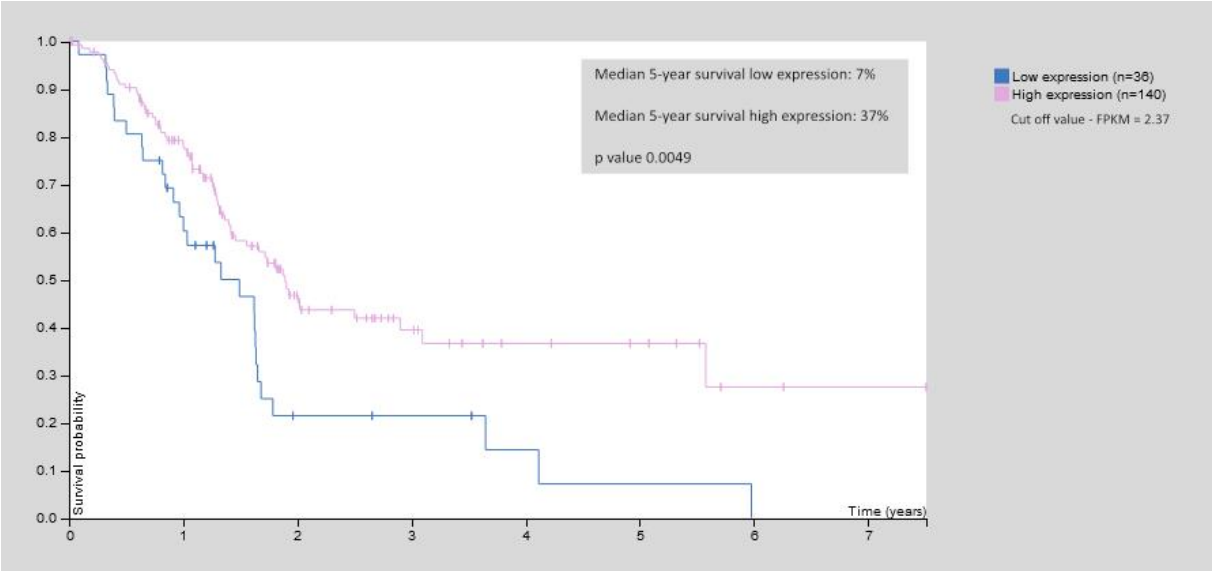

Figure III-4 Expression level of Txnrd2 influences survival in PDAC patients
Kaplan Meier curves of patients diagnosed with PDAC. Expression levels of mRNA of a total of 176 patients were obtained, cut off value was determined at FPKM = 2,37. Probability of event-free survival was observed over time. Image credit: Human Protein Atlas, available from v19.3.proteinatlas.org.

IV. Aims of this study

This study aimed to elucidate the role of mitochondrial thioredoxin reductase (Txrnd2) in *Kras^{G12D}* – driven pancreatic carcinogenesis. Firstly, *in vivo* models of *Kras$^{+/G12D}$; Txnrd2$^{\Delta Panc}$* and suitable controls (*Kras$^{+/G12D}$*) were analyzed at 12, 24 weeks and end of life.

Subsequently, a series of *in vitro* experiments were performed with pancreatic cancer cell lines explanted from *Kras$^{+/G12D}$; Txnrd2$^{\Delta Panc}$* and *Kras$^{+/G12D}$*mice:

i) Cellular proliferation, colony formation potential and cell cycle analyses were performed in order to determine the differences in tumor incidence observed
ii) To assess oxidative stress, levels of reactive oxygen species (ROS) were measured, expression of antioxidants as well as reaction towards exogenous oxidative stress monitored
iii) Mitochondrial respiration was investigated
iv) Insights into cell's signaling mechanisms were obtained, with analyzation of RAS-abundance and downstream signaling
v) Experiments involving NO - signaling were performed

All in all, we focused on *in vitro* experiments to assess the *in vivo* phenotype observed, trying to gain insight into the role of Txnrd2 in PDAC development and progression.

V. Materials and methods

V.1 Chemicals, Buffers and Supplies

V.1.1 Standard Chemicals

Chemical	Article Number	Supplying Company
Bovine Serum Albumin	A4503-100G	Sigma-Aldrich
Dimethyl Sulfoxide (DMSO)	472301-100mL	Honeywell / Riedel-de Haen
D-Mannitol	M4125-100G	Sigma-Aldrich
Dulbecco's Phosphate buffered Saline (PBS)	L 182 – 50	Biochrom AG
Ethanol, absolute	1.00983.1000	Merck
Ethylenediaminetetraacetic acid (EDTA)	E6511-100G	Sigma-Aldrich
Glycine	50046-1KG	Sigma-Aldrich
Isopropanol	109634	Merck
Magnesium Chloride	M8266-100G	Sigma-Aldrich
Methanol	8045	J. T. Baker
Nonidet P 40 Substitute	74385-1L	Sigma-Aldrich
PBS Dulbecco	L182-50	Merck
SDS granulated pure	A7249, 1000	AppliChem
Skim Milk Powder	70166-500G	Sigma-Aldrich
Sodium Chloride (NaCl)	71376-5KG	Sigma-Aldrich
Sodium Deoxycholate	D6750-500G	Sigma-Aldrich
Sodium Hydroxide (NaOH)	6771.1	Roth
Sucrose	S0389-500G	Sigma-Aldrich
Tris	5429.2	Roth
Tris-HCl	9090.3	Roth
Triton X 100	T9284-100ML	Sigma-Aldrich

Table V-1 Standard chemicals, supplying companies and article numbers

V.1.2 Standard buffers

PBS: PBS Dulbecco dissolved in deionized water (according to the manufacturer's instructions. Stored at room temperature.

TBS: 0.02 M TRIS-HCl, 0.137 M NaCl, pH 7.6 in deionized water. Stored refrigerated.

TBS-T: 0.1 % (v/v) Tween 20 in TBS. Prepared freshly.

V.1.3 Standard devices

Product	Supplying company
300 Tissue Processing Unit	Leica
Axiovert 200M	Zeiss
Centifuge 5810 R with rotor A -4-81	Eppendorf
Centrifuge 5147 R	Eppendorf
DuoMax 1300 shaker	Heidolph
Eppendorf Pipette Set Research Plus	Eppendorf
FLUOstar OPTIMA microplate reader	BMGs Labtech
Gallios™ Flow Cytometer	Beckman Coulter
Gel DocTM XR system	Bio-Rad
HeracellTM 240 incubator	ThermoFisher
Herasafe class II biological safety cabinet	ThermoFisher
LightCycler 480	Roche Diagnostics
LSRFortessa	BD
Mastercycler	Eppendorf
MICROM HM 355S microtome	ThermoFisher
Multiscan FC	ThermoFisher
NanoDrop 2000	ThermoFisher
Pipette Controllers	Falcon™
Silent Crusher M	Heidolph
Sub-Cell horizontal electrophoresis system	Bio-Rad
ThermoMixer compact	Eppendorf

Table V-2 Standard devices and supplying companies

V.2 *In Vivo* Techniques

V.2.1 Transgenic mouse lines

For this study, established genetic engineered mouse models (GEMM) of pancreatic cancer were used, as previously described by (Hingorani, Petricoin, et al., 2003). Under the Pt1fa-Promotor a Cre

– Recombinase was expressed (Pt1fa/p48 – $Cre^{ex1/+}$), leading to the expression of cre-Recombinase specific for exocrine pancreatic cells. Another mutation was in the Kras – gene, this is the mutation most commonly found in human cancers (Prior, Lewis, & Mattos, 2012), *LSL – Kras*^{G12D}. The cre-mediated point mutation results in *Kras*$^{+/G12D}$ mice – mice with an active, oncogenic *Kras*^{G12D} mutation on one allele while preserving the wildtype allele. These mice were used as control mice.

To study the loss of Txnrd2, both alleles were floxed, resulting in a Cre- mediated knockout of Txnrd2. These mice were then crossbred with *Kras*$^{+/G12D}$ mice until the Txnrd2 alleles were both floxed. The resulting animals *Kras*$^{+/G12D}$*; Txnrd2*$^{\Delta Panc}$ were used for our experimental setup.

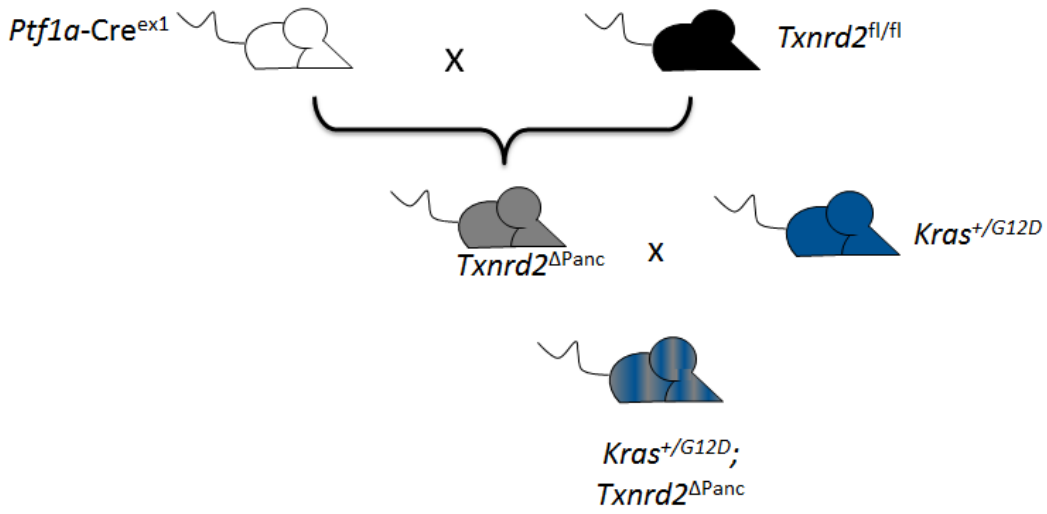

Figure V-1 Breeding strategy of **Kras$^{+/G12D}$; Txnrd2$^{\Delta Panc}$** ***mice***

V.2.2 Mouse husbandry

All animal experiments were conducted in accordance with German Federal Animal Protection Laws, under surveillance of the Institutional Animal Care and Use Committee of the Technische Universität München, Munich, Germany and approved by the Regierung von Oberbayern. The TVA under which all experiments were performed is listed under the following file number: ROB-55.2-2532.Vet_02-14-79.

The subject mice were kept in housing facilities at Zentrum für Präklinische Forschung at Klinikum rechts der Isar under specific pathogen free (SPF) conditions, according to the recommendations of the Federation of European Laboratory Animal Science Associations (FELASA). The mice were kept under 20 to 24 °C, 50 to 60% humidity, and a 12h/12 h light/dark cycle. All mice were given a standard diet (#Forti, Altromin Spezialfutter) and sterilized drinking water *ad libitum*.

At 3 weeks old the mice were separated from their parents and ears were marked. Biopsies were used for Genotyping (see DNA – Isolation, Polymerase Chain Reactionand Agarose Gel

Electrophoresis, respectively). At 8 weeks, suitable parent mice were selected for breeding, no CK animals were used for breeding. At indicated time points, animals were transferred to the laboratory, euthanized and prepped.

V.2.3 Mouse preparation and sample collection

Mice were sacrificed at indicated time points (4 / 12 / 24 weeks) or with severe impairments (abdominal enlargement, impaired social behavior, limping, impaired grooming, weight loss exceeding 15% of preceding weight). 2hrs prior to any euthanasia, the mice were intraperitoneally injected with Bromodeoxyuridine (BrdU) working solution at 10 µL/g body weight. Mice were euthanized using an Isoflurane (CP - Pharma G16B17A) – flooded chamber and consecutively exsanguinated. The following samples were collected:

Protein: Approximately 1 mm^3 piece of pancreas was snap-frozen in liquid nitrogen and stored in liquid nitrogen.

RNA: An approximately 1 mm^3 piece of pancreas was lysed in 612 µL RNA Lysis Buffer (Promega Z3051) supplemented with 2% (v/v) 1 - Thioglycerole (Promega A208B) using a Silent Crusher M (Heidolph), snap-frozen and stored at -80 °C.

DNA: An approximately 3 mm piece of the tail was taken for postmortem genotyping. It was lysed in DirectPCR-Tail Lysis Buffer (Peqgold VIAG102 – T) supplemented with 5% (v/v) Proteinase K recombinant (Roche 3115844001) at 55°C overnight under constant agitation and consecutive deactivation of Proteinase at 85°C for 45 min.

Histology: The remaining part of pancreas- along with the spleen, 2 individual lobes of the liver, a part of each lung, and the duodenum, as well as any additional macroscopically pathologic appearing organ were fixed in 4% (v/v) Paraformaldehyde (Science Service E15710 – S) in PBS at room temperature for at least 24 h. Then, the organs were dehydrated by a 300 Tissue Processing Unit (Leica) and consecutively embedded in Paraffin.

BrdU stock solution: 50 mg/µl BrdU (B5002-5G, Sigma-Aldrich) were dissolved in deionized water by adding 10 M sodium hydroxide (NaOH). Aliquots were stored at -20°C. Working solution was prepared by diluting stock solution 1 / 10 in sterile 0.9% (w/v) sodium chloride solution (Isotone Natriumchloridlösung, 5/12211753/0411 Braun).

V.2.4 Histological methods

As described in V.2.3, organ samples were embedded in Paraffin. Thereafter, the paraffin-blocks were cut into sections of 2 µm thickness with the MICROM HM 355S microtome (ThermoFisher)

and transferred to SUPERFROST PLUS microscope slides (ThermoFisher). The slides were dried at 37°C for at least 2 h before further processing.

V.2.4.1 Hemalaun-Eosin (H&E) Staining

H&E stainings were used as basic histological stainings. First, the paraffin sections from V.2.4 were deparaffinized by incubation in Roti-Histol (6640.4, Roth) for 5 min. This was repeated once again. Following this was a series of decreasing concentrations (100%, 96%, 70% and 0% (v/v)) of alcohol to rehydrate the organ structures. The slides were incubated in each concentration twice for 3 min. Then, basophilic organ structures were stained with Mayer's hemalaun solution (1.09249.2500, Merck) for 3 min and consecutive washing under tab water for 10 min. The counter-staining was performed with eosin (2C-140, Waldeck) for 3.5 min to color acidophilic structures. After staining, the slides were dehydrated by incubation in 96% (v/v) ethanol and isopropanol for 25 seconds each and incubated in Roti-Histol (6640.4, Carl Roth) twice for 2 min each. Next, the slides were mounted in pertex embedding medium (41-4012-00, Medite) and sheeted with coverslips (MENZEL-Gläser, BB024032A1, ThermoFisher).

Slides were scanned at the core facility of animal pathology of Zentrum der Präklinischen Forschung, TU München, by the lab of Katja Steiger.

V.3 *In Vitro* Techniques

V.3.1 Standard Equipment, supplies and procedures

Cell culture experiments were performed in a Herasafe class II biological safety cabinet (ThermoFisher) and cells were kept in a humidified (deionized water supplemented with Incuwater-Clean™) Heracell™ 240 incubator (ThermoFisher) at 37°C and 5% CO_2. Cell Culture dishes were purchased from Corning and BD (PRIMARIA™ Tissue Culture Flask, 353813, Corning; Corning 100 mm x 20 mm Style Dish Cell Culture, 430167, Corning; 6-Well Cell Culture Plates, 353224, BD; 24-Well Cell Culture Plates, 353047, BD), sterile, single-packed pipettes from Greiner Bio-One, pipette tips form Biozym (Safe-Seal-Tips professional) and autoclaved Pasteur pipettes from Eppendorf.

Cells were split 1 / 5 to 1 / 20 (depending on estimated growth rate) at confluency of 80 - 90% using Trypsin 0,05% + Ethylenediaminetetraacetic acid (EDTA; 25300-096, Invitrogen™). Standard medium was Dulbecco's modified Eagle Medium 4.5 g / dl D-Glucose (41965-039, gibco) supplemented with 10% (v/v) inactivated (45 min at 56 °C) and gamma-irradiated Fetal Bovine Serum (10270-106, Gibco), 1% (v/v) Pencillin-Streptomycin (15140-122, Gibco) and 1% (v/v) Minimum Esssential Medium Non-Essential Amino Acids (11140-035, Gibco). The Cells were washed with Dulbecco's Phosphate-buffered Saline (14190-144, Gibco).

V.3.2 Sample preparation

V.3.2.1 DNA – Isolation

Cells were seeded in a T25 cell culture flask on day prior. 24 h after and with 70 – 80% confluency, medium was aspirated, cells were washed with PBS and detached using Trypsin + EDTA. The cells were then pelleted (5 min at 300 rcf at room temperature), washed again with PBS and resuspended in DirectPCR Tail Lysis Buffer supplemented with Proteinase K (see V.2.3). After overnight incubation at 55 °C and consecutive proteinase deactivation for 45 min at 85 °C, genotyping and other experiments were performed (see V.4.1).

V.3.2.2 RNA – Isolation

Cells were seeded in a 10 cm – dish 48 h prior to experiment and medium was changed 24hrs before. At the time of cell collection, confluency measured approx. 60%. Cell medium was aspirated, and plates were washed twice with PBS while the flask was on ice. 612 µL of RNA Lysis Buffer supplemented with 1-Tioglycerole (see V.2.3) was added to flask and cells were detached using a cell scraper (Zellschaber S, 99002, TPP) and consecutively shock-frozen and stored at -80°C. RNA was isolated using the Maxwell Kit (AS1280, Promega) in the Maxwell 16 Instrument (Promega) according to the manufacturer's instructions. Extracted RNA was diluted in 20 – 30 µL PCR-grade water and RNA quality and quantity was measured using a NanoDrop 2000 (Thermo Fisher).

V.3.2.3 Protein – Isolation

Cells were seeded 48 h prior to experiment. Cells were treated with fresh medium, in one experiment containing 100 µM H_2O_2 for 2 h, control cells accordingly. In the remaining experiments, medium was changed 24 h prior to isolation.

At day of isolation, the confluency of cells was 60 - 80%. Medium was aspirated and plates were washed twice with PBS whilst on ice. 600 µL of freshly prepared RIPA-Buffer supplemented with 10% (v/v) Phosphatase Inhibitor Solution and 4% (v/v) Protease Inhibitor solution was added onto cell culture dish. Then cells were scraped and snap frozen.

RIPA – Buffer: 50 mM Tris Hydrochloride, 150 mM Sodium Chloride, 5% (m/v) Sodium Deoxycholate and 1% (v/v) NP-40 dissolved in 100mL deionized water

Phosphatase inhibitor solution: 1 Tablet (PhosSTOP EASYpack 04906837001, Roche) dissolved in 1 mL of deionized water

Protease inhibitor solution: (cOmplete Tablets Mini EASYpack, 04693124001, Roche) dissolved in 2 mL of deionized water

V.3.2.4 Isolation of Mitochondria

Mitochondria were isolated for enriched substrate for Western Blot of Txnrd2 protein. The protocol used (Clayton & Shadel, 2014) was adapted as following: Cells were grown in a 10 cm cell culture

dish until confluency reached 90%. Plate was washed twice with ice-cold PBS and scraped into an ice-cold Falkon Tube. Tubes were centrifuged at 500 rcf for 5 min at 4 °C and resuspended in 5.5 mL of ice-cold RSB Hypo Buffer. Cells were allowed to swell for 5 min, then membranes were destroyed using a 15 mL Dounce homogenizer. 4 mL of ice-cold 2.5X MS Homogenization Buffer was added and gently mixed. For differential centrifugation, tubes were firstly centrifuged at 1300 rcf for 5 min at 4 °C, then supernatant was pipetted into a new tube, volume was refilled with 1X MS Homogenization Buffer up to 15 mL and centrifugation was repeated twice. The supernatant was then pipetted into yet another tube and mitochondria were pelleted at 15000 rcf for 15 min at 4°C. Pellet of mitochondria was suspended in RIPA Buffer (see V.3.2.3) supplemented with Protease- and Phosphatase inhibitor, respectively.

RSB Hypo Buffer: 10 mM Sodium Chloride, 1.5 mM Magnesium Chloride, 10 mM Tris-HCl (pH 7.5). Stored at 4 °C.

2.5X MS Homogenization Buffer: 525 mM Mannitol, 175 mM Sucrose, 12.5 mM Tris-HCl (pH 7.5) and 2.5 mM EDTA in deionized water. Stored at 4 °C.

1X MS homogenization Buffer: 1 / 2.5 (v/v) of 2.5X MS Homogenization Buffer diluted in deionized water. Prepared freshly.

V.3.3 Standard Assays

V.3.3.1 Proliferation Assays

Proliferation assays were done with CyQuant Reagent (C7026, Thermo Fisher Scientific). Briefly, the provided dye binds double-stranded DNA and changes fluorescence, thus giving a linear fluorescent value for DNA amount and cell number, respectively. Cells were seeded in duplicates or triplicates in bottom-clear black 96 Well plates (costar 3603, Corning Incorporated) at a density of 1000 cells / well in standard cell culture medium. Blank wells without cells were always included. After 4h, t0-plate was washed once with PBS, frozen and stored at -80 °C whilst medium with respective conditions was changed. At time points 24, 48, 72 and 96 hours, plates were washed and stored at -80°C.

Assay was performed with all plates of the experiment simultaneously. Fluorescence was measured with a FLUOstar OPTIMA microplate reader (BMGs Labtech), with excitation wavelength of 480 nm and a filter of 520 nm for detection. Blank values were subtracted, and the duplicates / triplicates were averaged and related to t0 values to eradicate possible seeding errors.

V.3.3.2 Colony Formation Assays

Cells were seeded at a density of 100 cells / well in a 6 well plate. 4 h after seeding, Medium was changed. Colony Formation was examined daily, and on day 7 cells were fixed by washing once with PBS and adding 3 (1) mL of fixation solution, consecutive incubation at gentle agitation at room temperature for 30 min and multiple washing steps (tab water), until clear appearance of colonies. Colonized area was analyzed with Fiji Software.

Fixation solution: 6% (v/v) Glutaraldehyde (25%, 3778.1, Roth) and 0.5% (w/v) Crystal Violet (C3886-100G; Sigma-Aldrich) in deionized water. Stored at room temperature.

V.3.4 Flow Cytometry Experiments

V.3.4.1 Cell Cycle Flow Cytometry

Protocol was adapted from (abcam.com). Cells were seeded 2 days prior to experiment. Medium was changed 24h prior to experiment. Cells were detached using Trypsin 0,05% + EDTA and washed twice with PBS containing 1 mM EDTA. Cells resuspended in 500 µL were fixed by adding dropwise 5 ml of ice-cold 70% (v/v) Ethanol in deionized water and incubating for 30 min at 4°C. Afterwards, the cells were washed twice with PBS + EDTA and resuspended in 200 µL of staining solution. Samples were then scanned with the BD LSRFortessa (wavelengths of excitation: 585 nm, of emission: 615 nm) and analyzed using the FlowJo Software (Version v.X 0.8) by gating (Area vs. Width to exclude non-single cells) and auto-analysis Cell Cycle Tool.

PBS + EDTA: 9.55 g / L PBS Dulbecco was solved in 1 L of deionized water. 5 mM EDTA stock solution in deionized water was prepared by alkalizing with NaOH. EDTA was diluted to a final concentration of 1 mM in PBS. Stored at room temperature.

Staining solution: 2 mg/mL RNAse A (1007885, Qiagen), 200 µL of 1 mg/mL Propidium Iodide solution (P4864, Sigma-Aldrich) diluted in 10 mL of PBS supplemented with 0,1% (v/v) Triton X 100 and 1mM EDTA. Prepared freshly.

V.3.4.2 DAF FM Staining

Protocol was adapted after (Chris D. St. Laurent). Cells were seeded 24 h prior to any experiment. Cells were trypsinized, resuspended and washed with washing solution twice, centrifugation was persistently performed at 300 rcf for 5 min at room temperature. Positive controls (Nor-3 as NO donor, final concentration of 100 µM) and negative controls (PTIO as NO scavenger, final concentration of 1 mM), as well as unstained controls were done in each experiment. Cells were incubated with staining solution at 37°C for 30 min in the dark. Cells were then centrifuged, washed twice with washing solution and finally resuspended in washing solution, measured in a BD LSRFortessa (wavelengths of excitation: 500 nm, of emission: 515 nm) and analyzed using the FlowJo Software (Version v.X 0.8) by quantification of FITC-fluorescence.

Washing solution: Dulbecco's PBS supplemented with 1mM EDTA (see above) and 1% (v/v) Fetal Bovine Serum (see V.3.1). Prepared freshly.

Positive control – stock solution: 20 mM of Nor-3 ((±)-I-4-Ethyl-2-[I-hydroxyimino]-5-nitro-3-hexeneamide, ALX-430-011-M005, Enzo) dissolved in DMSO, stored at -20 °C.

Negative control – stock solution: 40 mM PTIO (2-Phenyl-4,4,5,5-tetramethylimidazoline-1-oxyl 3-oxide, P5084, Sigma-Aldrich) dissolved in deionized water, stored at -20 °C.

Staining solution: Washing solution + 10 µM DAF-FM DA (ab145295, abcam; stock solution 1 mM in DMSO stored at -20 °C). Prepared freshly.

V.3.4.3 Carboxy-H2DCFDA

Carboxy – H2DCFDA is a quantitative staining for ROS. Cells were seeded 24 h prior to experiment in 6 Well Plates and positive controls with 100 µM H_2O_2 treatment (2 h at 37 °C) were included. Cells were detached using Trypsin + EDTA (see above) and washed twice with PBS. Cells were stained with 50 µM of H2DCFDA (C400, Life Technologies) dissolved in PBS for 30 min at 37 °C. Cells were then measured with a Gallios™ Flow Cytometer (Beckman Coulter) with wavelengths of excitation of 485 nm and emission of 535 nm. Data was analyzed with FlowJo software (see above).

V.3.5 Immunofluorescent Stainings

V.3.5.1 MitoTracker Staining

Mitochondria were visualized with the MitoTracker™ Green FM dye (M7514, Invitrogen™). Cells were seeded on an 8 – Well Cover Slip (8-Well detachable Tissue Culture Chambers, 94.6170.802, Sarstedt) 24hrs prior to experiment. On the day of the experiment, the chamber slide was washed with PBS, then incubated with a 1 mM solution of MitoTracker™ in standard cell culture medium (see V.3.1) for 30 min at 37 °C. Chamber slide was then washed twice with PBS and stained cells were mounted with ProLong™ Gold antifade reagent with DAPI (P36931, 29nvitrogen™) and a cover slip (see V.2.4.1) was attached with regular nail polish.

Pictures were taken with a Axiovert 200M (Zeiss) and analyzed with Affinity Designer Software.

V.3.6 Cellular Respiration Experiments

V.3.6.1 Seahorse XF Analysis

Cells were seeded 24 h before measurement. 10 000 cells in 80 µL of Medium were seeded per well in an Agilent Seahorse Xfe96 Cell Culture Microplate and a regular 96 Well Plate (96-Well Plate, 353072, BD) for protein standardization. Plates were transferred to Garching Hochbrück (Lab of Martin Jastroch, HelmholtzZentrum München) and cartridge (Agilent Seahorse Xfe96 Extracellular Flux Assay Kit) was hydrated overnight. The following day, Medium was exchanged by adding 180 µL / well of Seahorse Medium (Agilent Seahorse XF Base Medium (0 mM Glucose) supplemented with 27.8 mM Glucose). The following substances were added during the measurement:

Medium	Substance	Final Concentration
Seahorse	Oligomycin	2 µg/mL
Seahorse	FCCP	1 µM
Seahorse	Pyruvat	5 mM
Seahorse	Rotenon	25 µM
Seahorse	AntimycinA	25 µM
Seahorse + 2-Deoxy Glucose		1 M

Table V-3 Additives with influence on cellular respiration used in the Seahorse – Assay

The medium of the second plate was aspirated, the plate was washed with PBS once and the cells were then lysed by adding 5 µL of RIPA Buffer supplemented by Protease and Phosphatase inhibitor, respectively, and storing the plate at – 80 °C. Protein amount was thus measured with the Pierce™ BCA Assay Kit (Thermo Fisher Scientific; 23225). Values were then adjusted as per protein content, following a subtraction of basal oxygen consumption (after addition of Antimycin A and Rotenon, red area).

Seahorse measurements allow assumptions on oxygen consumption, thus mitochondrial respiration, thus oxygen-dependent ATP production and spare capacity.

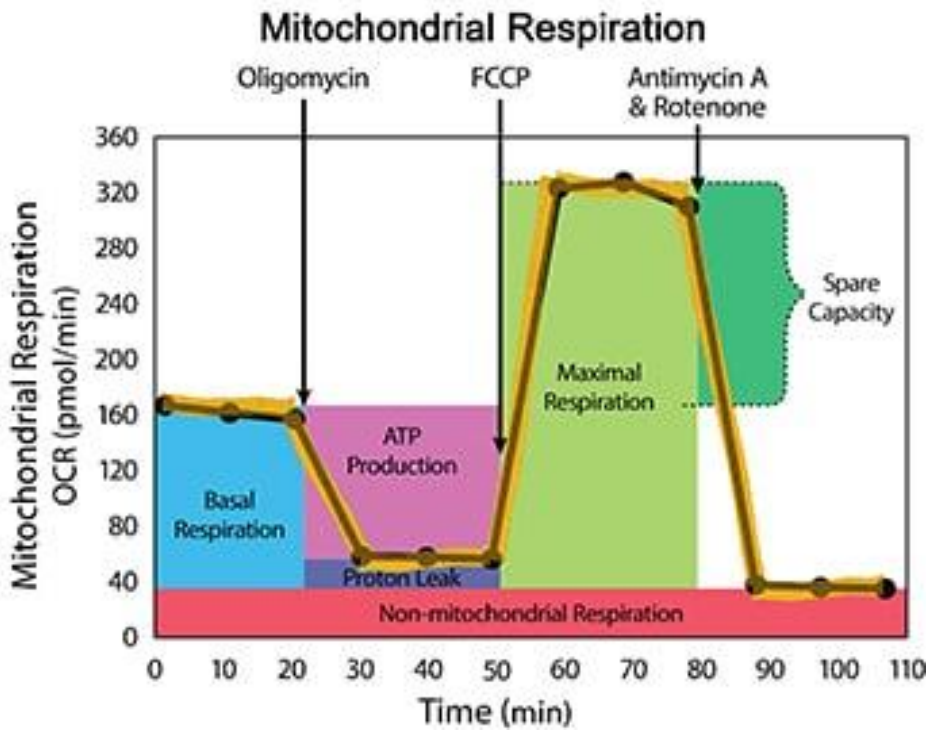

Figure V-2 Mitochondrial Respiration measurements
Oxygen consumption rates are measured under basal conditions and with the sequential addition of Oligomycin, FCCP, and Antimycin A with Rotenone (for concentrations see above). The obtained values allow determination of basal respiration, oxygen used of ATP production and upkeeping of proton leak, as well as maximal respiration and,

consequently, spare capacity.

V.4 Molecular Biological Methods

V.4.1 DNA – based methods

V.4.1.1 Polymerase Chain Reaction

Polymerase Chain Reaction (PCR) was performed to determine genotypes of 3 – week old mice. For each reaction, 5 µL of Red Taq mix (REDTaq ReadyMix™ PCR Reaction Mix, R2523, Sigma-Aldrich) were added to 6 µL PCR-grade water, 0.5 µL of 10 µM Primer Mix (see Table V-4) and 0.5 µL of DNA (see DNA – Isolation). Cre-Recombinase was tested twice, with general cre – Primers (giving signal for all cre recombinases in the mouse husbandry) and once with specific p48 cre primers. Primers were obtained from Eurofins genomics. One positive control (repeatedly positively tested DNA) and one negative control (no DNA) was performed with each tested gene.

Targeted gene	**Primer Sequences**	**Product size – mutated allele**	**Product Size – wildtype allele**
Cre – Recombinase	1. ACC AGC CAG CTA TCA ACT CG 2. TTA CAT TGG TCC AGC CAC C 3. CTA GGC CAC AGA ATT GAA AGA TCT 4. GTA GGT GGA AAT TCT AGC ATC ATC C	199 bp	324 bp
P48 Cre - Recombinase	1. GTC CAA TTT ACT GAC CGT ACA CCA A 2. CCT CGA AGG CGT CGT TGA TGG ACT GCA	1155 bp	600 bp
$Kras^{G12D}$	1. CAC CAG CTT CGG CTT CCT ATT 2. AGC TAA TGG CTC TCA AAG GAA TGT A 3. CCA TGG CTT GAG TAA GTC TGC	180 bp	280 bp
$Txnrd2^{floxed}$	1. CAG GTC ACT AGG CTG TAG AGT TTG C 2. ATG TCC CAG TGT ACT TAT GAT GAA TC	181 bp	133 bp

Table V-4 Primer sequences and product sizes for genotyping – PCR

V.4.1.2 Agarose Gel Electrophoresis

Ethidium-supplemented agarose gels were made using the Sub-Cell horizontal electrophoresis system (Bio-Rad). 2% (w/v) of Agarose (840004, Biozym) was dissolved in TAE Buffer by heating the solution. After a cooling period of approximately 10 min, 0.05% (v/v) of Ethidium Bromide (1%, 2218.2, Roth) was added and gels were casted.

Probes from Polymerase Chain Reaction were loaded onto gel, together with DNA Ladder-Mix (25-2040, Peqlab). Gels were run with constant voltages of 100 – 130 V (depending on gel length) and gels were photographed using the Gel Doc™ XR system (Bio-Rad).

TAE Buffer: 40 mM TRIS, 2 mM Titriplex III, 20 mM acetic acid, glacial in deionized water. Stored at room temperature.

V.4.1.3 Mitochondrial Copy Number Assay

Mitochondrial copy number was assessed as previously described by (Rooney et al., 2015). Primers were designed to amplify three individual stretches of mitochondrial DNA (see Table V-5). Amplicon Sizes were kept short, so that mitochondrial mutations and resulting interference of DNA – Polymerase were kept to a minimum.

DNA obtained as in V.3.2.1 described was measured in a NanoDrop 2000 (Thermo Fisher). Then a Polymerase Chain Reaction was performed, by adding LightCycler 480 SYBR Green 1 Master (10559520, Roche) with 5 µM of Primer Mix (see Table V-5) and 16 ng of DNA.

As a control gene for nuclear DNA content, Cyclophilin A was used and every reaction was duplicated.

The PCR was thus run in a LightCycler 480 (Roche Diagnostics) according to the program described in V.4.2.1.

The obtained C_P Values were averaged and, individually for each cell line, the relative mitochondrial DNA content was calculated as following:

$$Relative\ mitochondrial\ DNA\ content = \frac{E_{mito}\hat{}\ C_{P\ mito}}{E_{nuclear}\hat{}CP_{nuclear}}$$

Equation 10

The three gained values for the three individual mitochondrial DNA stretches were normalized to $Kras^{+/G12D}$ control cell lines and then averaged.

Target Gene	Primer Sequence	Amplicon Size	Primer Efficiency
Mito A	1. 5'-CCGTGAACCAAAACTCTAATCA-3' 2. 5'-CATTTTCAGTGCTTTGCTTTG-3'	89 bp	1.916
Mito B	1. 5'-TTCTATGGCCAATGCTCTGA-3' 2. 5'-CAATGGGCATAAAGCTATGG-3'	55 bp	1.945
Mito C	1. 5'-TGATGGTACGGACGAACAGA-3' 2. 5'-GATGTCTCCGATGCGGTTAT-3'	72 bp	1.960
Cyclophilin A	1. 5'-ATGGTCAACCCCACCGTG-3' 2. 5'-TTCTGCTGTCTTTGGAACTTTGTC-3'	99	1.893

Table V-5 Primers with sequences, amplicon sizes and efficiencies used for mitochondrial copy number assay

V.4.2 RNA – based methods

V.4.2.1 Quantitative Reverse Transcription-Polymerase Chain Reaction (qRTPCR)

qRT-PCR was performed to determine relative levels of mRNA by initiating reverse Transcriptase of RNA to DNA, followed by linear amplification and visualization of double-stranded DNA content. RNA was previously isolated (see RNA – Isolation) and reverse Transcription reaction was started by mixing 1 / 24 vol of Random Primers (C118A, Promega), 1 / 12 vol of 10 mM dNTP Mix (18427-013, invitrogen™) and 1 µg DNA of acceptable quality ($A_{260/280}$ = 2.0 ± 0.2 and $A_{260/230}$ = 2.2 ± 0.3), heated to 65 °C for 5 min and put on ice. 1 / 5 vol of First Strand Buffer (of SuperScript II Reverse Transcripase system; 18064-014, invitrogen™) and 0.1 M DTT (Y00147, invitrogen™) was added and solution was mixed at 25 °C for 2 min. Then, 1/25 vol of SuperScript II Enzyme was added, and reaction was started with 25 °C for 10min, 42 °C for 50 min and 70 °C for 15 min (all in a Mastercycler, Eppendorf).

DNA mix was 1 / 20 vol diluted in PCR-grade water and used for Polymerase Chain Reaction together with 1/2 vol of LightCycler 480 SYBR Green 1 Master (10559520, Roche) and 0.25 µM of Primer Mix. Reaction was performed in a LightCycler 480 (Roche Diagnostics). The PCR program consisted of an initial denaturation (95 °C, 10 min), 40 cycles of denaturation (95 °C, 20 sec), annealing (52 °C, 30 sec), and elongation (72 °C, 25 sec) with single acquisition, followed by a melt analysis consisting of 65 to 97 °C temperature gradient at a ramp rate of 0.11 °C/s with acquisition every 5 °C. Melting curves were obtained to confirm quality of primers, thus showing one specific PCR product. Filters used were 465 nm for excitation and 510 for emission.

Primers were obtained from Eurofins Genomics and tested for efficiency by 1 / 2 (v/v) serial dilutions of sample mix. Primers, efficiencies and amplicon sizes are shown in table.

Target gene	Primer Sequence	Amplicon Size	Primer Efficiency
Cyclophilin A	1. 5'-ATGGTCAACCCCACCGTG-3' 2. 5'-TTCTGCTGTCTTTGGAACTTTGTC-3'	99	1.893
Kras	1. 5'-GTCTCTTGGATATTCTCG -3' 2. 5'-CCTTGCTAACTCCTGAGCC -3'	254	1.502
Nras	1. 5'-TACAAACTGGTGGTGGTTGGAGCA-3' 2. 5'- ACTGGTCTCTCATGGCACTGTACT -3'	182	1.999
Hras	1. 5'-AAG CTT GTG GTG GTG GGC GCT AAA GGC -3' 2. 5'-CTT TCA CCC GCT TGA TCT GCT CCC TGT ACT -3'	274 bp	1.720
SOD 1	1. 5'CGGTGAACCAGTTGTGTTGT-3' 2. 5'-CAGGTCTCCAACATGCCTCT-3'	180	1.794

Glutathione Peroxidase 1	1. GTTCGGACACCAGGAGAATG-3' 2. 5'- CATTCCGCAGGAAGGTAAAG-3'	155	1.772
Glutathione Peroxidase 4	1. AGTACAGGGGTTTCGTGTGC-3' 2. 5'-GGCTGCAAACTCCTTGATTT -3'	195	1.703
Catalase	1. AGCGACCAGATGAAGCAGTG-3' 2. 5'-TCCGCTCTCTGTCAAAGTGTG -3'	181	1.631

Table V-6 Primer sequences with efficiencies, whether these are exon spanning and their amplicon sizes of primers used for qRT-PCR

Cyclophilin A mRNA expression was consistently used as a control, analysis of experiment was done with LightCycler 480 software (version 1.5.0.39, Roche Diagnostics).

V.4.3 Protein – based methods

V.4.3.1 Western Blot Analysis

Protein concentration was measured by the Pierce™ BCA Assay Kit (Thermo Fisher Scientific; 23225). Briefly, Cu^{2+} is reduced to Cu^{1+} by proteins in an alkaline medium. This leads to a linear change of absorbance at 562 nm, measured at a Multiscan FC (Thermo Scientific). Probes were diluted to equal concentrations with RIPA buffer supplemented with protease and phosphatase inhibitor. 1 / 6 vol 6x SDS sample buffer was added and samples were denatured for 5 min at 95 °C. SDS – Polyacrylamide Gel Electrophoreses gel preparation and running were performed with the mini-PROTEAN Tetra Cell system (Bio-Rad). Equal amounts of protein samples were added in the gel, the Fermentas Spectra™ Multicolor Broad Range Protein Ladder (11862124, ThemoFisher) was used as a marker and gels were run at 80 V in the stacking and 150 V in the separating gel.

Afterwards, proteins were transferred onto a Protran BA83 or BA85 Nitrocellulose Blotting Membrane (10402495 or 10401197, GE Healthcare) – depending on size of targeted protein – at 100 V for 1 – 2 h (also depending on protein size). Membrane was washed with TBS-T and blocked with 5% (w/v) Milk Powder dissolved in TBS-T for 1 h at room temperature. Afterwards, membranes were briefly washed with TBS-T and then incubated over night with the following antibody solutions:

Antibody:	**Distributing company:**	**Product number:**	**Dilution:**	**Dissolved in:**	**Antibody made in species:**
Anti-Erk 1,2	Cell Signalling	4695S	1 / 1000	5% (w/v) Milk in TBS-T	Rabbit
Anti-SOD 2	ADI	ADI-SOD-110-F	1 / 1000	5% (w/v) Milk in TBS-T	Rabbit

Anti-Hif-1α	Santa Cruz	Sc-10790	1 / 200	5% (w/v) BSA in TBS-T	Rabbit
Anti-Ras^{G12D}	Cell Signalling	14429	1 / 1000	5% (w/v) Milk in TBS-T	Rabbit
Anti-Kras	abcam	180772	1 / 1000	5% (w/v) Milk in TBS-T	Rabbit
Anti-phospho Braf	Cell Signalling	2696	1 / 1000	5% (w/v) BSA in TBS-T	Rabbit
Anti-Braf	Santa Cruz	Sc-5284	1 / 200	5% (w/v) Milk in TBS-T	Mouse
Anti-phospho MEK	Cell Signalling	9154	1 / 3000	5% (w/v) Milk in TBS-T	Rabbit
Anti-MEK	Cell Signalling	4694	1 / 1000	5% (w/v) Milk in TBS-T	Mouse
Anti-phospho Erk	Cell Signlling	4376S	1 / 1000	5% (w/v) BSA in TBS-T	Rabbit
Anti-phospho eNOS (Ser1177)	Cell Signalling	9571	1 / 1000	5% (w/v) BSA in TBS-T	Rabbit
Anti-eNOS	abcam	76198	1 / 1000	5% (w/v) Milk in TBS-T	Mouse

Table V-7 Primary antibodies used for Immunoblot Analysis with their distributing companies, product numbers, dilutions and host species

The following day, membranes were washed 3 times for 5 min at room temperature with TBS-T and then incubated with HRP-conjugated secondary antibody for 1h at room temperature:

Antibody against:	**Distributing company:**	**Product number:**	**Dilution:**	**Dissolved in:**	**Antibody made in species:**
rabbit	GE Healthcare	NA934-1ML	1 / 5000	5% (w/v) Milk in TBS-T	goat
mouse	GE Healthcare	NA931-1ML	1 / 5000	5% (w/v) Milk in TBS-T	goat

Table V-8 Secondary antibodies used for Immunoblot- Analysis with their distributing companies, product numbers, dilutions and host species

Membranes were again washed with TBS-T three times for 5 min each and secondary antibodies were then detected with Amersham ECL Western Blotting Detection Reagent (RPN2106, GE Healthcare) on ChemiDoc™ XRS+ (Bio-Rad). Western Blot bands were analyzed with Fiji Software and values were averaged for each cell line, except for RAS experiments, to highlight the heterogeneity of one Txnrd2-deficient cell line.

6 x SDS Sample buffer: 7 mL / 10 mL Stacking Gel buffer supplemented with 30% (v/v) glycerol, 10% (w/v) SDS, 0.012% (w/v) bromophenol blue (B0126-25G, Sigma-Aldrich)) and 0.6 M DTT (D9163-5G, Sigma-Aldrich) in deionized water. Stored at -80 °C in single-use aliquots.

4x Separation Gel buffer: 1 M TRIS-HCl, 0.4% (w/v) SDS, pH 8.8. Buffer was kept at 4°C.

Separation Gel: 8-12% (w/v) polyacrylamide (Rotiphorese Gel 30, 3029.2, Carl Roth), 6 µL / 1 mL APS (A3678-26G, Sigma-Aldrich; stock solution: 10% (w/v)), 2.4 µL/1 mL TEMED (T9281-100ML, Sigma-Aldrich), 1/4 vol Separation Gel buffer in deionized water. Prepared freshly.

4 x Stacking Gel buffer: 0.5 M TrisHCl, 0.4% (w/v) SDS, pH 6.8. Buffer was kept at 4 °C.

Stacking Gel: 4% (w/v) polyacrylamide (Rotiphorese Gel 30, 3029.2, Carl Roth), 10 µL/1 mL APS (A3678-26G, Sigma-Aldrich; stock solution: 10% (w/v)), 2 µL/1 mL TEMED (T9281-100ML, Sigma-Aldrich), 1/4 vol Stacking Gel buffer in deionized water. Prepared freshly.

5 x SDS-PAGE buffer: 0.125 M TRIS, 0.96 M glycine and 0.5% (w/v) SDS in deionized water. Buffer was kept at 4 °C.

10 x Transfer buffer: 0.25 M TRIS and 1.38 M glycine in deionized water. Buffer was kept at 4 °C.

1 x Transfer buffer: 20% (v/v) methanol, 1/10 vol 10 x Transfer buffer in deionized water. Prepared freshly.

V.4.3.2 RAS- activity assay

RAS activity was assessed by pulldown of active, GTP-bound RAS. Merck 17-218 Ras Activation Assay Kit was used.

Cells were grown for 48 h in 10 cm dishes. Medium was changed 2 h prior to experiment. All steps were performed on ice, according to manufacturer's instruction. For protein content adjustment, BCA assay (see above) was performed.

V.5 Statistical Analysis

Statistical analyses were performed with the GraphPad Prism Software, Version 7. Routinely, a two-sided student's t-test was used with each value representing the mean of 3 individual experiments. A p-value of less than 0.05 were considered significant.

VI. Results

VI.1 Thioredoxin reductase 2 deficiency leads to more precursor lesions, but fewer tumors

To investigate the impact of a deficiency in mitochondrial thioredoxin reductase (Txnrd2), *Kras*$^{+/G12D}$ mice with and without pancreatic knockout of *Txnrd2* were examined at 12 and 24 weeks (i.e., young and middle age, respectively). Although normal development was observed up to the indicated time points, we observed significant differences in the histology of mice pancreata at 12 weeks of age (Fig. VI-1 A): While *Kras*$^{+/G12D}$ animals had a largely normal pancreas with some preneoplastic lesions (PanINs), pancreata from *Kras*$^{+/G12D}$*; Txnrd2*$^{\Delta Panc}$ mice consisted of mostly dysplastic and pre-cancerous tissue. This effect equalized at 24 weeks of age between the groups (Fig. VI-1 D). Notably, when tumor incidence was analyzed in animals reaching endpoint criteria, the opposite effect was observed: Despite the significantly increased number of PanINs in *Kras*$^{+/G12D}$*; Txnrd2*$^{\Delta Panc}$ pancreata, these mice developed fewer tumors than *Kras*$^{+/G12D}$ mice (Fig. VI-2).

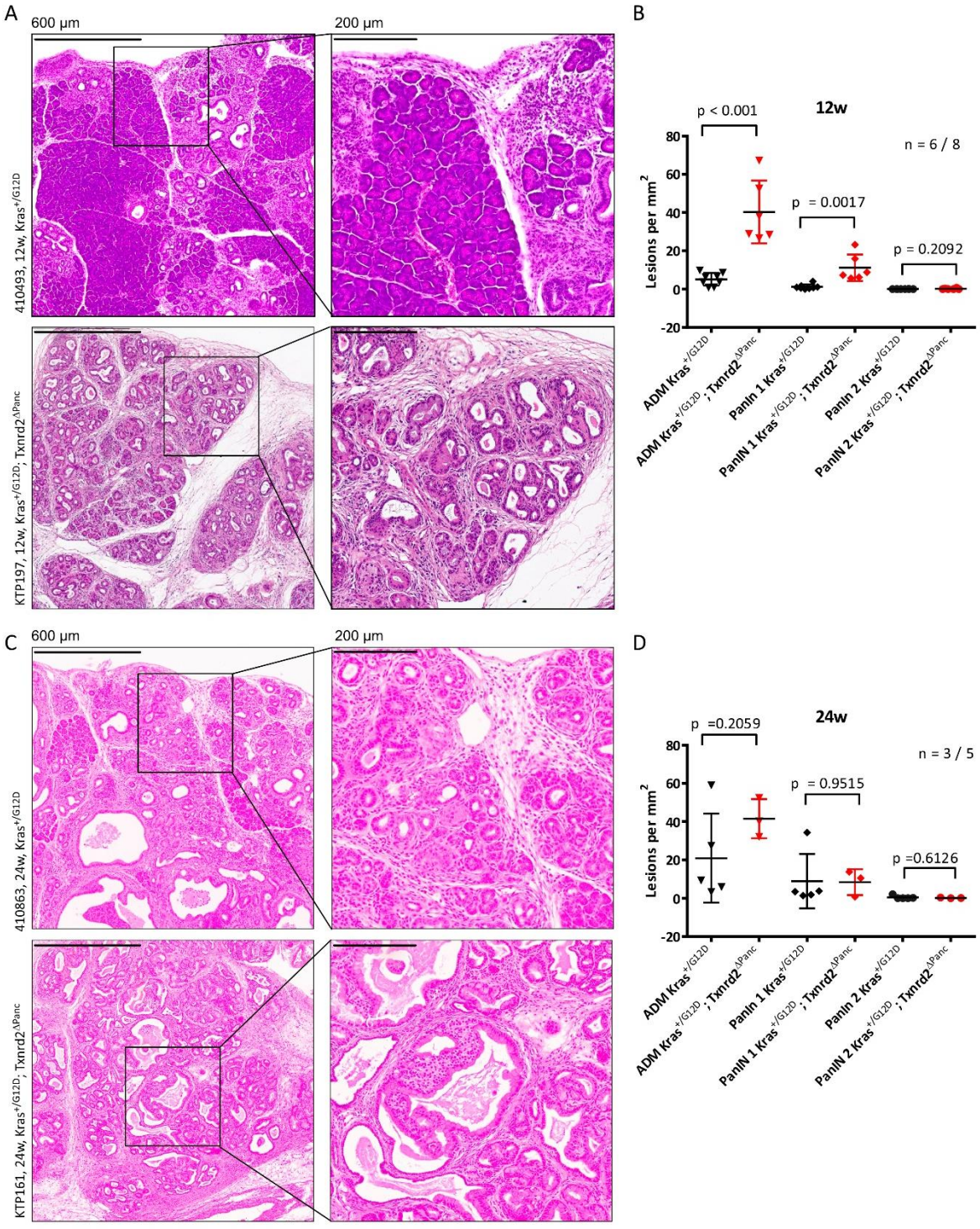

Figure VII-1 Pancreatic histology of 12- and 24-week-old **Kras$^{+/G12D}$** ***and*** **Kras$^{+/G12D}$; Txnrd2$^{\Delta Panc}$** ***mice***
Representative images of hematoxylin & eosin-stained pancreata from 12-week-old (A) and 24-week-old (C) Kras$^{+/G12D}$ *mice with and without pancreatic* Txnrd2 *deletion. Pancreatic sections of 6-8 animals of each genotype at 12 weeks and of 3-5 animals of each genotype at 24 weeks were scored (B, D), and lesions for which the appropriate score was*

uncertain were discussed with a trained animal pathologist. Data are represented as mean +/- SD. There were no PanIN 3 lesions or invasive cancer in scored pancreata.

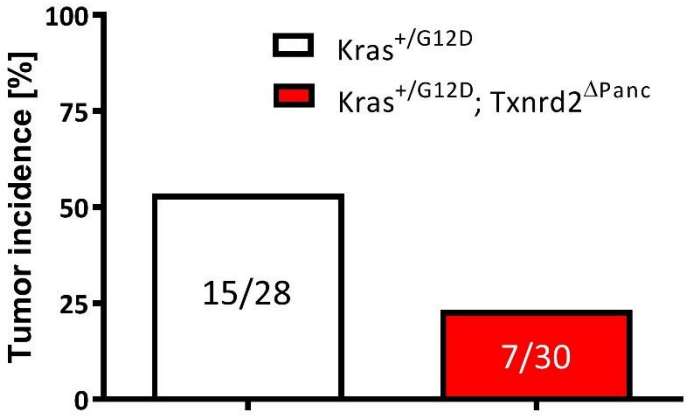

Figure VI-2 Tumor incidence of* Kras$^{+/G12D}$ *and* Kras$^{+/G12D}$; Txnrd2$^{\Delta Panc}$ *animals
Tumor incidence of mice that died naturally or were euthanized due to reaching endpoint criteria (abdominal enlargement, impaired social behavior, limping, impaired grooming, weight loss exceeding 15% of preceding weight, etc.). Pancreata and primary metastatic sites (liver, lung, retroperitoneum) were screened macroscopically and microscopically by a trained gastroenterologist (Dr. med Henrik Einwächter).

VI.2 Txnrd2 deficiency affects mitochondrial copy number and ROS levels, but not expression of antioxidants or H_2O_2 sensitivity

To examine the latency of tumor onset in *Kras$^{+/G12D}$; Txnrd2$^{\Delta Panc}$* mice, levels of Txnrd2 were assessed by western blot in cell lines extracted from *Kras$^{+/G12D}$; Txnrd2$^{\Delta Panc}$* and *Kras$^{+/G12D}$* mice (Fig. VI-3). We saw that the cell lines extracted from our genetically engineered mouse model show indeed no Txnrd2 expression.

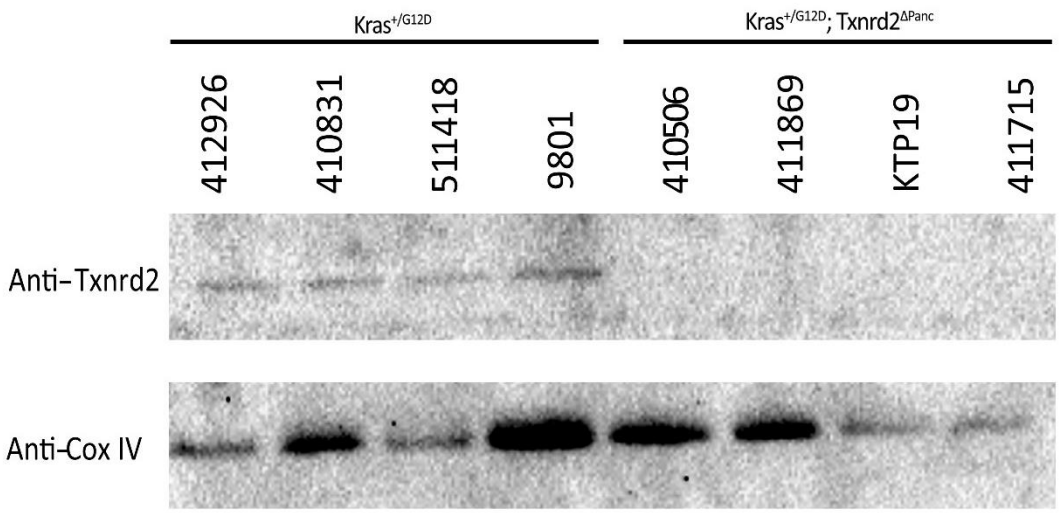

Figure VI-3 Western blot analysis of conditional Txnrd2 knockout
Levels of Txnrd2 were examined in cell lines derived from Kras$^{+/G12D}$ and Kras$^{+/G12D}$; Txnrd2$^{\Delta Panc}$ mice after mitochondrial isolation. Cox IV was used as a mitochondrial reference protein. Different levels of Cox IV were observed due differences in the efficacy of mitochondrial isolation. Gels used were 10% and membranes were 0.2 µm nitrocellulose.
Cox IV = Cytochrome c oxidase subunit 4

We first examined the impact of the absence of this enzyme on oxidant homeostasis. As Txnrd2 is a mitochondrial enzyme, we hypothesized that deficiency would affect the structure and quantity of mitochondria in Txnrd2 deficient cells. Indeed, we observed an increase in mitochondrial content in cells lacking Txnrd2 by both immunofluorescent staining (Fig. VI-4 A) and analysis of mitochondrial DNA (mtDNA) content (Fig. VI-4 B). Next, we measured levels of reactive oxygen species (ROS) in these cell lines by H2DCFDA staining. We saw a clear increase in ROS in cells lacking Txnrd2, pointing toward a necessity for Txnrd2 in the maintenance of the oxidant/antioxidant balance (Fig. VI-5).

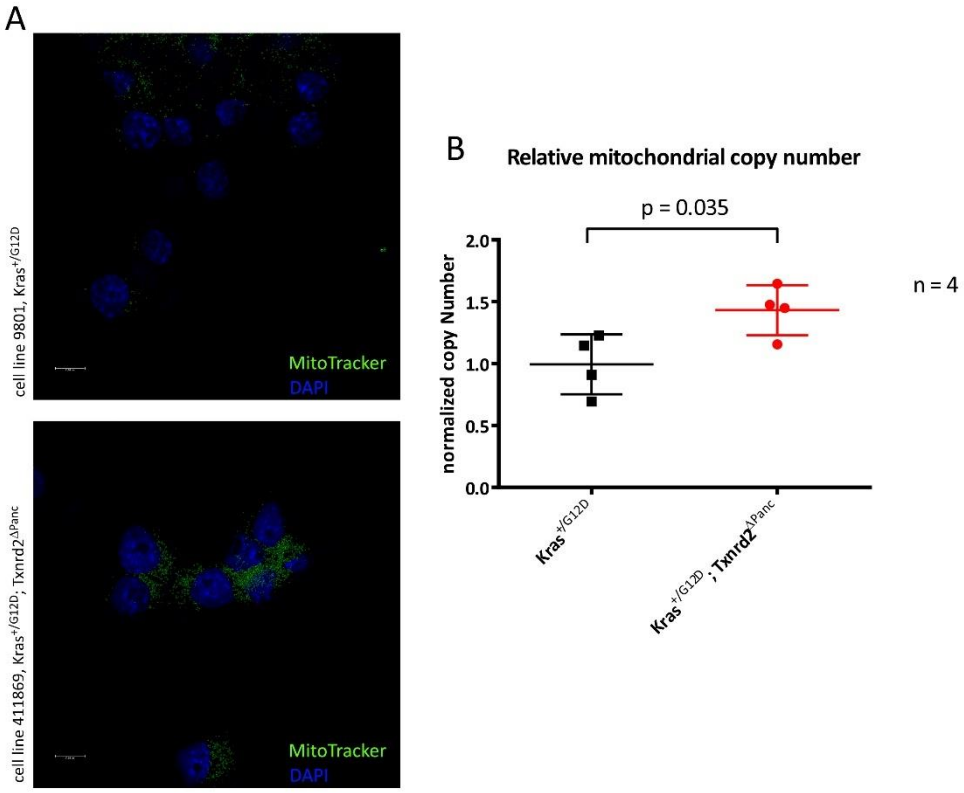

Figure VI-4 Mitochondrial content in cell lines derived from* Kras$^{+/G12D}$ *and* Kras$^{+/G12D}$; Txnrd2$^{\Delta Panc}$ *mice
(A) Mitochondrial content was assessed by MitoTracker staining and co-staining of cell nuclei with DAPI. Images of representative cell lines are shown.
(B) Mitochondrial copy number was assessed by quantitative real-time polymerase chain reaction of cell line DNA. Two individual DNA stretches were tested in three individual experiments, normalized to Kras$^{+/G12D}$ *samples, and averaged to generate one value for each cell line.*
Data are expressed as means ± SD and Student's t-test was used for statistical analysis.

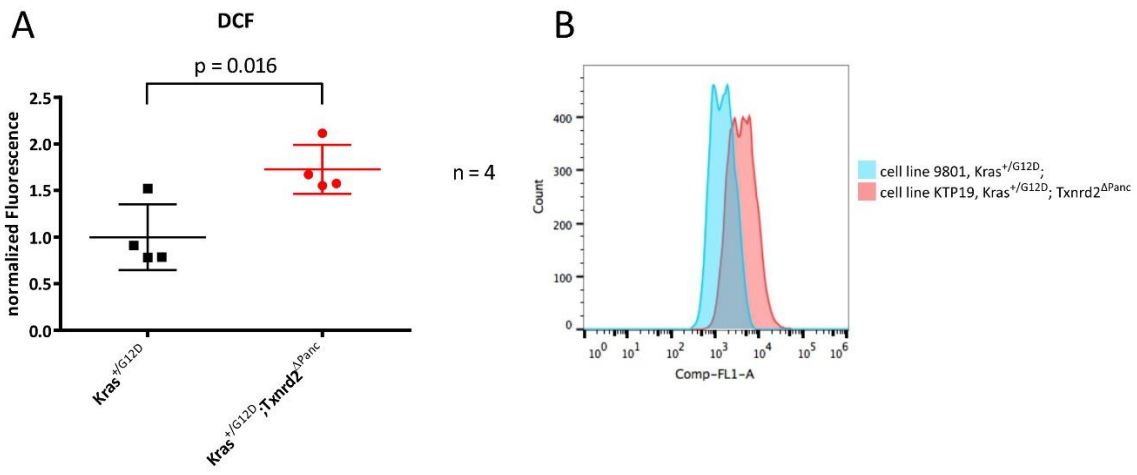

Figure VI-5 ROS levels in* Kras$^{+/G12D}$ *and* Kras$^{+/G12D}$; Txnrd2$^{\Delta Panc}$ *cell lines
(A) H2DCFDA staining was performed to measure the amount of reactive oxygen species in Kras$^{+/G12D}$ *and* Kras$^{+/G12D}$; Txnrd2$^{\Delta Panc}$ *cell lines by flow cytometry. Unstained controls were subtracted from fluorescent values to adjust for potential autofluorescence. Two individual experiments were performed, and values were averaged for each cell line. Data are expressed as means ± SD and Student's t-test was used for statistical analysis.*
(B) Two representative fluorescent curves for one Kras$^{+/G12D}$ *and* Kras$^{+/G12D}$; Txnrd2$^{\Delta Panc}$ *cell line each are shown.*
DCF = 2',7'-dichlorodihydrofluorescein diacetate

We next tested the effect of the knockdown of Txnrd2 on the expression of other players of the oxidate defense system. However, when we tested the mRNA levels of numerous antioxidant enzymes that play pivotal roles in oxidant defense (see III.2.3), including protein expression of SOD2, we did not observe any statistically significant differences between the groups (Fig. VI-6 A). To assess the oxidative stress response in these *Kras$^{+/G12D}$; Txnrd2$^{\Delta Panc}$* and *Kras$^{+/G12D}$* cell lines, sensitivity to high concentrations of H_2O_2 (20–1000 µM), an inducer of additional oxidative stress, was tested (Fig. VI-7 A). Both experiments showed that *Kras$^{+/G12D}$; Txnrd2$^{\Delta Panc}$* cell lines do not have impaired tolerance to oxidative stress compared to *Kras$^{+/G12D}$* cell lines.

Additionally, the function of *Tp53*, a gene that is a commonly mutated gene in pancreatic cancer (see III.1.2), was tested, as its loss leads to impaired cell cycle arrest, apoptosis initiation, and maintenance of genomic stability upon cellular stress (Miller, Shirole, Tian, Pal, & Sordella, 2016). Indeed, functional p53 was observed, as p21, a protein downstream of p53, was induced upon H_2O_2 treatment (Fig. VI-7 B).

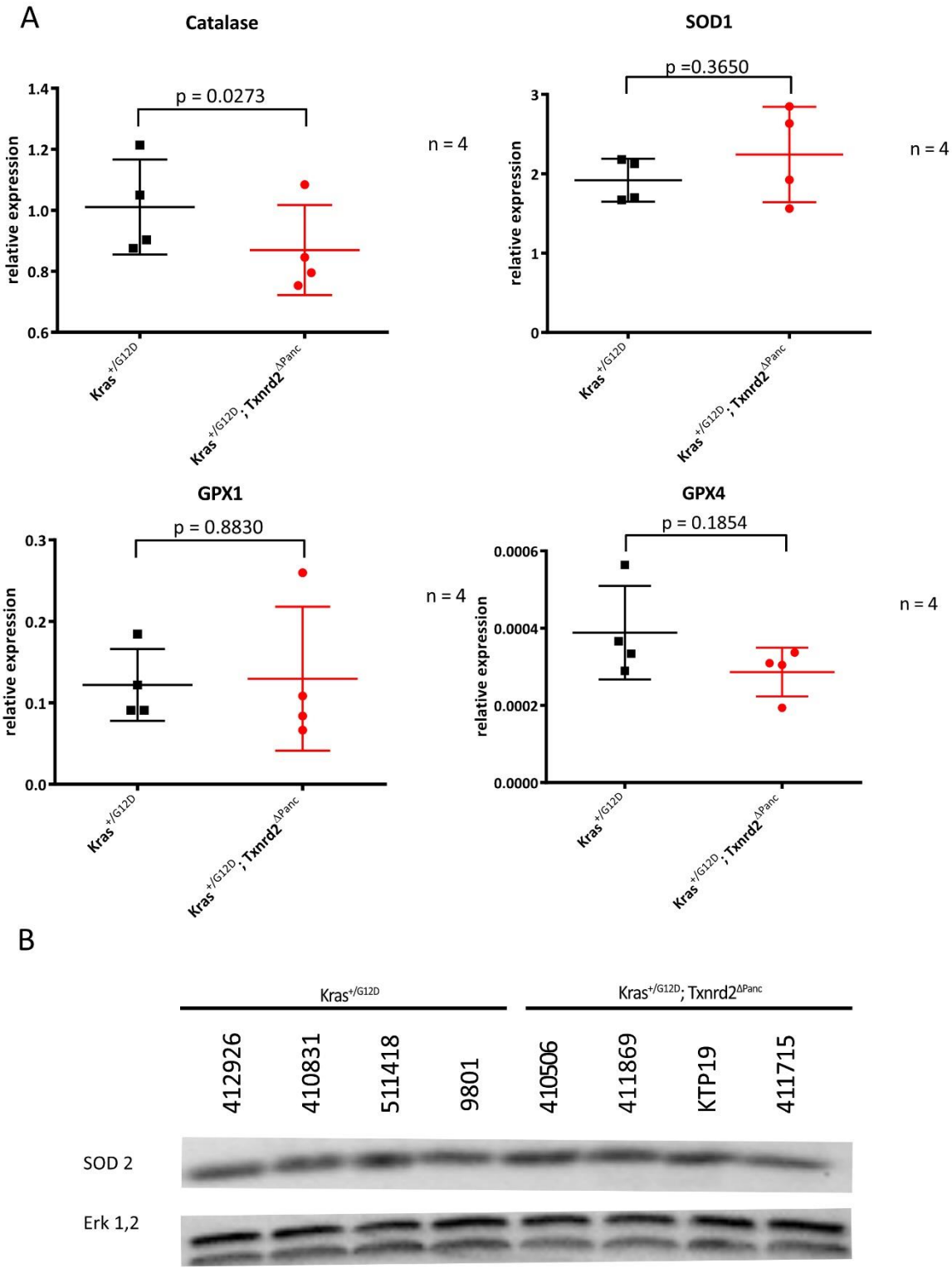

Figure VI-6 mRNA Expression and protein levels of antioxidants in* Kras$^{+/G12D}$ *and* Kras$^{+/G12D}$; Txnrd2$^{\Delta Panc}$ *cell lines

(A) Panel of antioxidant genes tested by quantitative reverse transcription polymerase chain reaction. Expression of catalase, cytosolic superoxide dismutase, and glutathione peroxidase dismutase 1 and 4 were assessed in Kras$^{+/G12D}$ *and* Kras$^{+/G12D}$; Txnrd2$^{\Delta Panc}$ *cell lines. Three individual experiments were performed, and values were averaged for each cell line.*

(B) Western blot analysis of mitochondrial superoxide dismutase. A 12% sodium dodecyl sulfate-polyacrylamide gel and a 0.2 µm nitrocellulose membrane were used. Erk 1 and 2 were used as reference proteins.
ns = not significant, GPX = glutathione peroxidase, SOD1 = cytosolic superoxide dismutase, SOD2 = mitochondrial superoxide dismutase
Data are expressed as means ± SD and Student's t-test was used for statistical analysis

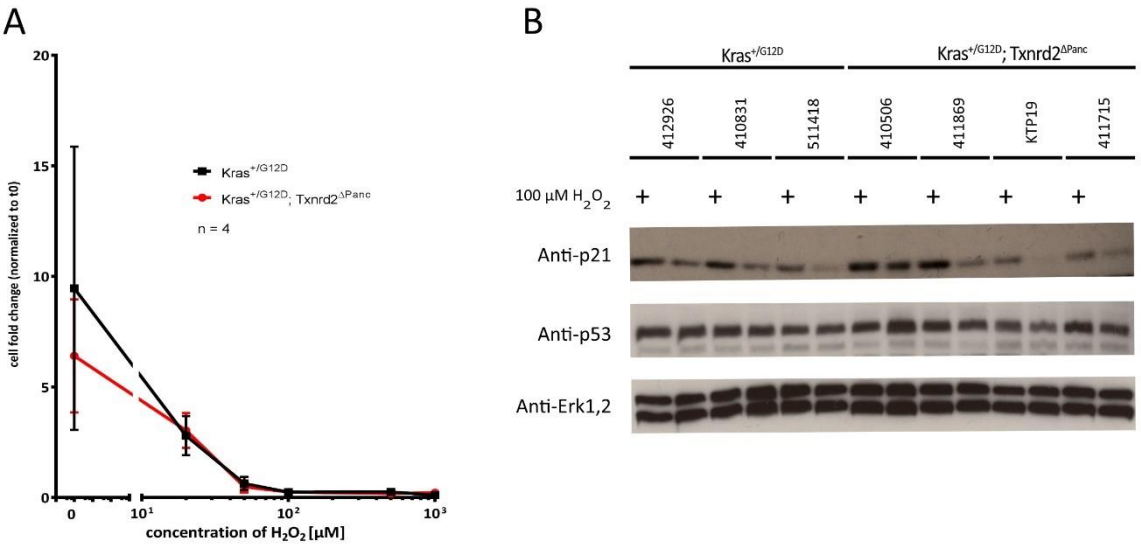

Figure VII-7 Oxidative stress in* Kras$^{+/G12D}$ *and* Kras$^{+/G12D}$; Txnrd2$^{\Delta Panc}$ *cell lines
(A) Kill curve of Kras$^{+/G12D}$ *and* Kras$^{+/G12D}$; Txnrd2$^{\Delta Panc}$ *cell lines treated with 0–1000 µM H_2O_2 for 72 h. Cell content was normalized to t_0 in order to adjust for seeding errors. Experiment was replicated 3 times and values were averaged for each genotype. Data are expressed as means ± SD and Student's t-test was used for statistical analysis.*
(B) Western blot analysis with protein extracted from Kras$^{+/G12D}$ *and* Kras$^{+/G12D}$; Txnrd2$^{\Delta Panc}$ *cell lines that were treated with 100 µM of H_2O_2 diluted in standard medium or medium only (control) for 2 h. A 12% sodium dodecyl sulfate-polyacrylamide gel and a 0.2 µm nitrocellulose membrane were used. Erk 1,2 were used as reference proteins.*

VI.3 Txnrd2-deficient cells proliferate more slowly than Txnrd2-sufficient cells due to impaired S-phase activity

To assess standard features of the cell lines described above, their proliferation and capacity for colony formation were measured. *Kras$^{+/G12D}$; Txnrd2$^{\Delta Panc}$* cell lines displayed slower proliferation compared to control cell lines (Fig. VI-8 A). In addition, the colony formation potential of *Kras$^{+/G12D}$; Txnrd2$^{\Delta Panc}$* cell lines was slightly but significantly impaired (VI-8 B). To further investigate the growth restriction, cell cycle analysis was performed (Fig. VI-9). This revealed differences in the number of cells in S-phase, suggesting impairments in DNA synthesis, but no differences in sub -G1 (apoptotic cells with fragmented DNA (Pozarowski & Darzynkiewicz, 2004)), G1, or G2/M phases in *Kras$^{+/G12D}$; Txnrd2$^{\Delta Panc}$* cell lines.

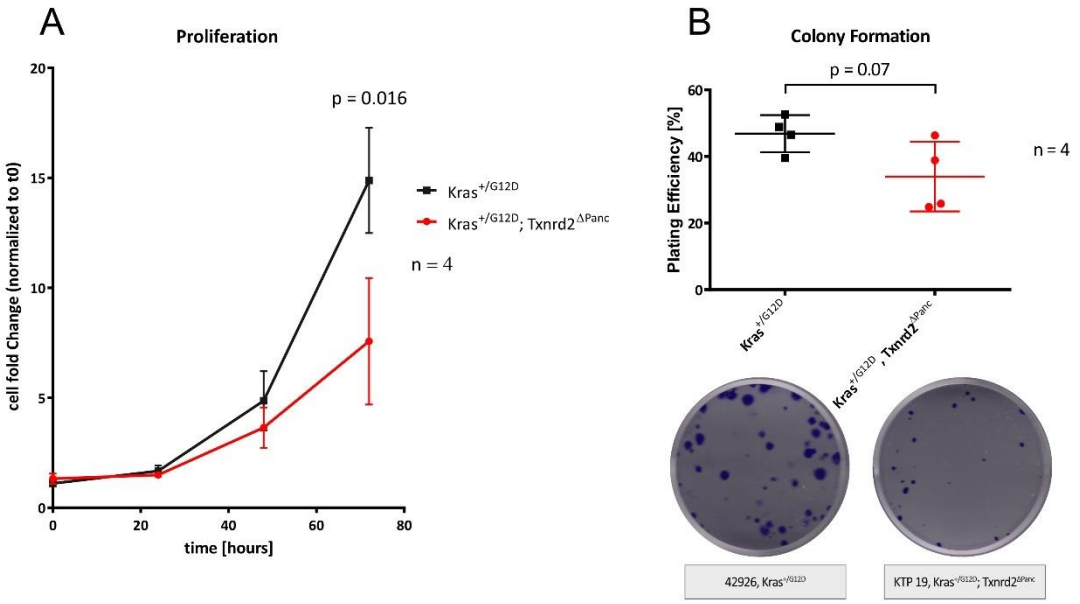

Figure VI-8 Proliferation and colony formation potential in* Kras$^{+/G12D}$ *and* Kras$^{+/G12D}$; Txnrd2$^{\Delta Panc}$ *cell lines
Basic characterization of the cell lines' biology. (A) Proliferation was measured at 24 h, 48 h, 72 h and 96 h after plating. . A CyQUANT assay was used to assess DNA content. Measurements were performed using a FLUOstar OPTIMA microplate reader (BMGs Labtech). Blank values were subtracted, and the triplicates were averaged and related to t_0 values to eliminate possible seeding errors. (B) Colony formation potential was assessed by standard colony formation assay. For each cell line, 100 cells were seeded in each well of a 6-well dish and incubated for 7 days. The dish was then fixed and dyed with Crystal Violet dissolved in Glutaraldehyde (for dilution see III.3.3.2), and colonies were analyzed with Fiji Software. Data from three individual experiments are shown.
Data are expressed as means ± SD and Student's t-test was used for statistical analysis.

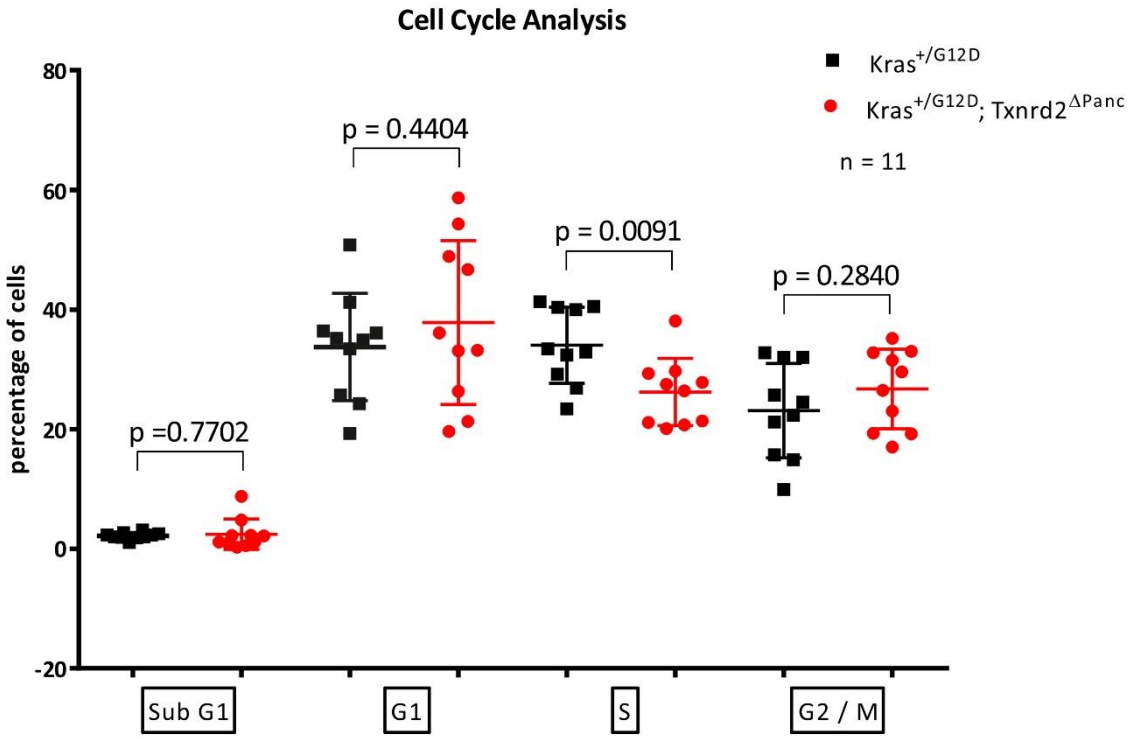

Figure VI-9 Cell cycle analysis in in* Kras$^{+/G12D}$ *and* Kras$^{+/G12D}$; Txnrd2$^{\Delta Panc}$ *cell lines

Fluorescence-activated cell sorting-based cell cycle analysis was performed using propidium iodide and prior fixation with ethanol. Samples were scanned with a BD LSRFortessa flow cytometer and analyzed using FlowJo Software (Version v.X 0.8) by gating (Area vs. Width to exclude non-single cells) and the auto-analysis Cell Cycle Tool. Each value represents an individual experiment.

Data are expressed as means ± SD and Student's t-test was used for statistical analysis.

VI.4 Txnrd2 deficiency does not alter mitochondrial respiration

The following experiments were conducted to elucidate the effect of Txnrd2 deficiency on glucose metabolism. Firstly, levels of hypoxia-inducible factor -1α (Hif-1α), a key regulator of the switch from oxidative phosphorylation to glycolysis (Warburg effect) (Maxwell, Pugh, & Ratcliffe, 2001; Semenza, 2007, 2009; Simon, 2006), were tested in *Kras$^{+/G12D}$* and *Kras$^{+/G12D}$; Txnrd2$^{\Delta Panc}$* cell lines (Fig. VI-10 A). In addition, oxygen consumption was tested by Seahorse measurements. Galactose medium, as previously described (Aguer et al., 2011), was used to decrease glycolytic output and thus enhance the possible defect in oxidative phosphorylation/mitochondrial function. We observed similar basal respiration rates upon glucose or galactose treatment (Fig. VI-10 B); however, uncoupling by addition of FCCP was impaired in galactose medium. Neither experiment showed impaired mitochondrial respiration in *Kras$^{+/G12D}$; Txnrd2$^{\Delta Panc}$* cells, thus indicating that impaired proliferation and reduced tumor incidence in *Kras$^{+/G12D}$; Txnrd2$^{\Delta Panc}$* cells is not a consequence of mitochondrial dysfunction.

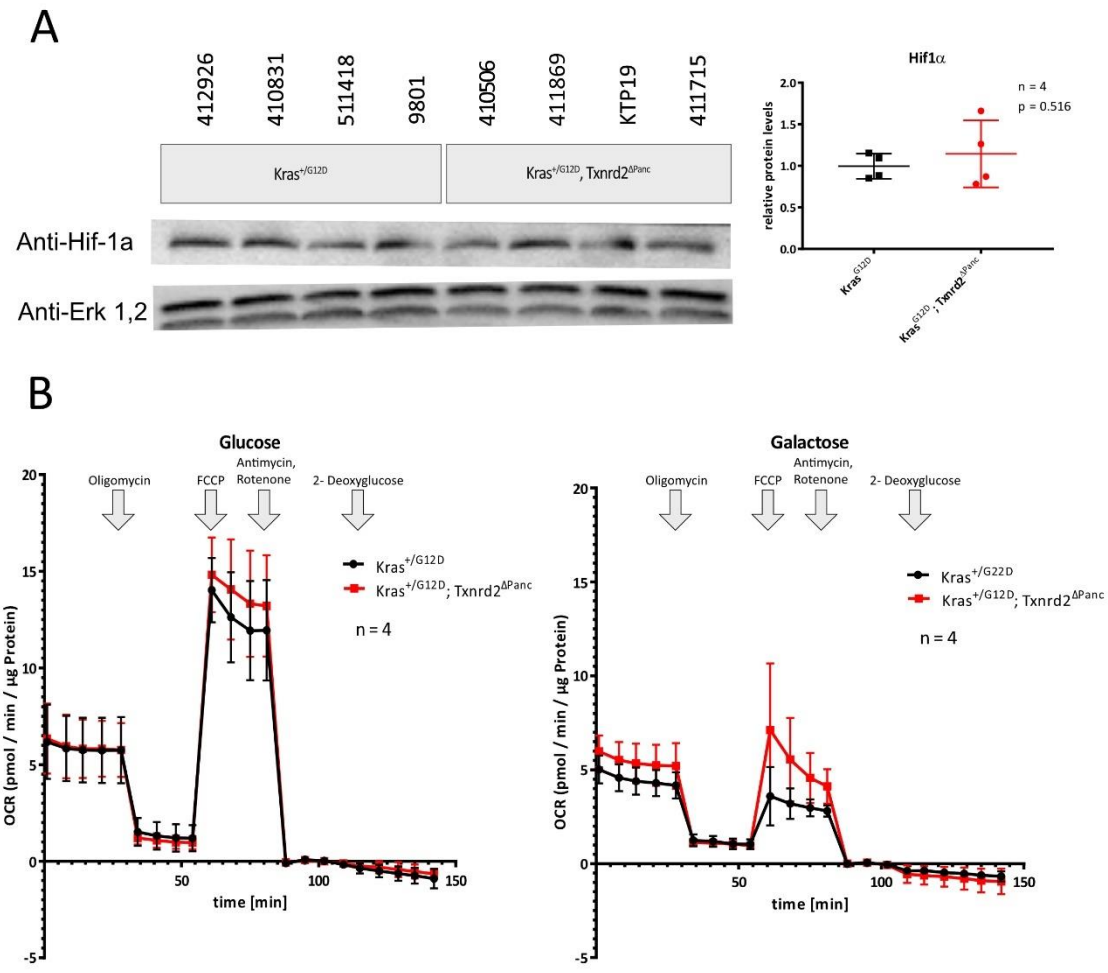

Figure VII-10 Metabolism in* Kras$^{+/G12D}$ *and* Kras$^{+/G12D}$; Txnrd2$^{\Delta Panc}$ *cell lines

(A) Hif-1α levels in Kras$^{+/G12D}$ *and* Kras$^{+/G12D}$; Txnrd2$^{\Delta Panc}$ *cell lines were detected by western blot analysis. Cobalt chloride (150 mM) was used as positive control (not shown). The gel used was 12% and the membrane used was 0.4 µm*

nitrocellulose. Erk 1,2 were used as reference proteins. Signals of three individual experiments were averaged for quantification.
(B) Oxygen consumption measurements of $Kras^{+/G12D}$ *and* $Kras^{+/G12D}$; $Txnrd2^{\Delta Panc}$ *cell lines were performed with the Seahorse assay. Firstly, basal respiration was measured. Then, by adding of 2 µg/mL oligomycin, ATP-linked oxygen consumption was stopped. By adding 1 µM FCCP, the proton gradient of the inner membrane of mitochondria was destructed and oxygen consumption rate was uncoupled. This was fueled by addition of pyruvate (5 mM). Subsequently, 25 µM each of antimycin A and rotenone were added to inhibit complex III and I, respectively, thus inhibiting mitochondrial respiration completely. Finally, by adding 2-deoxyglucose, cells were also deprived of glycolysis as an energy source. Each cell line was seeded in 4 individual wells and values were averaged for each genotype. All experiments were performed three times and values were averaged for each cell line. Mean +/- SD is depicted here. Galactose medium was used to increase the potential mitochondrial defect.*
FCCP = Carbonyl cyanide 4-(trifluoromethoxy)phenylhydrazone
Seahorse experiments were performed with the expertise of Dr. Martin Jastroch in his laboratory.

VI.5 Txnrd2 deficiency leads to decreased RAS activity

Subsequently, we hypothesized that the slower proliferation of Txnrd2-deficient cells is due to differences in RAS levels. To test this hypothesis, the following experiments were performed: First, the expression levels of RAS isoforms (KRAS, NRAS, and HRAS) were measured by qRT-PCR (Fig. VI-11 A), which revealed a slight, albeit insignificant decrease of RAS expression in *Kras*$^{+/G12D}$*; Txnrd2*$^{\Delta Panc}$ cell lines. Next, RAS activity was measured by pulldown of active GTP-bound RAS, which revealed reduced RAS activity in 3 out of 4 *Kras*$^{+/G12D}$*; Txnrd2*$^{\Delta Panc}$ cell lines (Fig. VI-11 B). This outlier cell line, with the internal number 411715, was an outlier throughout all RAS experiments. Lastly, levels of mutated KRAS (Kras^{G12D}) were measured by western blot analysis. In line with decreased RAS activity, levels of mutated KRAS were significantly lower in *Kras*$^{+/G12D}$*; Txnrd2*$^{\Delta Panc}$ cell lines compared to *Kras*$^{+/G12D}$ controls (Fig. VI-11 C).

To further investigate the differences in RAS activity, we analyzed several components of the RAS-Braf-MEK-cascade (Avruch et al., 2001)) and observed no significant differences in the active, phosphorylated form of these signaling molecules between *Kras*$^{+/G12D}$ and *Kras*$^{+/G12D}$*; Txnrd2*$^{\Delta Panc}$ cell lines (Fig. VI-12).

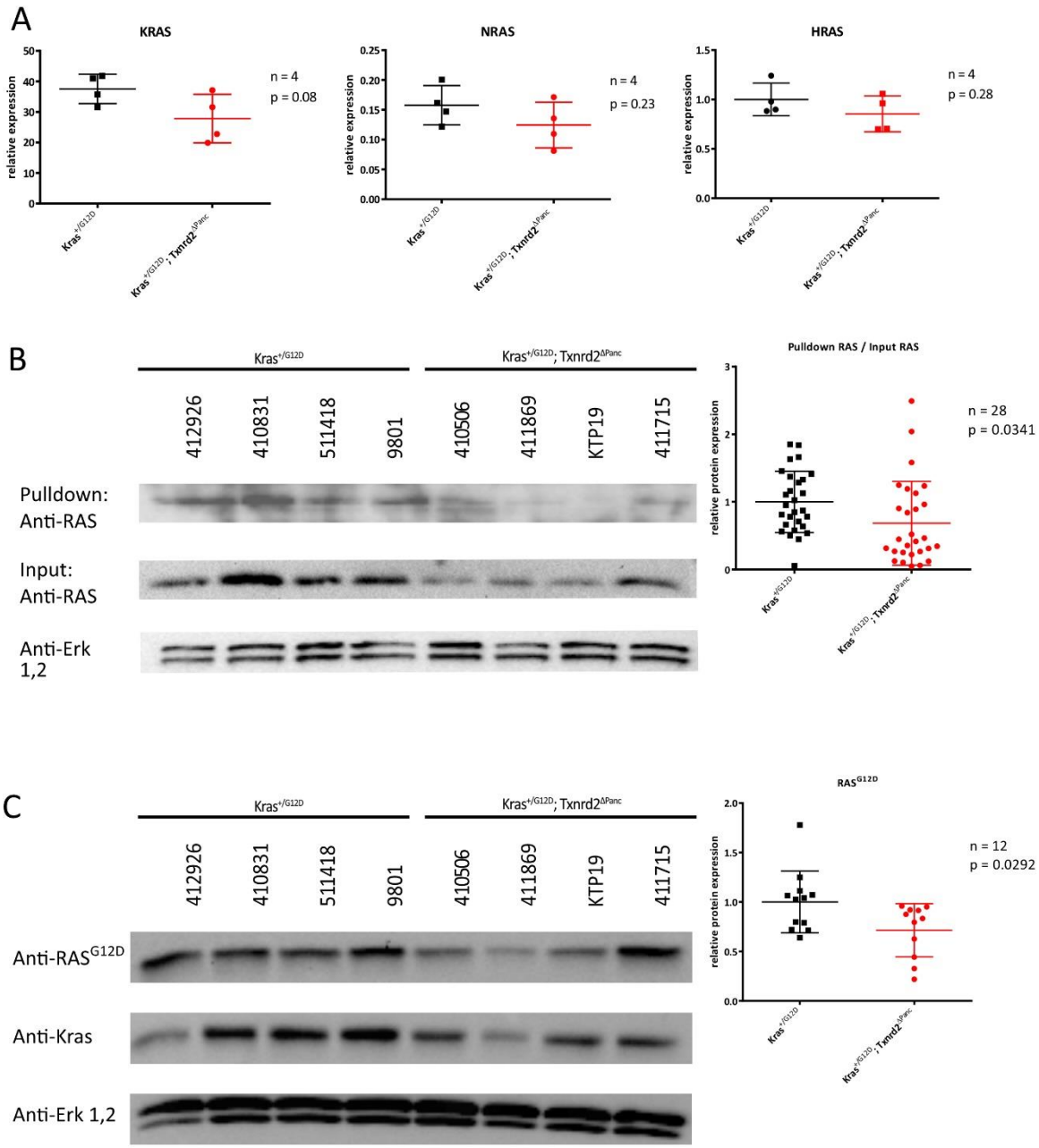

Figure VII-11 RAS in* Kras$^{+/G12D}$; Txnrd2$^{\Delta Panc}$ *cell lines

(A) Expression of RAS isoforms was quantified in Kras$^{+/G12D}$ *and* Kras$^{+/G12D}$; Txnrd2$^{\Delta Panc}$ *cell lines by quantitative reverse transcription polymerase chain reaction. Cyclophilin A was used as housekeeping gene. Each cell line was tested three times for each allele, and values were then averaged.*

(B) GTP-bound RAS in Kras$^{+/G12D}$ *and* Kras$^{+/G12D}$; Txnrd2$^{\Delta Panc}$ *cell lines was detected by RAS pulldown and subsequent western blot. Input was used for the loading control (Erk 1,2) and total RAS. The gels used were 15% and the membranes were 0.2 µm nitrocellulose. To quantify GTP-bound RAS, for each experiment, the fraction of Input-RAS/Pulldown-RAS was calculated for each cell line. Individual experiments are shown.*

(C) Mutant KRAS in Kras$^{+/G12D}$ *and* Kras$^{+/G12D}$; Txnrd2$^{\Delta Panc}$ *cell lines was assessed by western blot analysis with specific antibodies (see V.4.3.1). The gels used were 12% and the membranes used were 0.2 µm nitrocellulose. Erk 1,2 were used*

as the loading control. To quantify mutant KRAS, for each experiment, the levels of RAS^{G12D} were measured. Individual experiments are shown.

Data are expressed as means ± SD and Student's t-test was used for statistical analysis.

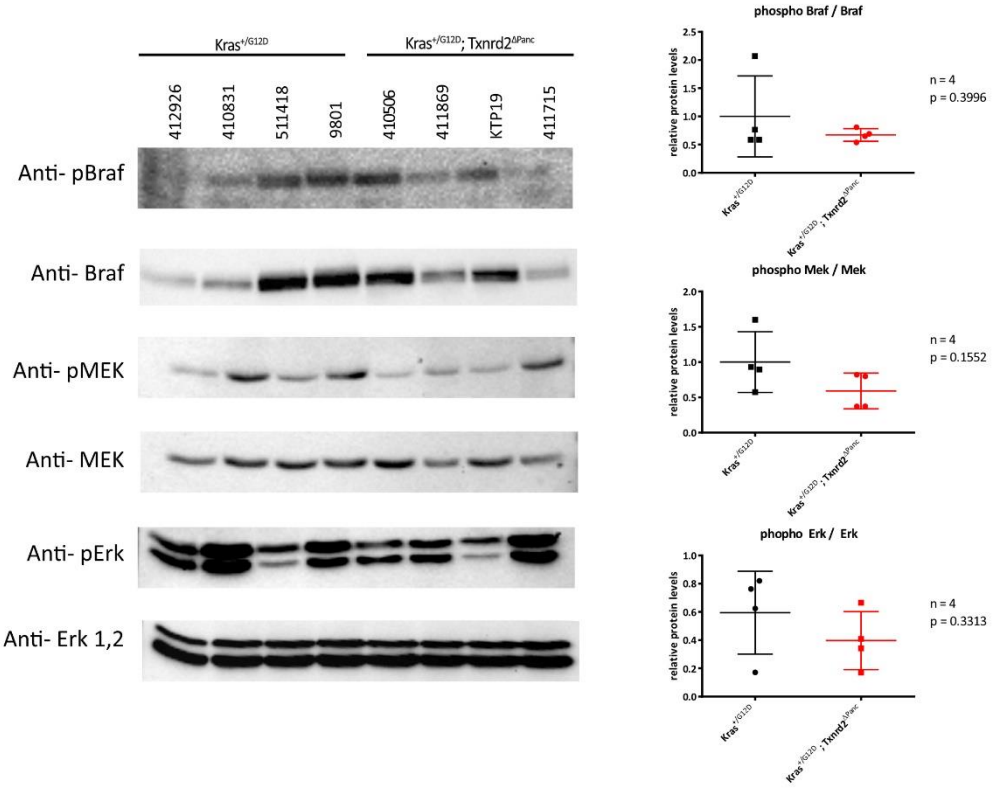

Figure VI-12 RAS–Raf–MEK–Erk cascade in* $Kras^{+/G12D}$; $Txnrd2^{\Delta Panc}$ *cell lines
Phospho-Braf (Ser445), Braf, phospho-MEK (Ser217/221), MEK, phospho-Erk (Thr202/Tyr204) and Erk levels were assessed via western blot analysis in $Kras^{+/G12D}$ *and* $Kras^{+/G12D}$; $Txnrd2^{\Delta Panc}$ *cell lines. All blots were performed using one set of isolated protein to exclude protein isolation differences. The gels used were 12% and membranes were 0.2 µm nitrocellulose. Three individual sets of western blots for each cell line were averaged for quantification.*
Data are expressed as means ± SD and Student's t-test was used for statistical analysis.

VI.6 Txnrd2 deficiency leads to endothelial nitric oxide synthase phosphorylation and increased nitric oxide signaling

The next set of experiments were aimed to elucidate nitric oxide (NO) signaling in *Kras*$^{+/G12D}$ and *Kras*$^{+/G12D}$*; Txnrd2*$^{\Delta Panc}$ cell lines. Recently, progress has been made in determining the role of endothelial NO synthase (eNOS) in pancreatic cancer (Lampson et al., 2012; Lim, Ancrile, Kashatus, & Counter, 2008), as well as linking it to thioredoxin in the vascular system (Hilgers et al., 2017) Thus, we analyzed the phosphorylation of eNOS (Fig. VI-13 A) and observed increased phosphorylation of eNOS in *Kras*$^{+/G12D}$*; Txnrd2*$^{\Delta Panc}$ cell lines compared to *Kras*$^{+/G12D}$ cell lines. The one *Kras*$^{+/G12D}$*; Txnrd2*$^{\Delta Panc}$ cell line that showed high RAS levels (411715) displayed low phosphorylation of eNOS.

Next, NO signaling was examined by staining with 4-Amino-5-Methylamino-2',7'-Difluorofluorescein Diacetate (DAF-FM DA) and detected via flow cytometry, a method accepted for measurements of the unstable intracellular NO in low concentrations (Vardi et al., 2006). This experiment revealed substantial differences in NO levels between *Kras*$^{+/G12D}$*; Txnrd2*$^{\Delta Panc}$ and *Kras*$^{+/G12D}$ control cell lines (Fig. VI-13 B). As we again found 411715 to be an outlier, we calculated the correlations between DAF and phospho-eNOS as well as RAS and phospho-eNOS. Both showed significant correlations, providing an indication for Txnrd2-dependent eNOS phosphorylation and, consequently, RAS inactivation.

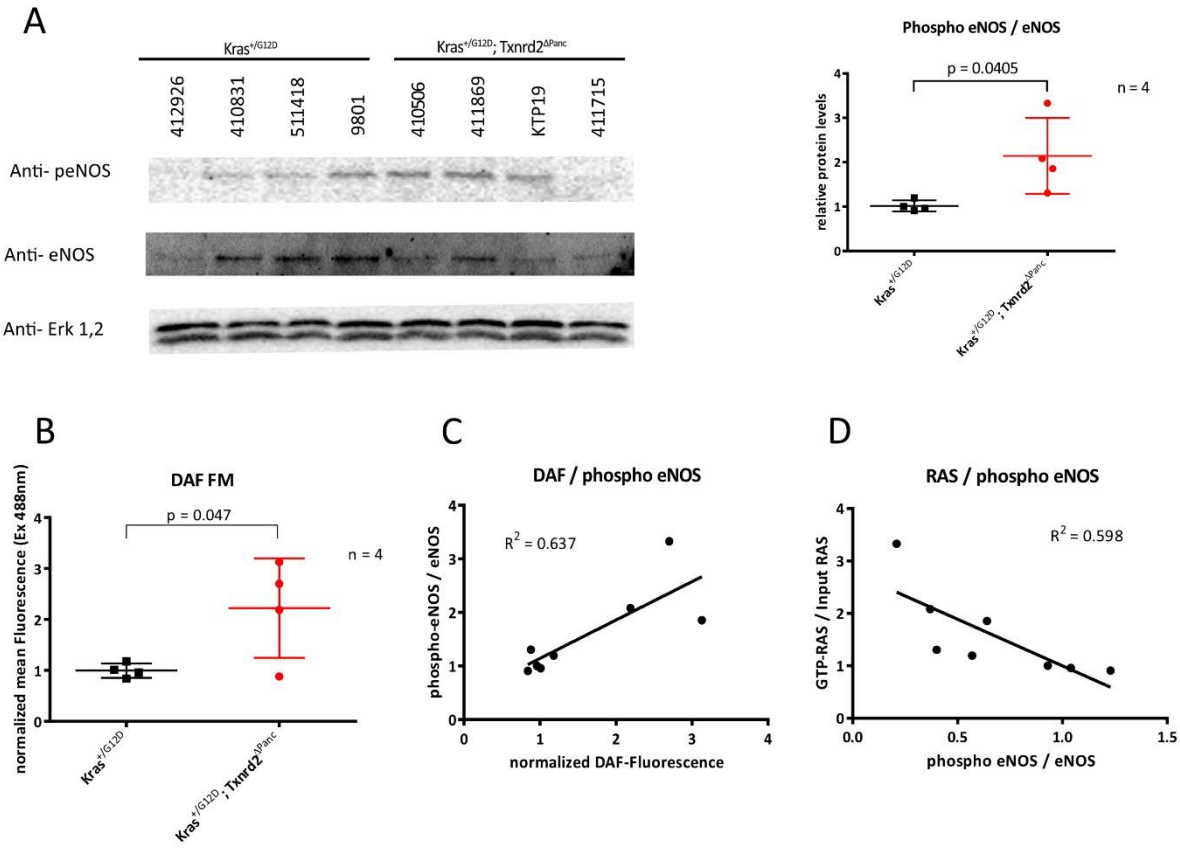

Figure VI-13 Levels of eNOS and NO in* Kras$^{+/G12D}$; Txnrd2$^{\Delta Panc}$ *cell lines

(A*) Phospho-eNOS (S1177) and eNOS levels in* Kras$^{+/G12D}$ *and* Kras$^{+/G12D}$; Txnrd2$^{\Delta Panc}$ *cell lines were assessed by western blot analysis. Gels used were 8% and membranes were 0.4 µm nitrocellulose. For each cell line, three individual experiments were averaged for quantification.*

(B) Nitric oxide levels were assessed by DAF-FM DA flow cytometry in Kras$^{+/G12D}$ *and* Kras$^{+/G12D}$; Txnrd2$^{\Delta Panc}$ *cells. Positive (Nor-3) and negative controls (PTIO) were included with each experiment (not shown). For each cell line, three individual experiments were averaged for each cell line.*

(C, D) Correlations between DAF and phospho-eNOS/eNOS (C) and between GTP-bound RAS and phospho eNOS/eNOS (D) were calculated by averaging at least three individual experiments for each cell line.

eNOS = epithelial nitric oxide synthase, DAF FM = 4-Amino-5-Methylamino-2',7'-Difluorofluorescein Diacetate, NO = nitric oxide, Nor-3 = ((±)-(E)-4-Ethyl-2-[(E)-hydroxyimino]-5-nitro-3-hexeneamide, PTIO = (2-Phenyl-4,4,5,5-tetramethylimidazoline-1-oxyl 3-oxide

Data are expressed as means ± SD and Student's t-test was used for statistical analysis.

VII. Discussion

In the present study, we examined the effect of *Txnrd2* knockout on pancreatic cancer development, a topic that has not yet been investigated.

As pancreatic cancer will be the most common cause of cancer-related death in Germany by 2030 (after lung cancer), and survival rates are very low, with a 5-year survival of less than 9% (Hidalgo, 2010; Jemal et al., 2011; R. Siegel et al., 2014; R. L. Siegel et al., 2019), there is an urgent need for basic and clinical science to find more approaches and regimes to treat patients and increase their survival.

Reactive oxygen species are known to be important players in carcinogenesis, and their role in pancreatic carcinogenesis are subject of current research. The level of ROS is of vital importance to the cells, as oxidative stress will lead to apoptosis (Martinez-Useros et al., 2017; Zhang et al., 2015). Yet a certain shift of the cells' RedOx state is needed for efficient tumor development (Liou et al., 2016).

We therefore set out to enlighten the role of Txnrd2, one of the key players of ROS defense (see III.2.3), in pancreatic tumor development and its effects on signaling and ROS homeostasis.

VII.1 Increased pancreatic precursor lesions in Txnrd2-deficient mice

We began by examining the number of precursor lesions in $Kras^{G12D}$; $Txnrd2^{\Delta Panc}$ and $Kras^{G12D}$ control animals. In 2003, Hingorani et al. showed that PanIN lesions act as precursor lesions for PDAC and that these PanIN lesions were induced by oncogenic KRAS ($Kras^{G12D}$)(Hingorani, Petricoin, et al., 2003). Since then, the oncogenic cascade of first acinar-to-ductal metaplasia (ADM), then pancreatic intraepithelial neoplasia (PanIN) lesions characterized by increasing dysplasia and oncogenic potency has been well established (see II.I.2).

Liou et al. showed in 2016 that mutation of KRAS leads to upregulation of mitochondrial ROS, resulting in increased oncogenic potential, as measured by increased numbers of ADM and PanIN lesions (Liou et al., 2016). Correspondingly, silencing of glutathione peroxidase-1 leads to increased levels of ROS and enhances epidermal-to-mesenchymal transition (Meng et al., 2018). Likewise, knockout of TP53INP1, a protein downstream of p53 and a regulator of intracellular stress response, leads to higher levels of ROS (Cano et al., 2009; N'Guessan et al., 2011). As a proof of concept, the inhibition of ROS by N- acetylcysteine or the mitochondrially targeted antioxidant mitoQ leads to a halt in tumor development (Al Saati et al., 2013; Liou et al., 2016).

We thus hypothesized that oncogenic potential is increased in mice that lack the antioxidant Txnrd2 via upregulation of mitochondrial ROS. Indeed, in this study, we observed higher levels of ADM low-grade PanIN lesions (PanIN 1 lesions) in Txnrd2-deficient mouse pancreata (see Fig. VI-1).

Peter Storz recently proposed a model for the connection between ROS levels and carcinogenesis in PDAC (Storz, 2017): During early carcinogenesis, levels of ROS increase due to altered glucose metabolism (e.g., the metabolic switch to glycolysis – the Warburg effect; see II.2.4), altered

mitochondrial metabolism, and altered expression of oxidants and antioxidants. In later stages, precancerous and cancerous cells avoid damage and cell death by maintaining redox homeostasis via upregulation of antioxidants (e.g., through Nrf2, a transcription factor responsible for maintaining a balanced redox state in both nontransformed and cancerous cells by inducing expression of multiple antioxidant response proteins, thus resulting in a more reduced intracellular state (DeNicola et al., 2011; Ma, 2013)). Nrf2 can be induced by oncogenic alleles (one of them being $Kras^{G12D}$) (DeNicola et al., 2011). As Storz et al. stated, it is essential for the cells to maintain ROS levels at a profiting level for tumor progression, and not let them exceed to a level to be harmful (Storz, 2017).

Remarkably, although we observed an increase in preneoplastic lesions, tumor incidence was reduced in $Kras^{G12D}$; $Txnrd2^{\Delta Panc}$ mice, indicating a halt in the initial acceleration of carcinogenesis and a possible block in tumor progression. While Storz et al. have underlined the significance of Kras-induced mitochondrial ROS on carcinogenesis, he emphasized the necessity for the cell to enhance antioxidant players in order to limit continuous cellular stress that would lead to senescence and apoptosis (Storz, 2017). It has been suggested that, as one key antioxidant is lacking in Txnrd2-deficient cells, they may struggle to maintain a control on ROS levels. That high levels of ROS lead to stalled tumor survival in PDAC has been shown by Mohammad et al.: The inhibition of glutathione S-transferase pi 1 (GSTP1) activity leads to high levels of ROS and induction of heme oxygenase-1 (HO-1). Inhibition of both GSTP1 and HO-1 in PDAC cells induced cell death (Mohammad et al., 2019). The concept of radiotherapy is based on this phenomenon: As cancerous cells have higher levels of endogenous ROS, induction of supplemental ROS (e.g., via ionizing radiation) leads to apoptosis and other forms of cell death (Zou, Chang, Li, & Wang, 2017).

It thus seems logical that depleting cells of Txnrd2 will lead to inhibited tumor progression. However, there are also other reasons that could contribute to this phenomenon. For example, loss of Txnrd2 might, by increasing levels of oncogenic ROS, lead to increased DNA mutations, as other authors have observed (Ishikawa et al., 2008). As some oxygen atoms are not electrically charged and can thus overcome cellular compartmentalization (see II.2.1), DNA damage can occur to mitochondrial and nuclear DNA. This might activate the cellular immune system (which has long been known to play a pivotal role in tumor development and defense (Schreiber, Old, & Smyth, 2011)), resulting in increased surveillance and apoptosis induced by cytotoxic T cells. Secondly, the reason for stalled tumor progression in *Txnrd2* - depleted mice is a switch in metabolism and mitochondrial integrity takes place that prevents $Txnrd2^{\Delta Panc}$ cell lines from effectively propagating and proliferating. It has been established that ROS can hinder mitochondrial functions; for example, even very small differences in membrane potential can lead to ineffective oxidative phosphorylation (Zorov, Juhaszova, & Sollott, 2014).

Taken together, there is conclusive evidence that increased levels of ROS are needed for effective cancer initiation (Cano et al., 2009; Meng et al., 2018; N'Guessan et al., 2011; Storz, 2017), but high levels of ROS lead to senescence and cell death (McPherson et al., 2019; Mohammad et al., 2019; Zorov et al., 2014; Zou et al., 2017). We observe that increased levels of ROS lead to increased carcinogenesis, but further tumor progression is halted due to the lack of a key antioxidant.

What remains elusive is the levels of ROS that lead to carcinogenesis vs. stalled tumor development, as well as means to measure or display the redox state of the cell in the context of carcinogenic growth. Given the poor prognosis of PDAC, future therapeutic approaches might depend on oxidants or antioxidants; thus, it is important to emphasize that the prevention of cancer will focus on reducing cellular redox states, while cancer therapy will aim to cause cellular stress and consequent senescence or cell death (Storz, 2017).

VII.2 Effect of Txnrd2 loss on cells' biology

We used cell lines isolated from mouse PDACs and established in cell culture. As the cell lines are derived from pancreatic cancer and not preneoplastic lesions, the former stage was examined in our experiments. Thus, the development of cancer and its biology, signaling, and metabolism during this period warrants further investigation.

We first examined cell proliferation and colony formation potential. We used widely accepted methods that show a tumor's growth potential (proliferation) as well as cells' potential to initiate colonies, differentiating between cells that are senescent (i.e., do not form colonies) and those that are not (Kabakov & Gabai, 2018).

As we observed decreased tumor incidence in mice lacking Txnrd2 expression in the pancreas, we hypothesized that tumor progression would also be slower. Indeed, cell proliferation and colony formation potential were decreased in cell lines lacking Txnrd2 (see Fig. VI-8).

It has been established that data obtained using cell lines *in vitro* correlate well with *in vivo* findings (Hellfritsch et al., 2015; Karp, Burke, Saylor, & Humphrey, 1984; Ruess et al., 2018). However, the complexity of the *in vivo* conditions, which include intercellular communication, integration in the 3D matrix, regulation of the immune system, and hormonal influences, cannot be modeled in simple 2D cell culture dish experiments.

Nonetheless, we aimed to elucidate the cause of the altered cell proliferation by performing cell cycle analyses. We observed differences in their cell cycles (see Fig. VI-9): Txnrd2-deficient cell lines had fewer cells in S phase than did the control cell lines. The other populations, including those in subG1 (cells that have less than 2N DNA content, i.e., cells that are undergoing necrosis or apoptosis), G1, or G2 phase, are similar in $Kras^{G12D}$; $Txnrd2^{\Delta Panc}$ and $Kras^{G12D}$ control cell lines.

S phase, or synthesis phase, is the replication phase of mitosis in which a copy of each chromosome is made, resulting in two sister chromatids per chromosome (2N → 4N). Entry into S phase is highly controlled, as DNA must be damage-free to duplicate safely and minimize risk of mutation.

Our results are in line with other findings in tumor biology: In VI-3, we showed that these $Kras^{G12D}$; $Txnrd2^{\Delta Panc}$ cell lines have slower proliferation and decreased colony formation potential compared

to *Kras*^{G12D} control cell lines. This is in accordance with the decreased tumor incidence in *Kras*^{G12D}; *Txnrd2*$^{\Delta Panc}$ mice.

One hypothesis for the low number of cells in S phase is a cell cycle arrest of Txnrd2-depleted cells at the G1/S checkpoint. This checkpoint, like the G2/M and metaphase checkpoints, is highly conserved (see (Malumbres & Barbacid, 2009)) and acts as a control for DNA damage before the cell begins to replicate its genome during S phase (for a review see (Bertoli, Skotheim, & de Bruin, 2013)).

Other potential contributors to the higher percentage of cells in S phase in Txnrd2-depleted cell lines is a S/G2 arrest in these cell lines, or an acquired ability of Kras^{G12D} cells to overcome this potential halt in the cell cycle. This arrest during S phase is triggered by DNA damage: Mistakes during synthesis of DNA will lead to (i) arrest of the cell cycle, (ii) prevention of the firing of late replication origins, (iii) stabilization of stressed replication forks, and (iv) promotion of DNA repair and restart of DNA replication (Flynn & Zou, 2011; Stokes et al., 2007), with these effects mediated by, for example, ataxia telangiectasia and Rad3-related (ATR) kinase (Cimprich & Cortez, 2008; Flynn & Zou, 2011). DNA mutations and/or alternative DNA damage response signaling could lead to initiation of this checkpoint, resulting in prolonged S phase and delaying advancement to G2 phase.

Another possible explanation is related to difficulties during the process of DNA synthesis itself. This could be due to higher level of oxidative stress. In order to examine the cellular redox state, we performed carboxy-H_2DCFDA staining. This assay aims to elucidate the level of ROS in cells, as ROS perform oxidation of 6-carboxy-2',7'-dichlorodihydrofluorescein diacetate (Carboxy-H_2DCFDA), resulting in 6-carboxy-2', 7' –dichlorodihydrofluorescein (Carboxy-H_2DCF) that provides the fluorescent signal measured by flow cytometry. The electron of the oxidation process is received by not H_2O_2 itself, but by a multitude of one-electron oxidizing species like hydroxyl radicals, hypochlorous acid, NO_2, and others (Kalyanaraman et al., 2012). It therefore acts as a rather unspecific measure of intracellular oxidizing compounds.
In our experiments, Carboxy-H_2DCFDA staining revealed higher levels of ROS in Txnrd2-depleted cell lines. ROS are potent initiators of DNA damage (see III.2.2), i.e., DNA-protein crosslinks and DNA interstrand crosslinks. It is common knowledge that DNA strand lesions hinder DNA synthase, thereby preventing efficient DNA synthesis (Maor-Shoshani, Ben-Ari, & Livneh, 2003; Seki et al., 2004). We thus hypothesize that the high levels of ROS observed generate lesions in the genome, resulting in turbulence during S phase, leading to lower proliferation rates and hence decreased tumor incidence.

VII.3 Effect of loss of Txnrd2 on mitochondrial respiration

As we observed differences in cellular proliferation and colony formation potential, we hypothesized that this was due to oxidative stress and/or hindered effective mitochondrial function. We thus analyzed levels of ROS via carboxy-H_2DCFDA staining (see above) and observed increased levels of ROS in *Txnrd2*$^{\Delta Panc}$ cell lines.

To further assess whether these cell lines not only show higher levels of ROS (which can act as intracellular messenger molecules; see II.2.2), but also other indications of oxidative stress, we measured the expression of antioxidant proteins. Oxidative stress generally leads to upregulation of antioxidants (Radi et al., 1991; Rhee et al., 2005; Sabens & Mieyal, (2009)) in response to a toxic imbalance of the redox state.

By showing that levels of antioxidant enzymes are not altered, we demonstrated that loss of Txnrd2 does not seem to lead to significant alterations in the cell's redox state, concordant with previous findings in mouse myocardia (Kiermayer et al., 2015).

Mitochondrial ROS originates from three main complexes: mitochondrial complex I, xanthine oxidase, and NADPH oxidase (Abramov, Scorziello, & Duchen, 2007; Zorov et al., 2014) (see also II.2.1). Under physiological conditions, approximately 2% of oxygen consumption is used to produce ROS (Chance, Sies, & Boveris, 1979). It has been shown that $Kras^{G12D}$ mutation leads to increased proton leak and increased production of ROS, leading to the hypothesis that reduction of mitochondrial efficiency increases the production of ROS (Liou et al., 2016).

We measured mitochondrial efficiency in the *$Kras^{G12D}$; $Txnrd2^{\Delta Panc}$* cell lines using the well-established Seahorse assay (Koopman et al., 2016). Initially, we hypothesized that eradicating Txnrd2 from the mitochondria would lead to significant changes in cellular oxygen consumption and mitochondrial function. However, we observed that lack of Txnrd2 did not alter the cellular respiration significantly. The following hypothesis can help to explain this result: Genes for mitochondrial proteins are mainly encoded in nuclear DNA; only a small portion is encoded in mtDNA. As most of the DNA encoding proteins involved in oxidative phosphorylation are thus not located in the mitochondria and would not be subjected to the increased levels of ROS that we observed in *$Kras^{G12D}$; $Txnrd2^{\Delta Panc}$* cells, one can postulate that the effect of the level of ROS acting as a mutagen in these cells is not as large as anticipated. It instead serves as an intracellular messenger, likewise to the results of various authors (D'Autreaux & Toledano, 2007; Nathan, 2003; Poole, Karplus, & Claiborne, 2004).

On the contrary, if ROS are indeed acting as a mutagen, they might compromise the efficiency of cellular respiration. As a result, mitochondrial fission could occur to increase the number of loci for cellular respiration in order to maintain the original level of ATP production via oxidative phosphorylation. To assess whether limited mitochondrial efficiency is balanced by increased numbers of mitochondria, we measured mtDNA content and used MitoTracker staining to verify our findings. Here, we observed that Txnrd2-depleted cell lines show increased mtDNA. We postulate that this can be attributed to either of the following causes:

i. As shown in VI.2, Txnrd2-deficient cells have more ROS. We can now speculate, that higher quantity of ROS leads to mutations and damages in dominantly mitochondrial DNA, as it has been known that e.g. chemicals mutagens tend to affect mitochondrial DNA more than nuclear DNA (Allen & Coombs, 1980; Backer & Weinstein, 1980; Shay & Werbin, 1987), and also Txnrd2 is located in the mitochondria, hence this is the locus of the lack of an antioxidant enzyme. Consequently, mtDNA is continuatively damaged, making it non-applicable for protein biosynthesis. Therefore, a higher amount of mitochondrial DNA is needed to maintain normal mitochondrial function.

However, it must be noted that approximately 99% of essential mitochondrial proteins are encoded in the cytoplasm; mtDNA encodes 2 rRNAs, 22 tRNAs, and 13 proteins that act as subunits of the respiratory chain (Boengler, Heusch, & Schulz, 2011).

Nevertheless, mutations in mtDNA can have a big impact: Ishikawa et al. showed that tumors with a high rate of mtDNA mutations have an increased metastatic potential. They showed that metastatic potential declines upon administration of an antioxidant, thus providing a proof of concept (Ishikawa et al., 2008).

ii. The ability of Txnrd2-depleted mitochondria to provide sufficient ATP and other sources of cellular energy may be limited, perhaps due to the higher levels of ROS we observed (see VI.2), leading to structural changes in the proteins of the respiratory chain. Thus, a higher quantity of proteins of the mitochondrial chain is required to maintain normal cellular respiration (measured by Seahorse technology; see Fig. VI-4).

Since cancerous cells depend heavily on glycolysis, also known as the Warburg effect (see II.2.4) (Warburg, 1924), we measured levels of one key regulator of this metabolic switch, Hif-1α (Courtnay et al., 2015; Semenza, 2007, 2009; Simon, 2006). We observed that the level of Hif-1α, measured by Western Blot analysis, is not altered in Txnrd2-deficient models.

Taken together, the data strongly suggests that cellular respiration and main energy production via glycolysis and oxidative phosphorylation are similar in $Kras^{G12D}$ and $Kras^{G12D}; Txnrd2^{\Delta Panc}$ cell lines.

VII.4 RAS activity links low tumor incidence to TXNRD2 deficiency in the $Kras^{G12D}$ background

Until now, there has been no published research reporting a connection between Txnrd2 and RAS, which is one of the key players in carcinogenesis in PDAC as well as in a variety of other cancers (see III.1.2).

Though viral agents able to induce cancerous growth were first described in the 1960s (Harvey, 1964; Kirsten & Mayer, 1967), it was not until 1982 that human homologues of Kirsten sarcoma gene (KRAS) and Harvey sarcoma gene (HRAS) were identified in Lowy's laboratory (Chang, Gonda, Ellis, Scolnick, & Lowy, 1982). HRAS and KRAS are two members of the RAS superfamily, a group of small GTPases. GTPases remain inactive until they bind to guanosine-5'-triphosphate (GTP), a conversion that is physiologically initiated by guanosine-exchange factors (GEFs) that transmit intra- or extracellular signals to RAS (Jancik, Drabek, Radzioch, & Hajduch, 2010). Upon binding of GTP, RAS undergoes conformational changes, resulting in activation of this signaling molecule (Jancik et al., 2010). RAS is inactivated via hydrolysis of the phosphate residues, a process that is facilitated by GTPase-activating proteins (GAPs) (Gideon et al., 1992).

When RAS bears an activating mutation (e.g., a glycine to aspartate mutation as seen in $Kras^{G12D}$), the protein loses its intrinsic GTPase activity, resulting in a permanently active state. As this mutation drives proliferation and survival and prevents apoptosis, differentiation, and cell-–cell interactions (Jancik et al., 2010), mutated Kras is hence considered an "oncogene."

We saw that even though *$Kras^{G12D}$; $Txnrd2^{\Delta Panc}$* and *$Kras^{G12D}$* control cell lines share the same *Kras* mutation, turning the protein into the "always-on" version, Txnrd2-depleted cell lines show lower RAS activity, as measured by pulldown of active (GTP-bound) RAS (Fig. VI-11 C). This is not due to altered expression of RAS proteins (Fig. VI-11 A).

The connection between RAS and ROS has previously been established (Chun et al., 2010; Liou et al., 2016; Storz, 2017; Weinberg et al., 2010). In pancreatic cancer cells, mutant KRAS leads to higher levels of ROS, thus ensuring a more oxidative and mutagenic cellular state. In a KRAS-mutant background, tumor growth depends on mtROS (Liou et al., 2016). However, tumor progression also depends on viable mitochondria, as depletion of mitochondrial transcription factor A (Tfam, a transcription factor for genes of the respiratory chain and relevant for oxidative phosphorylation (Larsson et al., 1998)) hinders carcinogenesis (Weinberg et al., 2010). In the present model, in which there is (i) a deficiency of one antioxidant and (ii) a mitochondrial aberration (as demonstrated by the higher number of mitochondria needed to achieve normal respiratory functions; see IV.2) in the cells that show less RAS activity, the connection is exposed. Others have shown that levels of active RAS are higher in cell lines overexpressing thioredoxin 1 (Arai et al., 2008). This can act as a proof of concept, as it is in line with our finding of more activated RAS in cell lines that show no impairment in thioredoxin reductase activity (*$Kras^{G12D}$* cell lines).

By finding a correlation between the level of RAS activity and the absence of Txnrd2, we have found an explanation for the low tumor incidence observed in the mouse model. A correlation between RAS and tumor development has long been a subject of investigation. Two examples show a conclusive link. First, Slebos et al. showed that in patients with adenocarcinoma of the lung, the described point mutation in the *KRAS* gene leads to a poor prognosis and very short tumor free-survival (Slebos et al., 1990). Second, Mueller et al. showed that RAS dosage determines the phenotype of PDAC, correlating a high dosage of RAS to a higher rate of metastasis and a more mesenchymal phenotype when the cells are in culture (Mueller et al., 2018).

We believe that Txnrd2 acts not only as an antioxidant, but also as an intracellular messenger. Knockout of Txnrd2 might therefore lead to altered signaling, resulting in reduced activity of KRAS. The scaling down of mutated KRAS activity is a topic of great scientific interest, as mutated KRAS drives oncogenesis of many tumors (see II.1.2). To date, only a few proteins have been found to decrease activity of mutated KRAS (Uprety & Adjei, 2020). One is Src homology region 2 domain-containing phosphatase-2 (SHP2): It has been shown that loss of this protein tyrosine phosphatase limits tumor development in a Kras-mutant tumor mouse model and sensitizes these tumors to MEK inhibition (Ruess et al., 2018). This phenomenon is similar to what we observed in this study: Our Txnrd2-deficient mouse model also develops fewer tumors; moreover, Txnrd2-deficient cells proliferate slower and intracellular signaling is altered (see Fig. IV.1, Fig. IV.8 and Fig. IV.11). Ruess et al. showed using transcriptomics analyses and extensive murine models that absence of SHP2 leads to down-signaling of KRAS signatures and thus managed to locate SHP2 upstream of RAS, as SHP2 deletion had no effect on constitutively active mutant MEK1 or PI3K (Ruess et al., 2018).

Similar examinations in our model will need to be undertaken to further investigate the underlying signaling mechanisms.

VII.5 S-nitrosylation links TXNRD2 and RAS activity

As recent literature has progressed in elucidating the role of eNOS in PDAC (Lampson et al., 2012; Lim et al., 2008), and eNOS was also linked to thioredoxin in a study focusing on hypertension and the effect of thioredoxin (injected and genetically enhanced) on lowering blood pressure (Hilgers et al., 2017), we investigated eNOS/NO in our model.

We saw that *in vivo* levels of NO, as measured by DAF staining and detected via flow cytometry, a well-established assay in redox research (A. M. Lewis, Matzdorf, & Rice, 2016; Schwendemann, Sehringer, Noethling, Zahradnik, & Schaefer, 2008), are significantly higher in cell lines lacking mitochondrial Txnrd (see Fig. VI-13).

The connection between the thioredoxin system and NO has previously been described. Expression of the thioredoxin system (but not other oxidative stress defense enzymes) is increased in cells that are subjected to NO stress. Cell lines that were transfected with TRX cDNA showed increased resilience to treatment with NO (Ferret, Soum, Negre, Wollman, & Fradelizi, 2000). In a likewise manner, thioredoxin interacting protein (TXNIP) is a regulator of thioredoxin activity that has been linked to both down- (Nishiyama et al., 1999) and upregulation (Schulze et al., 2006) of thioredoxin. In macrophages, administration of TXNIP (when administered together with iNOS) leads to higher levels of protein-SNOs (proteins modified with S-nitrosylation), thus acting as an inhibitor of the thioredoxin system (Forrester et al., 2009). In this system, TXNIP is also downregulated upon treatment with NO via iNOS, and low levels of TXNIP make the cells more resilient to NO stress (Forrester et al., 2009). Finally, in a colon cancer model, knockout of cytosolic thioredoxin reductase (Txnrd1) leads to increased cytotoxicity upon treatment with an NO donor (Edes, Cassidy, Shami, & Moos, 2010), thus providing a proof of concept.

The findings of our study are thus in line with what these authors have ubiquitously seen: Loss of the thioredoxin system leads to more NO signaling (Forrester et al., 2009), leading to the hypothesis that the cells will be less resilient toward NO stress.

As NO has a half-life of only a few seconds under normal cellular conditions, nitrosation is one means of conveying NO signaling. NO can origin from NO synthases or other NO donors (like N_2O_3 or $Fe^{II}NO^+$) (Heinrich et al., 2013). Nitrosation is the mechanism by which an NO^+ molecule is added to a nucleophilic group like amine or thiolate (Heinrich et al., 2013). In contrast, nitrosylation, a term that is commonly confused with nitrosation, describes the chemical process of coordination of NO to a metal center, forming a metal nitrosyl complex (Heinrich et al., 2013). Nitrosation (and nitrosylation) can result in S-nitrosothiols, the addition of an NO group onto a sulfur atom of a thiol (Heinrich et al., 2013). This can happen by i.) oxidation of NO, resulting in dinitrogen trioxide (N_2O_3), and subsequent transnitrosation or ii.) oxidative nitrosylation, in which first, the oxidation of thiol occurs, forming a thiyl radical, followed by a direct addition of NO (Heinrich et al., 2013). Under biological conditions, a direct addition of NO onto thiols does not occur (Heinrich et al., 2013).

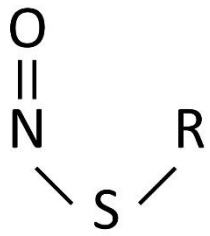

***Figure VIII-1 Structure of S-nitrosothiol**.*

R stands for organic residue. Data taken from (Heinrich et al., 2013).

The thioredoxin system is one of the mediators of nitrosation and de-nitrosation and is responsible for de-nitrosylation of the apoptotic marker caspase-3, resulting in enhanced activity of the apoptotic cascade (Benhar, Forrester, Hess, & Stamler, 2008; Mannick et al., 1999). They also showed that siRNA-mediated knockdown of thioredoxin or thioredoxin reductase, as well as treatment with auranofin (a chemical inhibitor of thioredoxin reductases) resulted in increased levels of S-nitrosylation of caspase-3 (Benhar et al., 2008). Moreover, they specifically linked knockdown of Txnrd2 with de-nitrosylation of caspase-3 (Benhar et al., 2008).

Hilgers et al., too, demonstrated a link between the thioredoxin system and NO signaling, although they used a different tissue. They injected human thioredoxin into mice with age-related hypertension and saw that it led to improved blood pressure parameters via enhanced release of NO and subsequent muscular relaxation (Hilgers et al., 2017). They also observed increased levels of eNOS in cells with active thioredoxin, as well as enhanced NO signaling (Hilgers et al., 2017). This, too, indicates a ubiquitous link between the thioredoxin system, NO signaling, and eNOS across different cell and tissue types.

Key generators of NO are nitric oxide synthases (NOS). The enzyme eNOS (also known as nitric oxide synthase 3 [NOS3]) was first discovered in the cardiovascular system as the key producer of NO, a main component in the regulation of blood vessel tone (P. L. Huang et al., 1995). Contrary to what its name suggests, eNOS expression is not limited to endothelial tissue, as one of its transcription factors (GATA-2) was also found in neuronal or myeloid cells (Fish et al., 2005; Lawson, Whyte, & Mellon, 1996; Ohneda & Yamamoto, 2002).

As eNOS has recently been investigated in pancreatic cancer (Lampson et al., 2012; Lim et al., 2008), we examined its levels and activity, as measured by phosphorylation. The phosphorylation of eNOS at serine 1177 has long been regarded as the key “on-switch” of NO synthesis (Kukreja & Xi, 2007), but recent investigations have revealed that the underlying principles might be somewhat more complicated than presumed (Eroglu, Saravi, Sorrentino, Steinhorn, & Michel, 2019). We found that

levels of phosphorylated eNOS were significantly higher in Txnrd2-depleted cell lines and that this correlated with the increased levels of NO (see Fig. VI-13).

The impact of eNOS on pancreatic carcinogenesis has been examined by Lim et al., who showed that active eNOS is crucial for tumor initiation and development. This effect is mediated by activation of endogenous RAS isoforms (i.e., Nras and Hras) by S-nitrosylation at Cys-118 (see V.4) (Lim et al., 2008). Soon thereafter, Lampson et al. showed that genetic deficiency of eNOS limits the development of PanINs as well as PDAC and that eNOS-deficient mice with advanced pancreatic cancer exhibited a trend toward an extended lifespan (Lampson et al., 2012). Both research teams attributed PDAC development to eNOS activation/phosphorylation inhibition of tumor development to inhibition of eNOS (either genetically or by administration of L-NAME). When comparing their findings to those of this study, at first glance, they may seem to be in opposition, as we observed decreased tumor development and enhanced levels of phosphorylated eNOS in the Txnrd2-deficient mice/cell lines. However, we believe this can be explained by the time at which Txnrd2 was depleted: In our model, Txnrd2 is depleted at early stages of embryonic development; hence, Kras-driven carcinogenesis proceeds in the background of altered signaling due to Txnrd2 depletion and its implications for eNOS and/or NO signaling. To examine this issue further, experiments with a conditional knockout of Txnrd2 should be undertaken in order to investigate the effect of late Txnrd2 depletion in later stages of carcinogenesis.

When examining levels of DAF staining and RAS activity, we observed a negative correlation between DAF staining and RAS activity: Txnrd2-depleted cell lines showed low activity of GTP-bound RAS and higher levels of NO.

The formation of S-nitrosothiols, a post-translational modification, is significant for cell signaling, affecting a variety of proteins (Gaston, Carver, Doctor, & Palmer, 2003). The signaling effect of S-nitrosation on the RAS molecule has also been established, as previously described (Raines, Bonini, & Campbell, 2007). In 1997, Lander et at. identified a site (Cys-118) on the RAS – protein responsible for NO signal transduction, resulting in guanine exchange and downstream signal transduction (Lander et al., 1997). More recently, Williams et al. showed that it is not the stable S-nitrosylation of the cysteine that leads to a guanine-exchange function, resulting in enhanced RAS activity, but the “actual chemical process of nitrosylation” (Williams, Pappu, & Campbell, 2003). Mice with a point mutation in Cys-118, thus disabling nitrosylation, show decreased tumor progression in a lung cancer model with the co-mutation $Kras^{G12D}$ (L. Huang, Carney, Cardona, & Counter, 2014).

This shows the dynamics of nitrosylation and de-nitrosylation and helps explain why we observed enhanced levels of NO signaling but decreased RAS activity: We postulate that, in Txnrd2-deficient cell lines, these processes are, through depletion of one major player of nitrosylation, more static. This results in low RAS activity.

The overall effect of Txnrd2-depletion → high eNOS phosphorylation → low RAS activity is reduced tumor incidence. What remains to be examined are the characteristics of the alterations of RAS isoforms. The experiments following this study will aim to elucidate this connection further, aiming to provide conclusive, mechanistic proof of the underlying nitrosylation signaling.

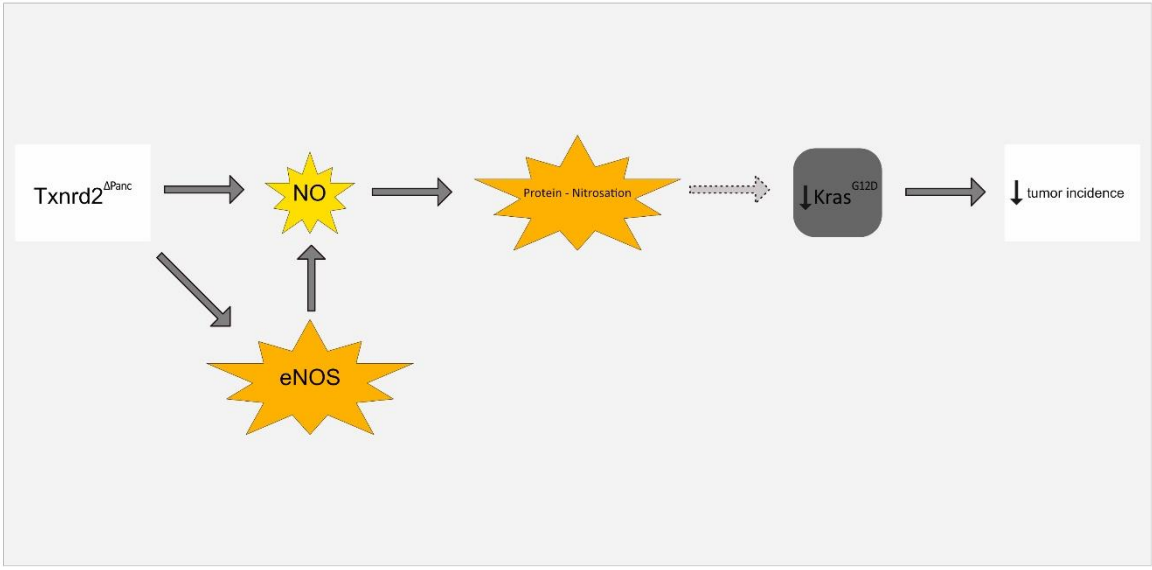

Figure VII-2 Underlying mechanisms in the* Kras$^{+/G12D}$; Txnrd2$^{\Delta Panc}$ *model.
In this study, we see that genetic depletion of Txnrd2 leads to higher levels of NO and higher acitivity of endothelial NO synthase (eNOS). This leads to altered protein nitrosylation. The effect is a lowered Kras activity as measured by GTP-bound RAS, which results in reduced tumor incidence in Kras$^{+/G12D}$; Txnrd2$^{\Delta Panc}$ *genetically engineered mouse models.*

VIII. Summary

In this project, the effect of loss of mitochondrial thioredoxin reductase (Txnrd2) on pancreatic carcinogenesis and pancreatic cancer cells was examined. We observed altered biology and higher levels of ROS, but no changes in mitochondrial respiration. Also, we observed a higher number of precursor lesions in *Kras*^{G12D}*; Txnrd2*$^{\Delta Panc}$ mice, but a smaller number of invasive PDAC. This effect might be due to the lower activity of mutated RAS, perhaps caused by S-nitrosylation, as we also observed higher amount of NO signaling and eNOS activity in TXNRD2-deficient cell lines.

IX. Amendments

IX.1 References

abcam.com. Flow cytometric analysis of cell cycle with propidium iodide DNA staining Retrieved from https://www.abcam.com/protocols/flow-cytometric-analysis-of-cell-cycle-with-propidium-iodide-dna-staining

Abramov, A. Y., Scorziello, A., & Duchen, M. R. (2007). Three distinct mechanisms generate oxygen free radicals in neurons and contribute to cell death during anoxia and reoxygenation. *J Neurosci, 27*(5), 1129-1138. doi:10.1523/JNEUROSCI.4468-06.2007

Aguer, C., Gambarotta, D., Mailloux, R. J., Moffat, C., Dent, R., McPherson, R., & Harper, M. E. (2011). Galactose enhances oxidative metabolism and reveals mitochondrial dysfunction in human primary muscle cells. *PLoS One, 6*(12), e28536. doi:10.1371/journal.pone.0028536

Aguirre, A. J., Bardeesy, N., Sinha, M., Lopez, L., Tuveson, D. A., Horner, J., . . . DePinho, R. A. (2003). Activated Kras and Ink4a/Arf deficiency cooperate to produce metastatic pancreatic ductal adenocarcinoma. *Genes Dev, 17*(24), 3112-3126. doi:10.1101/gad.1158703

Al Saati, T., Clerc, P., Hanoun, N., Peuget, S., Lulka, H., Gigoux, V., . . . Dufresne, M. (2013). Oxidative stress induced by inactivation of TP53INP1 cooperates with KrasG12D to initiate and promote pancreatic carcinogenesis in the murine pancreas. *Am J Pathol, 182*(6), 1996-2004. doi:10.1016/j.ajpath.2013.02.034

Allen, J. A., & Coombs, M. M. (1980). Covalent binding of polycyclic aromatic compounds to mitochondrial and nuclear DNA. *Nature, 287*(5779), 244-245. doi:10.1038/287244a0

Almoguera, C., Shibata, D., Forrester, K., Martin, J., Arnheim, N., & Perucho, M. (1988). Most human carcinomas of the exocrine pancreas contain mutant c-K-ras genes. *Cell, 53*(4), 549-554.

Arai, R. J., Ogata, F. T., Batista, W. L., Masutani, H., Yodoi, J., Debbas, V., . . . Monteiro, H. P. (2008). Thioredoxin-1 promotes survival in cells exposed to S-nitrosoglutathione: Correlation with reduction of intracellular levels of nitrosothiols and up-regulation of the ERK1/2 MAP Kinases. *Toxicol Appl Pharmacol, 233*(2), 227-237. doi:10.1016/j.taap.2008.07.023

Arner, E. S. (2009). Focus on mammalian thioredoxin reductases--important selenoproteins with versatile functions. *Biochim Biophys Acta, 1790*(6), 495-526. doi:10.1016/j.bbagen.2009.01.014

Arner, E. S., & Holmgren, A. (2000). Physiological functions of thioredoxin and thioredoxin reductase. *Eur J Biochem, 267*(20), 6102-6109.

Avruch, J., Khokhlatchev, A., Kyriakis, J. M., Luo, Z., Tzivion, G., Vavvas, D., & Zhang, X. F. (2001). Ras activation of the Raf kinase: tyrosine kinase recruitment of the MAP kinase cascade. *Recent Prog Horm Res, 56*, 127-155.

Backer, J. M., & Weinstein, I. B. (1980). Mitochondrial DNA is a major cellular target for a dihydrodiol-epoxide derivative of benzo[a]pyrene. *Science, 209*(4453), 297-299. doi:10.1126/science.6770466

Balkwill, F., & Mantovani, A. (2001). Inflammation and cancer: back to Virchow? *Lancet, 357*(9255), 539-545. doi:10.1016/S0140-6736(00)04046-0

Begas, P., Liedgens, L., Moseler, A., Meyer, A. J., & Deponte, M. (2017). Glutaredoxin catalysis requires two distinct glutathione interaction sites. *Nat Commun, 8*, 14835. doi:10.1038/ncomms14835

Benhar, M., Forrester, M. T., Hess, D. T., & Stamler, J. S. (2008). Regulated protein denitrosylation by cytosolic and mitochondrial thioredoxins. *Science, 320*(5879), 1050-1054. doi:10.1126/science.1158265

Bergeron, F., Auvre, F., Radicella, J. P., & Ravanat, J. L. (2010). HO* radicals induce an unexpected high proportion of tandem base lesions refractory to repair by DNA glycosylases. *Proc Natl Acad Sci U S A, 107*(12), 5528-5533. doi:10.1073/pnas.1000193107

Bertoli, C., Skotheim, J. M., & de Bruin, R. A. (2013). Control of cell cycle transcription during G1 and S phases. *Nat Rev Mol Cell Biol, 14*(8), 518-528. doi:10.1038/nrm3629

Bhabak, K. P., & Mugesh, G. (2010). Functional mimics of glutathione peroxidase: bioinspired synthetic antioxidants. *Acc Chem Res, 43*(11), 1408-1419. doi:10.1021/ar100059g

Biankin, A. V., Waddell, N., Kassahn, K. S., Gingras, M. C., Muthuswamy, L. B., Johns, A. L., . . . Grimmond, S. M. (2012). Pancreatic cancer genomes reveal aberrations in axon guidance pathway genes. *Nature, 491*(7424), 399-405. doi:10.1038/nature11547

Bienert, G. P., Moller, A. L., Kristiansen, K. A., Schulz, A., Moller, I. M., Schjoerring, J. K., & Jahn, T. P. (2007). Specific aquaporins facilitate the diffusion of hydrogen peroxide across membranes. *J Biol Chem, 282*(2), 1183-1192. doi:10.1074/jbc.M603761200

Boengler, K., Heusch, G., & Schulz, R. (2011). Nuclear-encoded mitochondrial proteins and their role in cardioprotection. *Biochim Biophys Acta, 1813*(7), 1286-1294. doi:10.1016/j.bbamcr.2011.01.009

Bonekamp, N. A., Volkl, A., Fahimi, H. D., & Schrader, M. (2009). Reactive oxygen species and peroxisomes: struggling for balance. *Biofactors, 35*(4), 346-355. doi:10.1002/biof.48

Borst, J. W., Visser, N. V., Kouptsova, O., & Visser, A. J. (2000). Oxidation of unsaturated phospholipids in membrane bilayer mixtures is accompanied by membrane fluidity changes. *Biochim Biophys Acta, 1487*(1), 61-73.

Burdick, A. D., Davis, J. W., 2nd, Liu, K. J., Hudson, L. G., Shi, H., Monske, M. L., & Burchiel, S. W. (2003). Benzo(a)pyrene quinones increase cell proliferation, generate reactive oxygen species, and transactivate the epidermal growth factor receptor in breast epithelial cells. *Cancer Res, 63*(22), 7825-7833.

Cadet, J., & Wagner, J. R. (2013). DNA base damage by reactive oxygen species, oxidizing agents, and UV radiation. *Cold Spring Harb Perspect Biol, 5*(2). doi:10.1101/cshperspect.a012559

Caldas, C., Hahn, S. A., da Costa, L. T., Redston, M. S., Schutte, M., Seymour, A. B., . . . Kern, S. E. (1994). Frequent somatic mutations and homozygous deletions of the p16 (MTS1) gene in pancreatic adenocarcinoma. *Nat Genet, 8*(1), 27-32. doi:10.1038/ng0994-27

Campbell, P. J., Yachida, S., Mudie, L. J., Stephens, P. J., Pleasance, E. D., Stebbings, L. A., . . . Futreal, P. A. (2010). The patterns and dynamics of genomic instability in metastatic pancreatic cancer. *Nature, 467*(7319), 1109-1113. doi:10.1038/nature09460

Cano, C. E., Gommeaux, J., Pietri, S., Culcasi, M., Garcia, S., Seux, M., . . . Carrier, A. (2009). Tumor protein 53-induced nuclear protein 1 is a major mediator of p53 antioxidant function. *Cancer Res, 69*(1), 219-226. doi:10.1158/0008-5472.CAN-08-2320

Chae, Y. K., Anker, J. F., Oh, M. S., Bais, P., Namburi, S., Agte, S., . . . Chuang, J. H. (2019). Mutations in DNA repair genes are associated with increased neoantigen burden and a distinct immunophenotype in lung squamous cell carcinoma. *Sci Rep, 9*(1), 3235. doi:10.1038/s41598-019-39594-4

Chan, D. W., Liu, V. W., Tsao, G. S., Yao, K. M., Furukawa, T., Chan, K. K., & Ngan, H. Y. (2008). Loss of MKP3 mediated by oxidative stress enhances tumorigenicity and chemoresistance of ovarian cancer cells. *Carcinogenesis, 29*(9), 1742-1750. doi:10.1093/carcin/bgn167

Chan, K., Han, X. D., & Kan, Y. W. (2001). An important function of Nrf2 in combating oxidative stress: detoxification of acetaminophen. *Proc Natl Acad Sci U S A, 98*(8), 4611-4616. doi:10.1073/pnas.081082098

Chance, B., Sies, H., & Boveris, A. (1979). Hydroperoxide metabolism in mammalian organs. *Physiol Rev, 59*(3), 527-605. doi:10.1152/physrev.1979.59.3.527

Chang, E. H., Gonda, M. A., Ellis, R. W., Scolnick, E. M., & Lowy, D. R. (1982). Human genome contains four genes homologous to transforming genes of Harvey and Kirsten murine sarcoma viruses. *Proc Natl Acad Sci U S A, 79*(16), 4848-4852. doi:10.1073/pnas.79.16.4848

Cheng, G., Cao, Z., Xu, X., van Meir, E. G., & Lambeth, J. D. (2001). Homologs of gp91phox: cloning and tissue expression of Nox3, Nox4, and Nox5. *Gene, 269*(1-2), 131-140.

Chris D. St. Laurent , T. C. M., and A. Dean Befus *Measurement of Nitric Oxide in Mast Cells*

with the Fluorescent Indicator DAF-FM Diacetate

Chun, S. Y., Johnson, C., Washburn, J. G., Cruz-Correa, M. R., Dang, D. T., & Dang, L. H. (2010). Oncogenic KRAS modulates mitochondrial metabolism in human colon cancer cells by inducing HIF-1alpha and HIF-2alpha target genes. *Mol Cancer, 9*, 293. doi:10.1186/1476-4598-9-293

Cimprich, K. A., & Cortez, D. (2008). ATR: an essential regulator of genome integrity. *Nat Rev Mol Cell Biol, 9*(8), 616-627. doi:10.1038/nrm2450

Clanton, T. L. (2007). Hypoxia-induced reactive oxygen species formation in skeletal muscle. *J Appl Physiol (1985), 102*(6), 2379-2388. doi:10.1152/japplphysiol.01298.2006

Clayton, D. A., & Shadel, G. S. (2014). Isolation of mitochondria from tissue culture cells. *Cold Spring Harb Protoc, 2014*(10), pdb prot080002. doi:10.1101/pdb.prot080002

Coluzzi, E., Colamartino, M., Cozzi, R., Leone, S., Meneghini, C., O'Callaghan, N., & Sgura, A. (2014). Oxidative stress induces persistent telomeric DNA damage responsible for nuclear morphology change in mammalian cells. *PLoS One, 9*(10), e110963. doi:10.1371/journal.pone.0110963

Conrad, M., Jakupoglu, C., Moreno, S. G., Lippl, S., Banjac, A., Schneider, M., . . . Brielmeier, M. (2004). Essential role for mitochondrial thioredoxin reductase in hematopoiesis, heart development, and heart function. *Mol Cell Biol, 24*(21), 9414-9423. doi:10.1128/MCB.24.21.9414-9423.2004

Courtnay, R., Ngo, D. C., Malik, N., Ververis, K., Tortorella, S. M., & Karagiannis, T. C. (2015). Cancer metabolism and the Warburg effect: the role of HIF-1 and PI3K. *Mol Biol Rep, 42*(4), 841-851. doi:10.1007/s11033-015-3858-x

Cullen, J. J., Weydert, C., Hinkhouse, M. M., Ritchie, J., Domann, F. E., Spitz, D., & Oberley, L. W. (2003). The role of manganese superoxide dismutase in the growth of pancreatic adenocarcinoma. *Cancer Res, 63*(6), 1297-1303.

D'Autreaux, B., & Toledano, M. B. (2007). ROS as signalling molecules: mechanisms that generate specificity in ROS homeostasis. *Nat Rev Mol Cell Biol, 8*(10), 813-824. doi:10.1038/nrm2256

Dansen, T. B., & Wirtz, K. W. (2001). The peroxisome in oxidative stress. *IUBMB Life, 51*(4), 223-230. doi:10.1080/152165401753311762

De La, O. J., Emerson, L. L., Goodman, J. L., Froebe, S. C., Illum, B. E., Curtis, A. B., & Murtaugh, L. C. (2008). Notch and Kras reprogram pancreatic acinar cells to ductal intraepithelial neoplasia. *Proc Natl Acad Sci U S A, 105*(48), 18907-18912. doi:10.1073/pnas.0810111105

de Sa Junior, P. L., Camara, D. A. D., Porcacchia, A. S., Fonseca, P. M. M., Jorge, S. D., Araldi, R. P., & Ferreira, A. K. (2017). The Roles of ROS in Cancer Heterogeneity and Therapy. *Oxid Med Cell Longev, 2017*, 2467940. doi:10.1155/2017/2467940

DeNicola, G. M., Karreth, F. A., Humpton, T. J., Gopinathan, A., Wei, C., Frese, K., . . . Tuveson, D. A. (2011). Oncogene-induced Nrf2 transcription promotes ROS detoxification and tumorigenesis. *Nature, 475*(7354), 106-109. doi:10.1038/nature10189

Dibra, D., Mishra, L., & Li, S. (2014). Molecular mechanisms of oncogene-induced inflammation and inflammation-sustained oncogene activation in gastrointestinal tumors: an under-appreciated symbiotic relationship. *Biochim Biophys Acta, 1846*(1), 152-160. doi:10.1016/j.bbcan.2014.05.001

DiMagno, E. P., Reber, H. A., & Tempero, M. A. (1999). AGA technical review on the epidemiology, diagnosis, and treatment of pancreatic ductal adenocarcinoma. American Gastroenterological Association. *Gastroenterology, 117*(6), 1464-1484.

Edes, K., Cassidy, P., Shami, P. J., & Moos, P. J. (2010). JS-K, a nitric oxide prodrug, has enhanced cytotoxicity in colon cancer cells with knockdown of thioredoxin reductase 1. *PLoS One, 5*(1), e8786. doi:10.1371/journal.pone.0008786

Ernster, L., & Dallner, G. (1995). Biochemical, physiological and medical aspects of ubiquinone function. *Biochim Biophys Acta, 1271*(1), 195-204.

Eroglu, E., Saravi, S. S. S., Sorrentino, A., Steinhorn, B., & Michel, T. (2019). Discordance between eNOS phosphorylation and activation revealed by multispectral imaging and chemogenetic methods. *Proc Natl Acad Sci U S A, 116*(40), 20210-20217. doi:10.1073/pnas.1910942116

Evans, J., Maccabee, M., Hatahet, Z., Courcelle, J., Bockrath, R., Ide, H., & Wallace, S. (1993). Thymine ring saturation and fragmentation products: lesion bypass, misinsertion and implications for mutagenesis. *Mutat Res, 299*(3-4), 147-156.

Fearon, E. R., & Vogelstein, B. (1990). A genetic model for colorectal tumorigenesis. *Cell, 61*(5), 759-767.

Felty, Q., Singh, K. P., & Roy, D. (2005). Estrogen-induced G1/S transition of G0-arrested estrogen-dependent breast cancer cells is regulated by mitochondrial oxidant signaling. *Oncogene, 24*(31), 4883-4893. doi:10.1038/sj.onc.1208667

Ferret, P. J., Soum, E., Negre, O., Wollman, E. E., & Fradelizi, D. (2000). Protective effect of thioredoxin upon NO-mediated cell injury in THP1 monocytic human cells. *Biochem J, 346 Pt 3*, 759-765.

Ferrington, D. A., & Kapphahn, R. J. (2004). Catalytic site-specific inhibition of the 20S proteasome by 4-hydroxynonenal. *FEBS Lett, 578*(3), 217-223. doi:10.1016/j.febslet.2004.11.003

Fish, J. E., Matouk, C. C., Rachlis, A., Lin, S., Tai, S. C., D'Abreo, C., & Marsden, P. A. (2005). The expression of endothelial nitric-oxide synthase is controlled by a cell-specific histone code. *J Biol Chem, 280*(26), 24824-24838. doi:10.1074/jbc.M502115200

Flynn, R. L., & Zou, L. (2011). ATR: a master conductor of cellular responses to DNA replication stress. *Trends Biochem Sci, 36*(3), 133-140. doi:10.1016/j.tibs.2010.09.005

Forrester, M. T., Seth, D., Hausladen, A., Eyler, C. E., Foster, M. W., Matsumoto, A., . . . Stamler, J. S. (2009). Thioredoxin-interacting protein (Txnip) is a feedback regulator of S-nitrosylation. *J Biol Chem, 284*(52), 36160-36166. doi:10.1074/jbc.M109.057729

Fraga, C. G., Shigenaga, M. K., Park, J. W., Degan, P., & Ames, B. N. (1990). Oxidative damage to DNA during aging: 8-hydroxy-2'-deoxyguanosine in rat organ DNA and urine. *Proc Natl Acad Sci U S A, 87*(12), 4533-4537.

Garodia, P., Ichikawa, H., Malani, N., Sethi, G., & Aggarwal, B. B. (2007). From ancient medicine to modern medicine: ayurvedic concepts of health and their role in inflammation and cancer. *J Soc Integr Oncol, 5*(1), 25-37.

Gaschler, M. M., & Stockwell, B. R. (2017). Lipid peroxidation in cell death. *Biochem Biophys Res Commun, 482*(3), 419-425. doi:10.1016/j.bbrc.2016.10.086

Gaston, B. M., Carver, J., Doctor, A., & Palmer, L. A. (2003). S-nitrosylation signaling in cell biology. *Mol Interv, 3*(5), 253-263. doi:10.1124/mi.3.5.253

Geiszt, M. (2006). NADPH oxidases: new kids on the block. *Cardiovasc Res, 71*(2), 289-299. doi:10.1016/j.cardiores.2006.05.004

Gideon, P., John, J., Frech, M., Lautwein, A., Clark, R., Scheffler, J. E., & Wittinghofer, A. (1992). Mutational and kinetic analyses of the GTPase-activating protein (GAP)-p21 interaction: the C-terminal domain of GAP is not sufficient for full activity. *Mol Cell Biol, 12*(5), 2050-2056. doi:10.1128/mcb.12.5.2050

Gong, F., Hou, G., Liu, H., & Zhang, M. (2015). Peroxiredoxin 1 promotes tumorigenesis through regulating the activity of mTOR/p70S6K pathway in esophageal squamous cell carcinoma. *Med Oncol, 32*(2), 455. doi:10.1007/s12032-014-0455-0

Grimsrud, P. A., Xie, H., Griffin, T. J., & Bernlohr, D. A. (2008). Oxidative stress and covalent modification of protein with bioactive aldehydes. *J Biol Chem, 283*(32), 21837-21841. doi:10.1074/jbc.R700019200

Guerra, C., Schuhmacher, A. J., Canamero, M., Grippo, P. J., Verdaguer, L., Perez-Gallego, L., . . . Barbacid, M. (2007). Chronic pancreatitis is essential for induction of pancreatic ductal adenocarcinoma by K-Ras oncogenes in adult mice. *Cancer Cell, 11*(3), 291-302. doi:10.1016/j.ccr.2007.01.012

Han, D., Canali, R., Rettori, D., & Kaplowitz, N. (2003). Effect of glutathione depletion on sites and topology of superoxide and hydrogen peroxide production in mitochondria. *Mol Pharmacol, 64*(5), 1136-1144. doi:10.1124/mol.64.5.1136

Hanahan, D., & Weinberg, R. A. (2000). The hallmarks of cancer. *Cell, 100*(1), 57-70.

Hanahan, D., & Weinberg, R. A. (2011). Hallmarks of cancer: the next generation. *Cell, 144*(5), 646-674. doi:10.1016/j.cell.2011.02.013

Harvey, J. J. (1964). An Unidentified Virus Which Causes the Rapid Production of Tumours in Mice. *Nature, 204*, 1104-1105. doi:10.1038/2041104b0

Heinrich, T. A., da Silva, R. S., Miranda, K. M., Switzer, C. H., Wink, D. A., & Fukuto, J. M. (2013). Biological nitric oxide signalling: chemistry and terminology. *Br J Pharmacol, 169*(7), 1417-1429. doi:10.1111/bph.12217

Hellfritsch, J., Kirsch, J., Schneider, M., Fluege, T., Wortmann, M., Frijhoff, J., . . . Beck, H. (2015). Knockout of mitochondrial thioredoxin reductase stabilizes prolyl hydroxylase 2 and inhibits tumor growth and tumor-derived angiogenesis. *Antioxid Redox Signal, 22*(11), 938-950. doi:10.1089/ars.2014.5889

Hezel, A. F., Kimmelman, A. C., Stanger, B. Z., Bardeesy, N., & Depinho, R. A. (2006). Genetics and biology of pancreatic ductal adenocarcinoma. *Genes Dev, 20*(10), 1218-1249. doi:10.1101/gad.1415606

Hidalgo, M. (2010). Pancreatic cancer. *N Engl J Med, 362*(17), 1605-1617. doi:10.1056/NEJMra0901557

Hilgers, R. H., Kundumani-Sridharan, V., Subramani, J., Chen, L. C., Cuello, L. G., Rusch, N. J., & Das, K. C. (2017). Thioredoxin reverses age-related hypertension by chronically improving vascular redox and restoring eNOS function. *Sci Transl Med, 9*(376). doi:10.1126/scitranslmed.aaf6094

Hingorani, S. R., Jacobetz, M. A., Robertson, G. P., Herlyn, M., & Tuveson, D. A. (2003). Suppression of BRAF(V599E) in human melanoma abrogates transformation. *Cancer Res, 63*(17), 5198-5202.

Hingorani, S. R., Petricoin, E. F., Maitra, A., Rajapakse, V., King, C., Jacobetz, M. A., . . . Tuveson, D. A. (2003). Preinvasive and invasive ductal pancreatic cancer and its early detection in the mouse. *Cancer Cell, 4*(6), 437-450.

Hodul, P. J., Dong, Y., Husain, K., Pimiento, J. M., Chen, J., Zhang, A., . . . Malafa, M. P. (2013). Vitamin E delta-tocotrienol induces p27(Kip1)-dependent cell-cycle arrest in pancreatic cancer cells via an E2F-1-dependent mechanism. *PLoS One, 8*(2), e52526. doi:10.1371/journal.pone.0052526

Holen, K. D., Klimstra, D. S., Hummer, A., Gonen, M., Conlon, K., Brennan, M., & Saltz, L. B. (2002). Clinical characteristics and outcomes from an institutional series of acinar cell carcinoma of the pancreas and related tumors. *J Clin Oncol, 20*(24), 4673-4678. doi:10.1200/JCO.2002.02.005

Homma, T., & Tsuchiya, R. (1991). The study of the mass screening of persons without symptoms and of the screening of outpatients with gastrointestinal complaints or icterus for pancreatic cancer in Japan, using CA19-9 and elastase-1 or ultrasonography. *Int J Pancreatol, 9*, 119-124.

Horstkotte, J., Perisic, T., Schneider, M., Lange, P., Schroeder, M., Kiermayer, C., . . . Kupatt, C. (2011). Mitochondrial thioredoxin reductase is essential for early postischemic myocardial protection. *Circulation, 124*(25), 2892-2902. doi:10.1161/CIRCULATIONAHA.111.059253

Huang, L., Carney, J., Cardona, D. M., & Counter, C. M. (2014). Decreased tumorigenesis in mice with a Kras point mutation at C118. *Nat Commun, 5*, 5410. doi:10.1038/ncomms6410

Huang, P. L., Huang, Z., Mashimo, H., Bloch, K. D., Moskowitz, M. A., Bevan, J. A., & Fishman, M. C. (1995). Hypertension in mice lacking the gene for endothelial nitric oxide synthase. *Nature, 377*(6546), 239-242. doi:10.1038/377239a0

Huggett, M. T., & Pereira, S. P. (2011). Diagnosing and managing pancreatic cancer. *Practitioner, 255*(1742), 21-25, 22-23.

Human Protein Atlas Retrieved from http://www.proteinatlas.org

Husain, K., Centeno, B. A., Coppola, D., Trevino, J., Sebti, S. M., & Malafa, M. P. (2017). delta-Tocotrienol, a natural form of vitamin E, inhibits pancreatic cancer stem-like cells and prevents pancreatic cancer metastasis. *Oncotarget, 8*(19), 31554-31567. doi:10.18632/oncotarget.15767

Iacobuzio-Donahue, C. A. (2012). Genetic evolution of pancreatic cancer: lessons learnt from the pancreatic cancer genome sequencing project. *Gut, 61*(7), 1085-1094. doi:10.1136/gut.2010.236026

Ishikawa, K., Takenaga, K., Akimoto, M., Koshikawa, N., Yamaguchi, A., Imanishi, H., . . . Hayashi, J. (2008). ROS-generating mitochondrial DNA mutations can regulate tumor cell metastasis. *Science, 320*(5876), 661-664. doi:10.1126/science.1156906

Jackson, E. L., Willis, N., Mercer, K., Bronson, R. T., Crowley, D., Montoya, R., . . . Tuveson, D. A. (2001). Analysis of lung tumor initiation and progression using conditional expression of oncogenic K-ras. *Genes Dev, 15*(24), 3243-3248. doi:10.1101/gad.943001

Jancik, S., Drabek, J., Radzioch, D., & Hajduch, M. (2010). Clinical relevance of KRAS in human cancers. *J Biomed Biotechnol, 2010*, 150960. doi:10.1155/2010/150960

Jemal, A., Bray, F., Center, M. M., Ferlay, J., Ward, E., & Forman, D. (2011). Global cancer statistics. *CA Cancer J Clin, 61*(2), 69-90. doi:10.3322/caac.20107

Johnson, L., Mercer, K., Greenbaum, D., Bronson, R. T., Crowley, D., Tuveson, D. A., & Jacks, T. (2001). Somatic activation of the K-ras oncogene causes early onset lung cancer in mice. *Nature, 410*(6832), 1111-1116. doi:10.1038/35074129

Jones, S., Zhang, X., Parsons, D. W., Lin, J. C., Leary, R. J., Angenendt, P., . . . Kinzler, K. W. (2008). Core signaling pathways in human pancreatic cancers revealed by global genomic analyses. *Science, 321*(5897), 1801-1806. doi:10.1126/science.1164368

Kabakov, A. E., & Gabai, V. L. (2018). Cell Death and Survival Assays. *Methods Mol Biol, 1709*, 107-127. doi:10.1007/978-1-4939-7477-1_9

Kalyanaraman, B., Darley-Usmar, V., Davies, K. J., Dennery, P. A., Forman, H. J., Grisham, M. B., . . . Ischiropoulos, H. (2012). Measuring reactive oxygen and nitrogen species with fluorescent probes: challenges and limitations. *Free Radic Biol Med, 52*(1), 1-6. doi:10.1016/j.freeradbiomed.2011.09.030

Kamiya, H., Miura, H., Murata-Kamiya, N., Ishikawa, H., Sakaguchi, T., Inoue, H., . . . et al. (1995). 8-Hydroxyadenine (7,8-dihydro-8-oxoadenine) induces misincorporation in in vitro DNA synthesis and mutations in NIH 3T3 cells. *Nucleic Acids Res, 23*(15), 2893-2899.

Kannan, K., & Jain, S. K. (2000). Oxidative stress and apoptosis. *Pathophysiology, 7*(3), 153-163.

Karp, J. E., Burke, P. J., Saylor, P. L., & Humphrey, R. L. (1984). Correlation of proliferative and clonogenic tumor cells in multiple myeloma. *Cancer Res, 44*(9), 4197-4200.

Kiermayer, C., Northrup, E., Schrewe, A., Walch, A., de Angelis, M. H., Schoensiegel, F., . . . Brielmeier, M. (2015). Heart-Specific Knockout of the Mitochondrial Thioredoxin Reductase (Txnrd2) Induces Metabolic and Contractile Dysfunction in the Aging Myocardium. *J Am Heart Assoc, 4*(7). doi:10.1161/JAHA.115.002153

Kirkman, H. N., & Gaetani, G. F. (2007). Mammalian catalase: a venerable enzyme with new mysteries. *Trends Biochem Sci, 32*(1), 44-50. doi:10.1016/j.tibs.2006.11.003

Kirsten, W. H., & Mayer, L. A. (1967). Morphologic responses to a murine erythroblastosis virus. *J Natl Cancer Inst, 39*(2), 311-335.

Koopman, M., Michels, H., Dancy, B. M., Kamble, R., Mouchiroud, L., Auwerx, J., . . . Houtkooper, R. H. (2016). A screening-based platform for the assessment of cellular respiration in Caenorhabditis elegans. *Nat Protoc, 11*(10), 1798-1816. doi:10.1038/nprot.2016.106

Kopp, J. L., von Figura, G., Mayes, E., Liu, F. F., Dubois, C. L., Morris, J. P. t., . . . Sander, M. (2012). Identification of Sox9-dependent acinar-to-ductal reprogramming as the principal mechanism for initiation of pancreatic ductal adenocarcinoma. *Cancer Cell, 22*(6), 737-750. doi:10.1016/j.ccr.2012.10.025

Kovac, S., Angelova, P. R., Holmstrom, K. M., Zhang, Y., Dinkova-Kostova, A. T., & Abramov, A. Y. (2015). Nrf2 regulates ROS production by mitochondria and NADPH oxidase. *Biochim Biophys Acta, 1850*(4), 794-801. doi:10.1016/j.bbagen.2014.11.021

Kukreja, R. C., & Xi, L. (2007). eNOS phosphorylation: a pivotal molecular switch in vasodilation and cardioprotection? *J Mol Cell Cardiol, 42*(2), 280-282. doi:10.1016/j.yjmcc.2006.10.011

Kuper, H., Adami, H. O., & Trichopoulos, D. (2000). Infections as a major preventable cause of human cancer. *J Intern Med, 248*(3), 171-183.

Labunskyy, V. M., Hatfield, D. L., & Gladyshev, V. N. (2014). Selenoproteins: molecular pathways and physiological roles. *Physiol Rev, 94*(3), 739-777. doi:10.1152/physrev.00039.2013

Lampson, B. L., Kendall, S. D., Ancrile, B. B., Morrison, M. M., Shealy, M. J., Barrientos, K. S., . . . Counter, C. M. (2012). Targeting eNOS in pancreatic cancer. *Cancer Res, 72*(17), 4472-4482. doi:10.1158/0008-5472.CAN-12-0057

Lander, H. M., Hajjar, D. P., Hempstead, B. L., Mirza, U. A., Chait, B. T., Campbell, S., & Quilliam, L. A. (1997). A molecular redox switch on p21(ras). Structural basis for the nitric oxide-p21(ras) interaction. *J Biol Chem, 272*(7), 4323-4326.

Larsson, N. G., Wang, J., Wilhelmsson, H., Oldfors, A., Rustin, P., Lewandoski, M., . . . Clayton, D. A. (1998). Mitochondrial transcription factor A is necessary for mtDNA maintenance and embryogenesis in mice. *Nat Genet, 18*(3), 231-236. doi:10.1038/ng0398-231

Lawson, M. A., Whyte, D. B., & Mellon, P. L. (1996). GATA factors are essential for activity of the neuron-specific enhancer of the gonadotropin-releasing hormone gene. *Mol Cell Biol, 16*(7), 3596-3605. doi:10.1128/mcb.16.7.3596

Leitlinienprogramm Onkologie der AWMF; Deutschen Krebsgesellschaft e.V. und Deutschen Krebshilfe e.V. (2013). S3-Leitlinie zum exokrinen Pankreaskarzinom.

Lewis, A. M., Matzdorf, S. S., & Rice, K. C. (2016). Fluorescent Detection of Intracellular Nitric Oxide in Staphylococcus aureus. *Bio Protoc, 6*(14). doi:10.21769/BioProtoc.1878

Lewis, C. A., Jr., Crayle, J., Zhou, S., Swanstrom, R., & Wolfenden, R. (2016). Cytosine deamination and the precipitous decline of spontaneous mutation during Earth's history. *Proc Natl Acad Sci U S A, 113*(29), 8194-8199. doi:10.1073/pnas.1607580113

Li, Q., & Engelhardt, J. F. (2006). Interleukin-1beta induction of NFkappaB is partially regulated by H2O2-mediated activation of NFkappaB-inducing kinase. *J Biol Chem, 281*(3), 1495-1505. doi:10.1074/jbc.M511153200

Li, X., Fang, P., Mai, J., Choi, E. T., Wang, H., & Yang, X. F. (2013). Targeting mitochondrial reactive oxygen species as novel therapy for inflammatory diseases and cancers. *J Hematol Oncol, 6*, 19. doi:10.1186/1756-8722-6-19

Liberti, M. V., & Locasale, J. W. (2016). The Warburg Effect: How Does it Benefit Cancer Cells? *Trends Biochem Sci, 41*(3), 211-218. doi:10.1016/j.tibs.2015.12.001

Lim, K. H., Ancrile, B. B., Kashatus, D. F., & Counter, C. M. (2008). Tumour maintenance is mediated by eNOS. *Nature, 452*(7187), 646-649. doi:10.1038/nature06778

Liou, G. Y., Doppler, H., DelGiorno, K. E., Zhang, L., Leitges, M., Crawford, H. C., . . . Storz, P. (2016). Mutant KRas-Induced Mitochondrial Oxidative Stress in Acinar Cells Upregulates EGFR Signaling to Drive Formation of Pancreatic Precancerous Lesions. *Cell Rep, 14*(10), 2325-2336. doi:10.1016/j.celrep.2016.02.029

Liou, G. Y., & Storz, P. (2010). Reactive oxygen species in cancer. *Free Radic Res, 44*(5), 479-496. doi:10.3109/10715761003667554

Lu, J., Sharma, L. K., & Bai, Y. (2009). Implications of mitochondrial DNA mutations and mitochondrial dysfunction in tumorigenesis. *Cell Res, 19*(7), 802-815. doi:10.1038/cr.2009.69

Ma, Q. (2013). Role of nrf2 in oxidative stress and toxicity. *Annu Rev Pharmacol Toxicol, 53*, 401-426. doi:10.1146/annurev-pharmtox-011112-140320

Madamanchi, N. R., & Runge, M. S. (2007). Mitochondrial dysfunction in atherosclerosis. *Circ Res, 100*(4), 460-473. doi:10.1161/01.RES.0000258450.44413.96

Makohon-Moore, A., & Iacobuzio-Donahue, C. A. (2016). Pancreatic cancer biology and genetics from an evolutionary perspective. *Nat Rev Cancer, 16*(9), 553-565. doi:10.1038/nrc.2016.66

Malumbres, M., & Barbacid, M. (2009). Cell cycle, CDKs and cancer: a changing paradigm. *Nat Rev Cancer, 9*(3), 153-166. doi:10.1038/nrc2602

Manna, S. K., Zhang, H. J., Yan, T., Oberley, L. W., & Aggarwal, B. B. (1998). Overexpression of manganese superoxide dismutase suppresses tumor necrosis factor-induced apoptosis and activation of nuclear transcription factor-kappaB and activated protein-1. *J Biol Chem, 273*(21), 13245-13254.

Mannick, J. B., Hausladen, A., Liu, L., Hess, D. T., Zeng, M., Miao, Q. X., . . . Stamler, J. S. (1999). Fas-induced caspase denitrosylation. *Science, 284*(5414), 651-654. doi:10.1126/science.284.5414.651

Mantovani, A., Allavena, P., Sica, A., & Balkwill, F. (2008). Cancer-related inflammation. *Nature, 454*(7203), 436-444. doi:10.1038/nature07205

Maor-Shoshani, A., Ben-Ari, V., & Livneh, Z. (2003). Lesion bypass DNA polymerases replicate across non-DNA segments. *Proc Natl Acad Sci U S A, 100*(25), 14760-14765. doi:10.1073/pnas.2433503100

Martinez-Useros, J., Li, W., Cabeza-Morales, M., & Garcia-Foncillas, J. (2017). Oxidative Stress: A New Target for Pancreatic Cancer Prognosis and Treatment. *J Clin Med, 6*(3). doi:10.3390/jcm6030029

Maxwell, P. H., Pugh, C. W., & Ratcliffe, P. J. (2001). Activation of the HIF pathway in cancer. *Curr Opin Genet Dev, 11*(3), 293-299.

McCain, J. (2013). The MAPK (ERK) Pathway: Investigational Combinations for the Treatment Of BRAF-Mutated Metastatic Melanoma. *P T, 38*(2), 96-108.

McPherson, L. A., Troccoli, C. I., Ji, D., Bowles, A. E., Gardiner, M. L., Mohsen, M. G., . . . Ford, J. M. (2019). Increased MTH1-specific 8-oxodGTPase activity is a hallmark of cancer in colon, lung and pancreatic tissue. *DNA Repair (Amst), 83*, 102644. doi:10.1016/j.dnarep.2019.102644

Meng, Q., Shi, S., Liang, C., Liang, D., Hua, J., Zhang, B., . . . Yu, X. (2018). Abrogation of glutathione peroxidase-1 drives EMT and chemoresistance in pancreatic cancer by activating ROS-mediated Akt/GSK3beta/Snail signaling. *Oncogene, 37*(44), 5843-5857. doi:10.1038/s41388-018-0392-z

Mihailovic, T., Marx, M., Auer, A., Van Lint, J., Schmid, M., Weber, C., & Seufferlein, T. (2004). Protein kinase D2 mediates activation of nuclear factor kappaB by Bcr-Abl in Bcr-Abl+ human myeloid leukemia cells. *Cancer Res, 64*(24), 8939-8944. doi:10.1158/0008-5472.CAN-04-0981

Miller, M., Shirole, N., Tian, R., Pal, D., & Sordella, R. (2016). The Evolution of TP53 Mutations: From Loss-of-Function to Separation-of-Function Mutants. *J Cancer Biol Res, 4*(4).

Miura, F., Takada, T., Amano, H., Yoshida, M., Furui, S., & Takeshita, K. (2006). Diagnosis of pancreatic cancer. *HPB (Oxford), 8*(5), 337-342. doi:10.1080/13651820500540949

Mochizuki, T., Furuta, S., Mitsushita, J., Shang, W. H., Ito, M., Yokoo, Y., . . . Kamata, T. (2006). Inhibition of NADPH oxidase 4 activates apoptosis via the AKT/apoptosis signal-regulating kinase 1 pathway in pancreatic cancer PANC-1 cells. *Oncogene, 25*(26), 3699-3707. doi:10.1038/sj.onc.1209406

Mohammad, J., Singh, R. R., Riggle, C., Haugrud, B., Abdalla, M. Y., & Reindl, K. M. (2019). JNK inhibition blocks piperlongumine-induced cell death and transcriptional activation of heme oxygenase-1 in pancreatic cancer cells. *Apoptosis, 24*(9-10), 730-744. doi:10.1007/s10495-019-01553-9

Moriya, M. (1993). Single-stranded shuttle phagemid for mutagenesis studies in mammalian cells: 8-oxoguanine in DNA induces targeted G.C-->T.A transversions in simian kidney cells. *Proc Natl Acad Sci U S A, 90*(3), 1122-1126.

Movafagh, S., Crook, S., & Vo, K. (2015). Regulation of hypoxia-inducible factor-1a by reactive oxygen species: new developments in an old debate. *J Cell Biochem, 116*(5), 696-703. doi:10.1002/jcb.25074

Mueller, S., Engleitner, T., Maresch, R., Zukowska, M., Lange, S., Kaltenbacher, T., . . . Rad, R. (2018). Evolutionary routes and KRAS dosage define pancreatic cancer phenotypes. *Nature, 554*(7690), 62-68. doi:10.1038/nature25459

Mulkeen, A. L., Yoo, P. S., & Cha, C. (2006). Less common neoplasms of the pancreas. *World J Gastroenterol, 12*(20), 3180-3185.

N'Guessan, P., Pouyet, L., Gosset, G., Hamlaoui, S., Seillier, M., Cano, C. E., . . . Carrier, A. (2011). Absence of tumor suppressor tumor protein 53-induced nuclear protein 1 (TP53INP1) sensitizes mouse thymocytes and embryonic fibroblasts to redox-driven apoptosis. *Antioxid Redox Signal, 15*(6), 1639-1653. doi:10.1089/ars.2010.3553

Nathan, C. (2003). Specificity of a third kind: reactive oxygen and nitrogen intermediates in cell signaling. *J Clin Invest, 111*(6), 769-778. doi:10.1172/JCI18174

Neoptolemos, J. P., Stocken, D. D., Friess, H., Bassi, C., Dunn, J. A., Hickey, H., . . . European Study Group for Pancreatic, C. (2004). A randomized trial of chemoradiotherapy and chemotherapy after resection of pancreatic cancer. *N Engl J Med, 350*(12), 1200-1210. doi:10.1056/NEJMoa032295

Nguyen, T., Nioi, P., & Pickett, C. B. (2009). The Nrf2-antioxidant response element signaling pathway and its activation by oxidative stress. *J Biol Chem, 284*(20), 13291-13295. doi:10.1074/jbc.R900010200

Nishiyama, A., Matsui, M., Iwata, S., Hirota, K., Masutani, H., Nakamura, H., . . . Yodoi, J. (1999). Identification of thioredoxin-binding protein-2/vitamin D(3) up-regulated protein 1 as a negative regulator of thioredoxin function and expression. *J Biol Chem, 274*(31), 21645-21650. doi:10.1074/jbc.274.31.21645

Oettle, H., Post, S., Neuhaus, P., Gellert, K., Langrehr, J., Ridwelski, K., . . . Riess, H. (2007). Adjuvant chemotherapy with gemcitabine vs observation in patients undergoing curative-intent resection of pancreatic cancer: a randomized controlled trial. *JAMA, 297*(3), 267-277. doi:10.1001/jama.297.3.267

Ohneda, K., & Yamamoto, M. (2002). Roles of hematopoietic transcription factors GATA-1 and GATA-2 in the development of red blood cell lineage. *Acta Haematol, 108*(4), 237-245. doi:10.1159/000065660

Oken, M. M., Creech, R. H., Tormey, D. C., Horton, J., Davis, T. E., McFadden, E. T., & Carbone, P. P. (1982). Toxicity and response criteria of the Eastern Cooperative Oncology Group. *Am J Clin Oncol, 5*(6), 649-655.

Opresko, P. L., Fan, J., Danzy, S., Wilson, D. M., 3rd, & Bohr, V. A. (2005). Oxidative damage in telomeric DNA disrupts recognition by TRF1 and TRF2. *Nucleic Acids Res, 33*(4), 1230-1239. doi:10.1093/nar/gki273

Pan, B., Lee, Y., Rodriguez, T., Lee, J., & Saif, M. W. (2012). Secondary tumors of the pancreas: a case series. *Anticancer Res, 32*(4), 1449-1452.

Paradies, G., Petrosillo, G., Pistolese, M., Di Venosa, N., Federici, A., & Ruggiero, F. M. (2004). Decrease in mitochondrial complex I activity in ischemic/reperfused rat heart: involvement of reactive oxygen species and cardiolipin. *Circ Res, 94*(1), 53-59. doi:10.1161/01.RES.0000109416.56608.64

Paradise, B. D., Barham, W., & Fernandez-Zapico, M. E. (2018). Targeting Epigenetic Aberrations in Pancreatic Cancer, a New Path to Improve Patient Outcomes? *Cancers (Basel), 10*(5). doi:10.3390/cancers10050128

Park, S. A., Na, H. K., Kim, E. H., Cha, Y. N., & Surh, Y. J. (2009). 4-hydroxyestradiol induces anchorage-independent growth of human mammary epithelial cells via activation of IkappaB kinase: potential role of reactive oxygen species. *Cancer Res, 69*(6), 2416-2424. doi:10.1158/0008-5472.CAN-08-2177

Park, Y. H., Kim, S. U., Kwon, T. H., Kim, J. M., Song, I. S., Shin, H. J., . . . Yu, D. Y. (2016). Peroxiredoxin II promotes hepatic tumorigenesis through cooperation with Ras/Forkhead box M1 signaling pathway. *Oncogene, 35*(27), 3503-3513. doi:10.1038/onc.2015.411

Pathania, V., Syal, N., Pathak, C. M., & Khanduja, K. L. (1999). Vitamin E suppresses the induction of reactive oxygen species release by lipopolysaccharide, interleukin-1beta and tumor necrosis factor-alpha in rat alveolar macrophages. *J Nutr Sci Vitaminol (Tokyo), 45*(6), 675-686.

Pelzer, U., Schwaner, I., Stieler, J., Adler, M., Seraphin, J., Dorken, B., . . . Oettle, H. (2011). Best supportive care (BSC) versus oxaliplatin, folinic acid and 5-fluorouracil (OFF) plus BSC in patients for second-line advanced pancreatic cancer: a phase III-study from the German CONKO-study group. *Eur J Cancer, 47*(11), 1676-1681. doi:10.1016/j.ejca.2011.04.011

Perrier, S., Hau, J., Gasparutto, D., Cadet, J., Favier, A., & Ravanat, J. L. (2006). Characterization of lysine-guanine cross-links upon one-electron oxidation of a guanine-containing oligonucleotide in the presence of a trilysine peptide. *J Am Chem Soc, 128*(17), 5703-5710. doi:10.1021/ja057656i

Petrosillo, G., Ruggiero, F. M., Di Venosa, N., & Paradies, G. (2003). Decreased complex III activity in mitochondria isolated from rat heart subjected to ischemia and reperfusion: role of reactive oxygen species and cardiolipin. *FASEB J, 17*(6), 714-716. doi:10.1096/fj.02-0729fje

Ponten, F., Jirstrom, K., & Uhlen, M. (2008, Dec). The Human Protein Atlas--a tool for pathology. *J Pathol.* 2008/10/15. Retrieved from https://www.ncbi.nlm.nih.gov/pubmed/18853439

Poole, L. B., Karplus, P. A., & Claiborne, A. (2004). Protein sulfenic acids in redox signaling. *Annu Rev Pharmacol Toxicol, 44*, 325-347. doi:10.1146/annurev.pharmtox.44.101802.121735

Pozarowski, P., & Darzynkiewicz, Z. (2004). Analysis of cell cycle by flow cytometry. *Methods Mol Biol, 281*, 301-311. doi:10.1385/1-59259-811-0:301

Prior, I. A., Lewis, P. D., & Mattos, C. (2012). A comprehensive survey of Ras mutations in cancer. *Cancer Res, 72*(10), 2457-2467. doi:10.1158/0008-5472.CAN-11-2612

Quante, A. S., Ming, C., Rottmann, M., Engel, J., Boeck, S., Heinemann, V., . . . Strauch, K. (2016). Projections of cancer incidence and cancer-related deaths in Germany by 2020 and 2030. *Cancer Med, 5*(9), 2649-2656. doi:10.1002/cam4.767

Quinn, M. T., & Gauss, K. A. (2004). Structure and regulation of the neutrophil respiratory burst oxidase: comparison with nonphagocyte oxidases. *J Leukoc Biol, 76*(4), 760-781. doi:10.1189/jlb.0404216

Radi, R., Turrens, J. F., Chang, L. Y., Bush, K. M., Crapo, J. D., & Freeman, B. A. (1991). Detection of catalase in rat heart mitochondria. *J Biol Chem, 266*(32), 22028-22034.

Rahib, L., Smith, B. D., Aizenberg, R., Rosenzweig, A. B., Fleshman, J. M., & Matrisian, L. M. (2014). Projecting cancer incidence and deaths to 2030: the unexpected burden of thyroid, liver, and pancreas cancers in the United States. *Cancer Res, 74*(11), 2913-2921. doi:10.1158/0008-5472.CAN-14-0155

Raines, K. W., Bonini, M. G., & Campbell, S. L. (2007). Nitric oxide cell signaling: S-nitrosation of Ras superfamily GTPases. *Cardiovasc Res, 75*(2), 229-239. doi:10.1016/j.cardiores.2007.04.013

Reddy, J. K., & Mannaerts, G. P. (1994). Peroxisomal lipid metabolism. *Annu Rev Nutr, 14*, 343-370. doi:10.1146/annurev.nu.14.070194.002015

Redston, M. S., Caldas, C., Seymour, A. B., Hruban, R. H., da Costa, L., Yeo, C. J., & Kern, S. E. (1994). p53 mutations in pancreatic carcinoma and evidence of common involvement of homocopolymer tracts in DNA microdeletions. *Cancer Res, 54*(11), 3025-3033.

Redza-Dutordoir, M., & Averill-Bates, D. A. (2016). Activation of apoptosis signalling pathways by reactive oxygen species. *Biochim Biophys Acta, 1863*(12), 2977-2992. doi:10.1016/j.bbamcr.2016.09.012

Reichert, M., Blume, K., Kleger, A., Hartmann, D., & von Figura, G. (2016). Developmental Pathways Direct Pancreatic Cancer Initiation from Its Cellular Origin. *Stem Cells Int, 2016*, 9298535. doi:10.1155/2016/9298535

Rhee, S. G., Chae, H. Z., & Kim, K. (2005). Peroxiredoxins: a historical overview and speculative preview of novel mechanisms and emerging concepts in cell signaling. *Free Radic Biol Med, 38*(12), 1543-1552. doi:10.1016/j.freeradbiomed.2005.02.026

Rooney, J. P., Ryde, I. T., Sanders, L. H., Howlett, E. H., Colton, M. D., Germ, K. E., . . . Meyer, J. N. (2015). PCR based determination of mitochondrial DNA copy number in multiple species. *Methods Mol Biol, 1241*, 23-38. doi:10.1007/978-1-4939-1875-1_3

Ruess, D. A., Heynen, G. J., Ciecielski, K. J., Ai, J., Berninger, A., Kabacaoglu, D., . . . Algul, H. (2018). Mutant KRAS-driven cancers depend on PTPN11/SHP2 phosphatase. *Nat Med, 24*(7), 954-960. doi:10.1038/s41591-018-0024-8

Rygiel, T. P., Mertens, A. E., Strumane, K., van der Kammen, R., & Collard, J. G. (2008). The Rac activator Tiam1 prevents keratinocyte apoptosis by controlling ROS-mediated ERK phosphorylation. *J Cell Sci, 121*(Pt 8), 1183-1192. doi:10.1242/jcs.017194

Sabens, E. A., & Mieyal, J. J. ((2009)). *Glutaredoxin and Thioredoxin Enzyme Systems: Catalytic Mechanisms and Physiological Functions: Chapter 7, in Glutathione and sulfur amino acids in human health and diseas*: e (eds R. Masella and G. Mazza), John Wiley, Hoboken, N.J.

Schreiber, R. D., Old, L. J., & Smyth, M. J. (2011). Cancer immunoediting: integrating immunity's roles in cancer suppression and promotion. *Science, 331*(6024), 1565-1570. doi:10.1126/science.1203486

Schulze, P. C., Liu, H., Choe, E., Yoshioka, J., Shalev, A., Bloch, K. D., & Lee, R. T. (2006). Nitric oxide-dependent suppression of thioredoxin-interacting protein expression enhances thioredoxin activity. *Arterioscler Thromb Vasc Biol, 26*(12), 2666-2672. doi:10.1161/01.ATV.0000248914.21018.f1

Schwendemann, J., Sehringer, B., Noethling, C., Zahradnik, H. P., & Schaefer, W. R. (2008). Nitric oxide detection by DAF (diaminofluorescein) fluorescence in human myometrial tissue. *Gynecol Endocrinol, 24*(6), 306-311. doi:10.1080/09513590801994063

Seki, M., Masutani, C., Yang, L. W., Schuffert, A., Iwai, S., Bahar, I., & Wood, R. D. (2004). High-efficiency bypass of DNA damage by human DNA polymerase Q. *EMBO J, 23*(22), 4484-4494. doi:10.1038/sj.emboj.7600424

Semenza, G. L. (2004). Hydroxylation of HIF-1: oxygen sensing at the molecular level. *Physiology (Bethesda), 19*, 176-182. doi:10.1152/physiol.00001.2004

Semenza, G. L. (2007). HIF-1 mediates the Warburg effect in clear cell renal carcinoma. *J Bioenerg Biomembr, 39*(3), 231-234. doi:10.1007/s10863-007-9081-2

Semenza, G. L. (2009). Regulation of cancer cell metabolism by hypoxia-inducible factor 1. *Semin Cancer Biol, 19*(1), 12-16. doi:10.1016/j.semcancer.2008.11.009

Shay, J. W., & Werbin, H. (1987). Are mitochondrial DNA mutations involved in the carcinogenic process? *Mutat Res, 186*(2), 149-160. doi:10.1016/0165-1110(87)90028-5

Sibbing, D., Pfeufer, A., Perisic, T., Mannes, A. M., Fritz-Wolf, K., Unwin, S., . . . von Beckerath, N. (2011). Mutations in the mitochondrial thioredoxin reductase gene TXNRD2 cause dilated cardiomyopathy. *Eur Heart J, 32*(9), 1121-1133. doi:10.1093/eurheartj/ehq507

Siegel, R., Ma, J., Zou, Z., & Jemal, A. (2014). Cancer statistics, 2014. *CA Cancer J Clin, 64*(1), 9-29. doi:10.3322/caac.21208

Siegel, R. L., Miller, K. D., & Jemal, A. (2018). Cancer statistics, 2018. *CA Cancer J Clin, 68*(1), 7-30. doi:10.3322/caac.21442

Siegel, R. L., Miller, K. D., & Jemal, A. (2019). Cancer statistics, 2019. *CA Cancer J Clin, 69*(1), 7-34. doi:10.3322/caac.21551

Simon, M. C. (2006). Coming up for air: HIF-1 and mitochondrial oxygen consumption. *Cell Metab, 3*(3), 150-151. doi:10.1016/j.cmet.2006.02.007

Slebos, R. J., Kibbelaar, R. E., Dalesio, O., Kooistra, A., Stam, J., Meijer, C. J., . . . et al. (1990). K-ras oncogene activation as a prognostic marker in adenocarcinoma of the lung. *N Engl J Med, 323*(9), 561-565. doi:10.1056/NEJM199008303230902

Song, J., Li, J., Qiao, J., Jain, S., Mark Evers, B., & Chung, D. H. (2009). PKD prevents H2O2-induced apoptosis via NF-kappaB and p38 MAPK in RIE-1 cells. *Biochem Biophys Res Commun, 378*(3), 610-614. doi:10.1016/j.bbrc.2008.11.106

Stokes, M. P., Rush, J., Macneill, J., Ren, J. M., Sprott, K., Nardone, J., . . . Comb, M. J. (2007). Profiling of UV-induced ATM/ATR signaling pathways. *Proc Natl Acad Sci U S A, 104*(50), 19855-19860. doi:10.1073/pnas.0707579104

Storz, P. (2017). KRas, ROS and the initiation of pancreatic cancer. *Small GTPases, 8*(1), 38-42. doi:10.1080/21541248.2016.1192714

Storz, P., Doppler, H., Ferran, C., Grey, S. T., & Toker, A. (2005). Functional dichotomy of A20 in apoptotic and necrotic cell death. *Biochem J, 387*(Pt 1), 47-55. doi:10.1042/BJ20041443

Swords, D. S., Firpo, M. A., Scaife, C. L., & Mulvihill, S. J. (2016). Biomarkers in pancreatic adenocarcinoma: current perspectives. *Onco Targets Ther, 9*, 7459-7467. doi:10.2147/OTT.S100510

Tang, Z., Li, C., Kang, B., Gao, G., Li, C., & Zhang, Z. (2017). GEPIA: a web server for cancer and normal gene expression profiling and interactive analyses. *Nucleic Acids Res, 45*(W1), W98-W102. doi:10.1093/nar/gkx247

Torgovnick, A., & Schumacher, B. (2015). DNA repair mechanisms in cancer development and therapy. *Front Genet, 6*, 157. doi:10.3389/fgene.2015.00157

Tremblay, S., & Wagner, J. R. (2008). Dehydration, deamination and enzymatic repair of cytosine glycols from oxidized poly(dG-dC) and poly(dI-dC). *Nucleic Acids Res, 36*(1), 284-293. doi:10.1093/nar/gkm1013

Ueno, H., Kosuge, T., Matsuyama, Y., Yamamoto, J., Nakao, A., Egawa, S., . . . Kanemitsu, K. (2009). A randomised phase III trial comparing gemcitabine with surgery-only in patients with resected pancreatic cancer: Japanese Study Group of Adjuvant Therapy for Pancreatic Cancer. *Br J Cancer, 101*(6), 908-915. doi:10.1038/sj.bjc.6605256

Uprety, D., & Adjei, A. A. (2020). KRAS: From undruggable to a druggable Cancer Target. *Cancer Treat Rev, 89*, 102070. doi:10.1016/j.ctrv.2020.102070

van Heek, N. T., Meeker, A. K., Kern, S. E., Yeo, C. J., Lillemoe, K. D., Cameron, J. L., . . . Maitra, A. (2002). Telomere shortening is nearly universal in pancreatic intraepithelial neoplasia. *Am J Pathol, 161*(5), 1541-1547. doi:10.1016/S0002-9440(10)64432-X

Vaquero, E. C., Edderkaoui, M., Pandol, S. J., Gukovsky, I., & Gukovskaya, A. S. (2004). Reactive oxygen species produced by NAD(P)H oxidase inhibit apoptosis in pancreatic cancer cells. *J Biol Chem, 279*(33), 34643-34654. doi:10.1074/jbc.M400078200

Vardi, A., Formiggini, F., Casotti, R., De Martino, A., Ribalet, F., Miralto, A., & Bowler, C. (2006). A stress surveillance system based on calcium and nitric oxide in marine diatoms. *PLoS Biol, 4*(3), e60. doi:10.1371/journal.pbio.0040060

Volmar, K. E., Routbort, M. J., Jones, C. K., & Xie, H. B. (2004). Primary pancreatic lymphoma evaluated by fine-needle aspiration: findings in 14 cases. *Am J Clin Pathol, 121*(6), 898-903. doi:10.1309/UAD9-PYFU-A82X-9R9U

Waddell, N., Pajic, M., Patch, A. M., Chang, D. K., Kassahn, K. S., Bailey, P., . . . Grimmond, S. M. (2015). Whole genomes redefine the mutational landscape of pancreatic cancer. *Nature, 518*(7540), 495-501. doi:10.1038/nature14169

Wang, M., Kirk, J. S., Venkataraman, S., Domann, F. E., Zhang, H. J., Schafer, F. Q., . . . Oberley, L. W. (2005). Manganese superoxide dismutase suppresses hypoxic induction of hypoxia-inducible factor-1alpha and vascular endothelial growth factor. *Oncogene, 24*(55), 8154-8166. doi:10.1038/sj.onc.1208986

Wang, Y., Huang, X., Cang, H., Gao, F., Yamamoto, T., Osaki, T., & Yi, J. (2007). The endogenous reactive oxygen species promote NF-kappaB activation by targeting on activation of NF-kappaB-inducing kinase in oral squamous carcinoma cells. *Free Radic Res, 41*(9), 963-971. doi:10.1080/10715760701445045

Warburg, O. (1924). Uber den Stoffwechsel der Karzinomezellen. *Biochem Z, 152*, 309-344.

Weinberg, F., Hamanaka, R., Wheaton, W. W., Weinberg, S., Joseph, J., Lopez, M., . . . Chandel, N. S. (2010). Mitochondrial metabolism and ROS generation are essential for Kras-mediated tumorigenicity. *Proc Natl Acad Sci U S A, 107*(19), 8788-8793. doi:10.1073/pnas.1003428107

Weitzman, S. A., & Gordon, L. I. (1990). Inflammation and cancer: role of phagocyte-generated oxidants in carcinogenesis. *Blood, 76*(4), 655-663.

Williams, J. G., Pappu, K., & Campbell, S. L. (2003). Structural and biochemical studies of p21Ras S-nitrosylation and nitric oxide-mediated guanine nucleotide exchange. *Proc Natl Acad Sci U S A, 100*(11), 6376-6381. doi:10.1073/pnas.1037299100

Wong-Ekkabut, J., Xu, Z., Triampo, W., Tang, I. M., Tieleman, D. P., & Monticelli, L. (2007). Effect of lipid peroxidation on the properties of lipid bilayers: a molecular dynamics study. *Biophys J, 93*(12), 4225-4236. doi:10.1529/biophysj.107.112565

Wood, M. L., Dizdaroglu, M., Gajewski, E., & Essigmann, J. M. (1990). Mechanistic studies of ionizing radiation and oxidative mutagenesis: genetic effects of a single 8-hydroxyguanine (7-hydro-8-oxoguanine) residue inserted at a unique site in a viral genome. *Biochemistry, 29*(30), 7024-7032.

Wu, Y., Antony, S., Juhasz, A., Lu, J., Ge, Y., Jiang, G., . . . Doroshow, J. H. (2011). Up-regulation and sustained activation of Stat1 are essential for interferon-gamma (IFN-gamma)-induced dual oxidase 2 (Duox2) and dual oxidase A2 (DuoxA2) expression in human pancreatic cancer cell lines. *J Biol Chem, 286*(14), 12245-12256. doi:10.1074/jbc.M110.191031

Xia, X., Wu, W., Huang, C., Cen, G., Jiang, T., Cao, J., . . . Qiu, Z. (2015). SMAD4 and its role in pancreatic cancer. *Tumour Biol, 36*(1), 111-119. doi:10.1007/s13277-014-2883-z

Yamaguchi, J., Yokoyama, Y., Kokuryo, T., Ebata, T., & Nagino, M. (2018). Cells of origin of pancreatic neoplasms. *Surg Today, 48*(1), 9-17. doi:10.1007/s00595-017-1501-2

Yoshioka, J. (2015). Thioredoxin Reductase 2 (Txnrd2) Regulates Mitochondrial Integrity in the Progression of Age-Related Heart Failure. *J Am Heart Assoc, 4*(7). doi:10.1161/JAHA.115.002278

Yuen, A., & Diaz, B. (2014). The impact of hypoxia in pancreatic cancer invasion and metastasis. *Hypoxia (Auckl), 2*, 91-106. doi:10.2147/HP.S52636

Zhang, C., Cao, S., Toole, B. P., & Xu, Y. (2015). Cancer may be a pathway to cell survival under persistent hypoxia and elevated ROS: a model for solid-cancer initiation and early development. *Int J Cancer, 136*(9), 2001-2011. doi:10.1002/ijc.28975

Zhou, J., Chen, Y., Lang, J. Y., Lu, J. J., & Ding, J. (2008). Salvicine inactivates beta 1 integrin and inhibits adhesion of MDA-MB-435 cells to fibronectin via reactive oxygen species signaling. *Mol Cancer Res, 6*(2), 194-204. doi:10.1158/1541-7786.MCR-07-0197

Zorov, D. B., Juhaszova, M., & Sollott, S. J. (2014). Mitochondrial reactive oxygen species (ROS) and ROS-induced ROS release. *Physiol Rev, 94*(3), 909-950. doi:10.1152/physrev.00026.2013

Zou, Z., Chang, H., Li, H., & Wang, S. (2017). Induction of reactive oxygen species: an emerging approach for cancer therapy. *Apoptosis, 22*(11), 1321-1335. doi:10.1007/s10495-017-1424-9

Zuo, S., Boorstein, R. J., & Teebor, G. W. (1995). Oxidative damage to 5-methylcytosine in DNA. *Nucleic Acids Res, 23*(16), 3239-3243.

IX.2 List of Figures

IX.3 List of Tables

IX.4 Declaration on publication

Part of this study has been published as follows:

Txnrd2 deficiency leads to low RAS-activity and decreased tumor development in a KrasG12D - driven pancreatic carcinogenesis mouse model

Pfister K, Aichler M, Jastroch M, Brielmeier M, Einwächter H, Schmid RM

Presentation from Pancreas I (Posters) at UEG Week 2019

X. Acknowledgments

Throughout the work of this dissertation, I received great support and assistance. Firstly, I would like to thank Prof. Dr. R. Schmid and Dr. Henrik Einwächter for accepting me into their working group, their guidance in theory and methodology and their continuous advice and encouragement. Your passion for pancreatic cancer was and is a great inspiration.

Secondly, I would like to thank my colleagues at AG Schmid / Einwächter, firstly Thorsten, who introduced me to science and lab work, who showed great patience and immense knowledge and who was of big guidance and influence throughout the whole project. Thank you so much! Also, Anja and Mathilde with their great practical knowledge and sympathetic ear. Thank you for your help and your friendship. Last, but not least, thank you Shankar and Chao for the vivid scientific discussions and good collaboration.

A big thanks to my colleagues at 2. Medizinische Klinik: Kivanc, Chao-Yu, Ezgi, Katrin, Theresa, Melanie, Jonas, and all the others: Thank you for the 10 pm dinners after a 14 - hour day, thank you for the nice evenings on the rooftop terrace, and thank you for the chats and the encouragement.

Also, I would like to thank my friends and family who proofread this thesis: Thank you Luke, Rick, and Amanda. I feel very lucky to be able to call you my overseas home-away-from-home.

Lastly, I want to thank my parents for their continuous believe in me and my skills, for their support, their encouragement and great advice. This thesis would not have happened without you. Thank you, Pascal, for understanding the drills of dissertation writing and continuous encouragement. The final thank you will be addressed to my partner Philipp for his love and support during the ups and downs during the work of this dissertation. Thank you for listening to my everyday problems, even though KRAS and TXNRD2 are very far away from your daily topics and thank you for the everlasting encouragement and support.